

Dissertation zur Erlangung des Doktorgrades der Fakultät für Chemie und Pharmazie
der Ludwig-Maximilians-Universität München

Global analysis of mRNA metabolism by comparative dynamic transcriptome analysis



Mai Sun

aus Beijing, Volksrepublik China

2013

Erklärung

Diese Dissertation wurde im Sinne von §7 der Promotionsordnung vom 28. November 2011 von Herrn Professor Dr. Patrick Cramer betreut.

Eidesstattliche Versicherung

Diese Dissertation wurde eigenändig und ohne unerlaubte Hilfe erarbeitet.

München,

.....
Mai Sun

Dissertation eingereicht am: 16.04.2013

1. Gutachter: Prof. Dr. Patrick Cramer

2. Gutachter: PD. Dr. Dietmar Martin

Mündliche Prüfung am: 28.05.2013

Acknowledgements

Before I began my PhD, I heard from many people who already have a PhD, that this would be a painful four or five or even longer years to go through. And many people who thought themselves to be engaged into academia eventually quit this field. It sounded really horrible. But I didn't believe that. Time flies very fast, and I'm now here at the end of my PhD, I must say, I enjoyed these years. Cramer group is very colorful and gives a very nice work atmosphere. I want to thank many people, but the most thanks to Prof. Patrick Cramer. I remember the first day in Cramer lab, is also my first day at the University Munich. During this years, Patrick is always a good mentor and have been supportive. Not like some of the professors, Patrick really cares the interest of the students and gives wise suggestions. I have had a lot of crazy ideas during the time in this lab, and Patrick took them seriously, some of them resulted in this dissertation. For all of these, I thank my supervisor Patrick. As I said, the Cramer lab is a colorful lab, because many excellent colleagues contribute to the nice atmosphere. Among them I appreciate my colleague and friend Andreas Mayer. We shared a bench and later were bench neighbour. For the years we shared ideas, helped each other with experiments, exchange news from within and without science. It was great time as bench-mate with you, so thank you very much.

Special thanks to Nicole Pirkl, what you have done was not just a favor to me, but a great contribution to this study. You were an excellent technical assistant. And now since you go back to the school, I wish you a good and fruitful time in school and a brilliant career later.

I want to thank my collaborator Björn Schwalb for great computational support for cDTA data. Thank you for being patient when I come down to your office for hours of discussion. It took you so much time sometimes just to optimize the visual effect of the plots in order to make it understandable for me. And I also want to thank Daniel Schulz. You were so generous and shared with me your data, which eventually made the first cDTA paper much better. And I want to thank your critical comments to the protocol. Based on that, we together optimized the cDTA.

I am also very grateful to Dr. Laurent Larivière, Dr. Martin Seizl, Claudia Buchen, Dr. Heidi Feldmann, Dr. Dietmar Martin, and Kerstin Maier for help, being critical and for giving advices to the practical bench work including many small tricks. Thanks to all the other members of the Cramer lab for help, discussions, and just being nice colleague and for the very nice working atmosphere.

Last but not least, I thank my family, my father and mother. You always supported me, so I could study and do research so many years in Germany. And thank all my friends in Europe and in China. And my beloved girlfriend Zhou Ji, thank you for being with me, and I wish we could get our PhD together soon.

Abstract

mRNA metabolism is a highly complicated process. It begins with co-transcriptional events including RNA capping, splicing, cleavage and polyadenylation. During transcription, various proteins are loaded onto the mRNA. This mRNA protein complex is known as mRNP. The structure and composition of mRNP determine the fate of mRNA. Before transported to the cytoplasm, mRNAs are inspected by the nuclear surveillance mechanisms, the aberrant molecules are eliminated. In the cytosol, the cap of mRNA is protected by the translation initiation factor eIF4E. The eIF4E interacts with poly(A)-binding protein and circularize mRNA to ensure effective translation. Cytosolic mRNA degradation competes with translation and can reduce the translatability by shortening the poly(A)-tail. Poly(A)-tail shortening eventually triggers decapping and mRNA degradation. Various surveillance events also take place in the cytosol to prevent formation of aberrant proteins.

To monitor eukaryotic mRNA metabolism, we developed in this study comparative Dynamic Transcriptome Analysis (cDTA). cDTA provides absolute rates of mRNA synthesis and decay in *Saccharomyces cerevisiae* (*Sc*) cells with the use of *Schizosaccharomyces pombe* (*Sp*) as internal standard. cDTA uses non-perturbing metabolic labeling that supersedes conventional methods for mRNA turnover analysis. cDTA reveals that *S. cerevisiae* and *S. pombe* transcripts that encode orthologous proteins have similar synthesis rates, whereas decay rates are five-fold lower in *S. pombe*, resulting in similar mRNA concentrations despite the larger *S. pombe* cell volume. cDTA of *S. cerevisiae* mutants reveals that a eukaryote can buffer mRNA levels. Impairing transcription with a point mutation in RNA polymerase (Pol) II causes decreased mRNA synthesis rates as expected, but also decreased decay rates. Impairing mRNA degradation by deleting deadenylase subunits of the Ccr4-Not complex causes decreased decay rates as expected, but also decreased synthesis rates. Extended kinetic modeling reveals mutual feedback between mRNA synthesis and degradation that may be achieved by a factor that inhibits synthesis and enhances degradation. We further use cDTA to determine the transcription rate and degradation

rate of mRNAs in 46 yeast strains lacking genes involved in mRNA degradation and metabolism. In these strains, changes in mRNA degradation rates are generally compensated by changes in mRNA synthesis rates, resulting in a buffering of mRNA levels. We show that buffering of mRNA levels requires the RNA exonuclease Xrn1. The buffering is rapidly established when mRNA synthesis is impaired, but is delayed when mRNA degradation is impaired, apparently due to Xrn1p-dependent transcription repressor induction. Cluster analysis of the data defines the general mRNA degradation machinery, reveals different substrate preferences for the two mRNA deadenylase complexes Ccr4-Not and Pan2p-Pan3p, and unveils an interwoven cellular mRNA surveillance network.

Publication List

This thesis is based on two first author papers:

- 2012 **Global analysis of eukaryotic mRNA degradation reveals Xrn1-dependent buffering of transcript levels** Mai Sun¹, Björn Schwalb¹, Nicole Pirkl, Kerstin C. Maier, Arne Schenk, Henrik Failmezger, Achim Tresch, and Patrick Cramer, *Manuscript submitted*

¹ These authors contributed equally

M. Sun, B.S., and P.C. conceived and designed the study. B.S. and A.T. designed and B.S., A.T. A.S., and H.F. carried out computational analyses. M.S., N.P., K.M., designed and performed experiments. P.C. and A.T wrote the manuscript, with input from all authors.

- 2012 **Comparative dynamic transcriptome analysis (cDTA) reveals mutual feedback between mRNA synthesis and degradation** Mai Sun¹, Björn Schwalb¹, Daniel Schulz¹, Nicole Pirkl, Stefanie Etzold, Laurent Larivière, Kerstin C. Maier, Martin Seizl, Achim Tresch, Patrick Cramer, *Genome Research*, **2012** 22(7):1350-9

¹ These authors contributed equally

M. Sun, B.S., L.L., and P.C. conceived and designed the study. M. Sun and D.S. implemented and evaluated experimental methods. S.E. und M. Seizl conducted the *rpb1-1* experiments. B.S. and A.T. designed and carried out computational analyses. M.S., D.S., N.P., K.M., S.E., and M. Seizl designed and performed experiments. P.C. and A.T wrote the manuscript, with input from all authors.

Other publications

- 2012 **Measurement of genome-wide RNA synthesis and decay rates with Dynamic Transcriptome Analysis (DTA)** Björn Schwalb, Daniel Schulz, Mai Sun, Benedikt Zacher, Sebastian Dömcke, Dietmar Martin, Patrick Cramer, Achim Tresch, *Bioinformatics*, **2012** 28(6):884-5.

- 2012 **CTD Tyrosine Phosphorylation Impairs Termination Factor Recruitment to RNA Polymerase II** Andreas Mayer, Martin Heidemann, Michael Lidschreiber, Amelie Schrieck, Mai Sun, Corinna Hintermair, Elisabeth Kremmer, Dirk Eick, Patrick Cramer, *Science*, **2012**. 336:1723-1725.
- 2010 **A Tandem SH2 Domain in Transcription Elongation Factor Spt6 Binds the Phosphorylated RNA Polymerase II C-terminal Repeat Domain (CTD)** Mai Sun, Laurent Larivière, Stefan Dengl, Andreas Mayer, Patrick Cramer, *J Biol Chem*, 2010. 285:41597-41603.
- 2009 **Structure and *in Vivo* Requirement of the Yeast Spt6 SH2 Domain** Stefan Dengl, Andreas Mayer, Mai Sun, Patrick Cramer, *J Mol Biol*, **2009**. 389:211-225.
- 2009 **LiCl-mediated preparation of functionalized benzylic indium(III) halides and highly chemoselective palladium-catalyzed cross-coupling in a protic cosolvent** Yi-Hung Chen, Mai Sun, Paul Knochel, *Angew Chem Int Ed Engl*, **2009**. 48:2236-2239.

Contents

Declaration	iii
Acknowledgements	v
Abstract	vii
Publications	ix
Contents	ix
1 Introduction	1
1.1 The complexity of mRNA metabolism	1
1.2 mRNA degradation is an important platform for gene regulation	2
1.2.1 The mRNA degradation pathways	2
1.2.2 Deadenylation	4
1.2.3 Decapping	6
1.2.4 Bulk degradation by exonuclease Xrn1p	7
1.2.5 Bulk degradation by the exosome complex	8
1.2.6 mRNA degradation as surveillance	9
1.3 Methods of investigating mRNA degradation	10
1.3.1 Dissecting the degradation events	10
1.3.2 Monitoring mRNA metabolism using genome wide gene expres- sion methods	10
1.3.3 Dynamic transcriptome analysis (DTA)	11
1.4 Aims and scope of this work	12
2 Materials	16
2.1 List of Strains	16

2.2	List of Plasmids	20
2.3	List of important primers	20
2.4	Growth media	23
2.5	Buffers and Solutions	24
3	Methods	27
3.1	Common Methods	27
3.1.1	Molecular cloning using <i>Escherichia coli</i>	27
3.1.2	Cryo-stocks of yeast strains	28
3.1.3	Generation of knock-out strains	28
3.1.4	Colony PCR	29
3.1.5	Generation of point mutants	29
3.1.6	Molecular cloning of tagged protein	29
3.2	comparative <u>D</u> ynamic <u>T</u> ranscriptomic <u>A</u> nalysis (cDTA)	30
3.2.1	Metabolic labeling of the cells	30
3.2.2	Microarray procedure	30
3.2.3	Brief about data analysis	31
3.3	Other biochemical methods	32
3.3.1	Flow cytometry analysis	32
3.3.2	<i>in vitro</i> transcription assay	32
3.3.3	RT-qPCR	32
4	Results	34
4.1	cDTA analysis reveals a mutual feedback loop between mRNA transcrip- tion and degradation	34
4.1.1	Establishment of cDTA based on DTA	34
4.1.2	Rate extraction from cDTA data	37
4.1.3	cDTA supersedes conventional methods	44
4.1.4	Comparison of mRNA metabolism in distant yeast species	46
4.1.5	Impaired mRNA synthesis is compensated by decreased degra- dation	49
4.1.6	Impaired degradation is compensated by decreased synthesis	53
4.1.7	A transcription inhibitor and degradation enhancer may buffer mRNA levels	55

4.2	Global analysis of eukaryotic mRNA degradation reveals Xrn1-dependent buffering of transcript levels	56
4.2.1	Global analysis of mRNA degradation	56
4.2.2	Generality of mRNA level buffering	58
4.2.3	mRNA level buffering requires Xrn1p activity	58
4.2.4	Xrn1p represses mRNA synthesis indirectly	61
4.2.5	Induction of transcription repressor Nrg1p	64
4.2.6	Delayed mRNA buffering upon degradation inhibition	65
4.2.7	Rapid buffering upon mRNA synthesis inhibition	67
4.2.8	Cluster analysis reveals mRNA degradation complexes	68
4.2.9	General mRNA degradation machinery	70
4.2.10	Deadenylase complexes differ in substrate preference	72
4.2.11	Scavenger decapping factors Dcs1p and Dcs2p are global antagonists	72
4.2.12	An interwoven mRNA surveillance network	74
5	Discussion	75
5.1	cDTA reveals mutual feedback loop of transcription and degradation of mRNA	75
5.2	Global analysis of mRNA degradation indicates Xrn1p as a buffering factor	77
5.3	Outlook	79
	References	81
	Abbreviations	100
	Curriculum Vitae	101

Chapter 1

Introduction

1.1 The complexity of mRNA metabolism

In most species studied, the amount of RNA is defined by RNA synthesis (Fuda et al., 2009) and degradation (Garneau et al., 2007; Parker and Sheth, 2007). These two major processes determine cellular mRNA levels and thus govern genome expression (Figure 1.1). Transcription is regulated at different levels: the DNA sequence defines the location, and to some extent the strength of transcription. It includes the core promoter sequence, which is bound by the general transcription factors (GTFs); and the sequence upstream of the core promoter, which can be bound by either activators or repressors, and can thus interact with GTFs. Thousands of factors regulate transcription, the majority of these are proteins, and some are regulatory non-coding RNAs (Liu et al., 2013). After the several nucleotide are synthesized, the mRNA is capped, intron sequence is spliced, the nascent mRNA is cleaved before termination and polyadenylated. During transcription, various proteins are loaded onto the mRNA. The structure of the mRNA and the composition of the proteins loaded onto the mRNA determine its fate. Before transport to the cytoplasm, mRNAs are inspected by the nuclear surveillance mechanisms and the aberrant molecules are eliminated. In the cytosol, mRNA cap is protected by the translation initiation factor eIF4E. eIF4E interacts with poly(A)-binding protein and circularizes mRNAs to ensure effective translation. Cytosolic mRNA degradation competes with translation and can reduce the translatability by shortening the poly(A)-tail. poly(A) shortening eventually triggers decapping and mRNA degradation. Various surveillance events also take place in the cytosol to prevent the formation of aberrant protein. The cellular degradation is governed by

multiple mechanisms. There are four general pathways (Figure 1.1): deadenylation dependent decapping followed by $5' \rightarrow 3'$ degradation, $3' \rightarrow 5'$ degradation by exosome, the endonucleolytic digestion and quality control pathways.

1.2 mRNA degradation is an important platform for gene regulation

1.2.1 The mRNA degradation pathways

In eukaryotes, mRNAs are synthesized in the nucleus by RNA polymerase II (Pol II). The 5'-end of the nascent mRNA is protected by a 7-methyl guanosine cap (m^7G -cap) structure, which is added immediately after a few nucleotides are synthesized (Shatkin, 1976; Topisirovic et al., 2011). When Pol II reaches the 3'-poly(A) site, cleavage happens, the nascent mRNA is released into the nucleoplasm and subsequently polyadenylated (Colgan and Manley, 1997; Millevoi and Vagner, 2010). This poly(A) tail prevents mRNA from degradation at the 3'-end. The mRNAs are coated with various functional proteins to form messenger ribonucleoproteins (mRNPs) (Lee and Tarn, 2013); some of them facilitate mRNA export to the cytoplasm, where they are translated (Rodríguez-Navarro and Hurt, 2011). The poly(A) tail of mRNA is bound by poly(A)-binding protein (PABP), and the 5'- m^7G -cap is bound by cap binding proteins (CBPs). These two complexes interact with each other, determine the translation efficiency and protect mRNAs from degradation (Topisirovic et al., 2011). However, mRNAs are constantly deadenylated in cytoplasm. Shortening the poly(A) tail reduces the ability of mRNAs to be translated and eventually leads to translational inhibition and degradation.

In yeast poly(A) shortening leads to decapping and thereby exposing the RNAs to $5' \rightarrow 3'$ digestion by exonuclease (Decker and Parker, 1993; Muhlrad et al., 1994). *In vivo* the mRNAs are protected from decapping in a poly(A) dependent manner (Caponigro and Parker, 1995; Decker and Parker, 1993). The poly(A) binding protein Pab1p plays a major role in the decapping inhibition (Caponigro and Parker, 1995). The ability of Pab1p to inhibit decapping is intrinsic and is independent of the binding to poly(A) (Coller et al., 1998). Decapping is conserved throughout eukaryotic organisms. Evidence shows that in yeast the $5' \rightarrow 3'$ degradation following decapping is faster than the $3' \rightarrow 5'$ degradation. However, in some yeast mRNA $3' \rightarrow 5'$ degradation will be the dominant decay mechanism.

Degradation also plays an important role in surveillance. Although Pol II has proof-reading activity and has a very low error rate (Cheung and Cramer, 2011; Wang et al., 2009), splicing is an error prone process and often leads to frame shift in mRNA (Jaillon et al., 2008; Zhang et al., 2009). Frame shifts eventually cause premature stop codon formation and produces truncated peptides. In the nucleus, aberrant transcripts can be recognized and polyadenylated by the TRAMP complex, and subjected to degradation by exosomes (Schmidt and Butler, 2013). In the cytosol, non-sense mediated decay (NMD) is a translation dependent surveillance pathway, which recruits the degradation machinery and is involved in the subsequent clearance of the aberrant mRNAs (González et al., 2001). Some RNAs also contain secondary structure, which can obstruct translating ribosomes. No-go mediated decay (NGD) cope with these situations and triggers mRNA degradation as well (Inada, 2013).

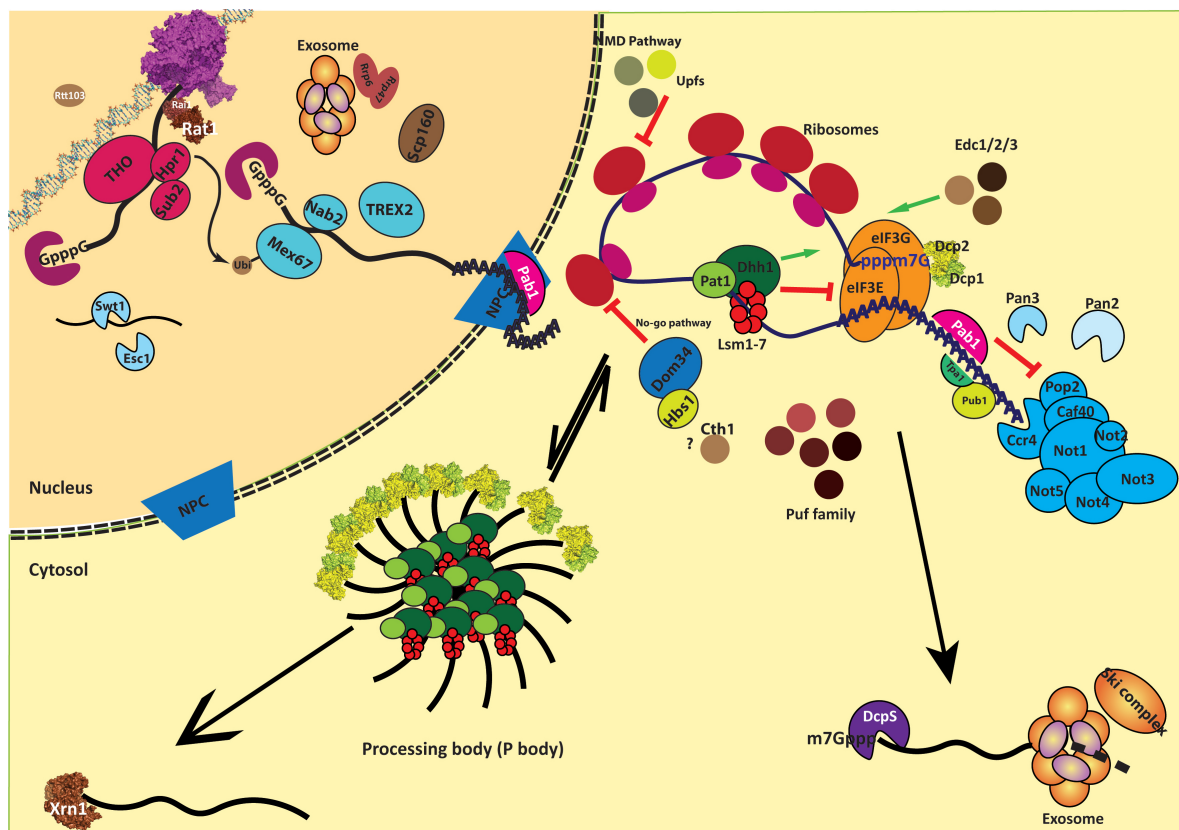


Figure 1.1: The mRNA degradation pathway

1.2.2 Deadenylation

Although mRNA can be degraded from both ends by exoribonucleases or in the middle by endoribonucleases, studies show that poly(A)-shortening is the initial step in mRNA degradation. In eukaryotic cells, deadenylation is carried out by the large Ccr4-Not complex (Chen et al., 2002; Tucker et al., 2001). Eukaryotes possess another protein complex, Pan2p-Pan3p, with deadenylase activity, which was discovered even before the discovery of deadenylase activity of Ccr4-Not complex (Sachs and Deardorff, 1992). In yeast as well as in drosophila, evidence shows that Pan2p-Pan3p trims the poly(A) tail in the nucleus during mRNA processing. In the cytoplasm, Pan2p-Pan3p initiates deadenylation before the Ccr4-Not complex takes action (Brown and Sachs, 1998; Tucker et al., 2001). In deletion strains of Ccr4p, Pan2p-Pan3p seems to have residual deadenylation activity, but deletion of Pan2p-Pan3p does not affect the cellular deadenylation. In mammalian cells, several cis-regulating elements can enhance deadenylation, such as AU-rich elements (AREs), miRNA recognition sites, and non-sense codon (Chen and Shyu, 2011). Here I briefly review the character of these deadenylase complexes.

Ccr4-Not complex Ccr4-Not complex is one of the global regulator of gene expression (Collart, 2003). It contains 9 subunits and regulates RNA turnover at several steps (Bai et al., 1999). Ccr4-Not complex was identified solely as transcription factor in 1980 (Reed, 1980), and it is important in the regulation of TFIID distribution on promoters (Lenssen et al., 2005, 2007). Since the two subunits of this complex, Ccr4p and Caf1p, are deadenylases (Tucker et al., 2001), Ccr4-Not complex also contributes to mRNA degradation. Ccr4-Not complex even functions in protein degradation, since Not4p was identified as an E3 ligase (Albert et al., 2002). Latest *in vitro* studies confirm Ccr4-Not complex functions in transcription elongation (Kruk et al., 2011) by performing ChIP assays. Ccr4p is also found in the Cdc73p-Paf1p-Pol II-containing complex (Paf1p complex), which also includes Ctr9p, Rtf1p, Leo1p, Gal11p, Ccr4p, Hpr1p, and the general initiation factors TFIIB and TFIIF, but lacks Tbp1p, TFIIH, and transcription elongation factor TFIIS, as well as the SRBps.

Ccr4-Not complex is structurally and functionally divided into two modules, the Ccr4-Pop2 module and the Not2-Not5 module. The former one conducts the exnuclease activity *in vivo*, whereas the latter one take part in transcription repression, protein degradation (Cui et al., 2008).

The catalytic subunits of the Ccr4-Not complex Ccr4p is a 3'-exoribonuclease with a preference for poly(A)-substrates. The yeast Ccr4p contains 3 functional domains: the N-terminal extension, which is unique to *Saccharomyces cerevisiae* and not found in higher eukaryotes; the central leucine-rich repeat(LRR), which is important for the contact between Ccr4p and Pop2p; and the C-terminal nuclease domain. Pop2p is one of the two catalytic subunits in Ccr4-Not complex (Tucker et al., 2001).

Pop2p belongs to the DEDD nuclease family, and possesses 3' → 5'-exonuclease activity with preference for poly(A) sequence *in vitro*. However, mutations of Pop2p to disrupt the catalytic activity do not cause deadenylation defects in *in vivo*. Partial disruption of Pop2p inhibits the association of Ccr4p with the Not1p and Not2p proteins (Bai et al., 1999; Liu et al., 1998). Besides the structural function of Pop2p in Ccr4-Not complex, it also has other separate functions in deadenylation *in vivo* (Ohn et al., 2007). Deadenylation end point defect is observed in several Pop2p mutants, in which a conserved region is mutated or deleted(Ohn et al., 2007). Furthermore, *pop2Δ* was shown to be synthetic lethal with *dhh1Δ*, whereas *ccr4Δ* is not synthetic lethal with *dhh1Δ* (Maillet and Collart, 2002).

The non-catalytic subunits of the Ccr4-Not complex The largest subunit of the Ccr4-Not complex is Not1p, which is an L-shaped protein. Not1p is thus believed to be the structure scaffold which holds this complex together. The N-terminal of Not1p around 1000 amino acids is structured. Part of this region interacts with Pop2p and Ccr4p (Bai et al., 1999). Structural analysis pinpointed the stretch Not1₇₅₄₋₁₀₀₀ recruits Ccr4p-Pop2p and is essential for yeast viability. Interruption of the Not1p-Pop2p interface resembles the phenotype of *pop2Δ* (Basquin et al., 2012).

Not4p has a variety of functions at protein level regulation. It is known as ubiquitin E3 ligase and can ubiquitinate subunits without association of Ccr4-Not complex. Not4p regulates the stability of stress-induced transcription factors (Cooper et al., 2012).

Not2p, Not3p and Not5p have more direct functions in transcription. Not5p and Not2p interact with transcription factor TFIID (Badarinarayana et al., 2000; Deluen et al., 2002) and SAGA (Cui et al., 2008). Not2p and Not3p are detected at multiple promoters by cross-linking. The Not module also plays diverse essential roles in higher eukaryotes e.g. during embryogenesis (Neely et al., 2010).

The Ccr4-Not complex contains Caf40p and Caf130p, but they have distinct function

than the deadenylase module and Not module.

Pan2p-Pan3p complex Pan2p is a divalent ion dependent ribonuclease, and can digest single stranded ribonucleic acid from the 3'-end. Pan2p has a substrate preference towards poly(A)-stretches.

In contrast Pan3p has no enzymatic activity, but rather interacts with poly(A) binding protein (PABP) and Pan2p. *In vitro*, Pan3p stimulates the activity of Pan2p upon binding to PABP (Uchida et al., 2004).

1.2.3 Decapping

Following deadenylation, mRNAs can be further degraded by the exosome from the 3'-end and subsequently decapped by the so called scavenger decapping factors DcpS. The majority of mRNA is decapped by decapping complex Dcp1p-Dcp2p and translationally deactivated. Eukaryotes form RNA processing bodies in the cytoplasm called P-body. Where proteins essential for mRNA metabolism are stored. Among them, the decapping machinery builds up a conserved core in P-body, which consists of the decapping enzyme complex Dcp1p-Dcp2p, the decapping activator and the translation repressor Dhh1p and Pat1p, the Sm-like decapping activator complex Lsm1-7p (Sheth and Parker, 2003) and the Sm-domain protein Scd6p (Muhlrad and Parker, 2005), enhancer of decapping Edc3p (Kshirsagar and Parker, 2004), and the 5' → 3'-exoribonuclease Xrn1p (Sheth and Parker, 2003). Translationally inactivated mRNAs accumulate in P-bodies. There they will be degraded or stored for reuse (Parker and Sheth, 2007).

Deadenylation triggered decapping by Dcp1p/Dcp2p Many experiments show that Dcp2p is the catalytic subunit of the decapping machinery, whereas Dcp1p functions to enhance the activity of Dcp2p. Dcp1p and Dcp2p form a complex where Dcp1p acts as co-activator and Dcp2p catalyses the m⁷G-cap-hydrolysis reaction (Coller and Parker, 2004). Dcp2p contains a NUDIX/MutT domain; deletion of this domain leads to inactivation of Dcp2p *in vivo* and *in vitro* (Dunckley and Parker, 1999). The NUDIX domain of Dcp2p can bind the 5'-cap and the RNA body and the catalytic activity of Dcp2p is enhanced upon binding (Deshmukh et al., 2008). Actively translated mRNAs are prevented from decapping. Structure features of a translatable mRNA, such as cap

binding protein eIF4E (Ramirez et al., 2002), the poly(A)-tail and poly(A)-binding proteins, inhibit decapping activity (Tucker and Parker, 2000).

The regulation of decapping The decapping process is regulated by both inhibition and enhancement. An example is the poly(A) binding protein Pab1p; deletion of Pab1p causes decapping prior to deadenylation (Caponigro and Parker, 1995; Morrissey et al., 1999). Other proteins that bind to the cap, e.g. eIF4E also inhibit decapping. There are several groups of proteins, which enhance decapping. The decapping activator Dhh1p and Pat1p function by moving mRNAs from polysomes into the translationally inert state that accumulates in P-bodies. Dhh1p and Pat1p interact with subunits in the translation initiation complex and repress translation, thus promoting P-body formation. Under glucose starvation, translational repression is observed in WT cell in response to the environment cue. But in *dhh1* Δ and *pat1* Δ strain, translational repression is only slightly impaired. Dhh1p represses translation possibly by directly binding to translation initiation factors. Experiments show that Dhh1p inhibits the formation of 48S complex *in vitro* (Coller and Parker, 2005). Dhh1p enhances the decapping event in the deadenylated mRNA, since in the *dhh1* Δ strain capped mRNA lacking poly(A)-tail is accumulated, impaired Dhh1p does not affect the mRNA deadenylation rate. Experiments also showed that, Dhh1p is not required for the NMD pathway (Coller et al., 2001; Fischer and Weis, 2002). Pat1p, a topoisomerase II associated deadenylation dependent mRNA decapping factor, is also required for faithful chromosome transmission, maintenance of rDNA locus stability, and protection of mRNA 3'-UTRs. It is functionally linked to Pab1p. It contains a Pumilio domain and thus binds to mRNA. The confirmed binary interaction partners of Pat1p are Dhh1p, Lsm1p, Lsm2p, and Lsm4p. The Edc1p and Edc2p proteins are identified as decapping enhancers since their overexpression can compensate the synthetic lethality of the temperature sensitive allele of *DCP1* and *DCP2* and *ski7* Δ . Edc1p and Edc2p bind to Dcp1p, the general decapping activator, via its EVH1 domain, and thus enhance the decapping activity of Dcp2p by 1000-fold (Borja et al., 2011; Schwartz et al., 2003).

1.2.4 Bulk degradation by exonuclease Xrn1p

The cap structure prevents mRNA from degradation, accumulation of mRNA without 5'-cap is observed in *xrn1* Δ yeast (Hsu and Stevens, 1993). Xrn1p is a conserved

processive exonuclease (Johnson and Kolodner, 1991). Xrn1p preferentially degrades mRNA carrying a 5'-monophosphate end, which is the product of decapping (Stevens, 2001). Xrn1p is also a component of P-bodies thus interacting with Dcp1p-Dcp2p, Lsm proteins, Pat1p, and Dhh1p (Parker and Sheth, 2007). Recently, Xrn1p was also found to have functions in the nucleus. Deletion of Xrn1p leads to accumulation of non-coding RNAs, the majority of these are anti-sense transcripts. This finding implies a potential nuclear function for Xrn1p (van Dijk et al., 2011).

1.2.5 Bulk degradation by the exosome complex

Exosome The eukaryotic exosome comprises a nine-subunit core and catalytic subunits (Chlebowski et al., 2013). The core is ring shaped and is conserved throughout eukaryotes. In contrast to its prokaryotic counterpart, the core does not although six of the eukaryotic exosome core subunits are structural homologue to RNase PH, they don't have catalytic activity (Liu et al., 2006).

The enzymatic activity of the eukaryotic exosome is driven by the RNR superfamily ribonuclease Dis3p. The catalytic activity of Dis3p is built up by four aspartate subunits and is situated at the bottom of the ring-like exosome core, where the mRNA exits. Dis3p binds to the exosome core in the cytoplasm, and degrades deadenylated mRNAs in 3' → 5' direction. The Rrp6p subunit is believed to catalyze the nuclear degradation of mRNAs in quality control. Recent structural analysis elucidated that Rrp6p plays an important role in stabilizing the exosome structure (Makino et al., 2013). Exosome eliminate the aberrant RNAs and also takes part in the maturation of RNAs in nucleus by trimming them in a 3' → 5' direction (Houseley et al., 2006).

The scavenger decapping enzyme DcpS There is another type of decapping enzyme, that degrades the short capped RNAs produced by exosome dependent 5' → 3' degradation (Wang and Kiledjian, 2001). Long RNA substrates cannot be degraded by DcpS. It also hydrolyzes the m⁷G-cap to produce m⁷G-cap and phosphate. DcpS contains a HIT domain, and it reacts specifically with methylated cap analogs *in vitro*. It cannot hydrolyze unmethylated cap and intact capped RNA (Liu et al., 2002). In the cytoplasm exosome leaves short mRNAs with m⁷G-cap structure, the canonical decapping enzyme has low activity towards this group of mRNAs and the cap is thus removed by DcpS.

1.2.6 mRNA degradation as surveillance

Nuclear surveillance As mentioned above, the RNAs which failed to be processed properly and thus contain mutations are subjected to degradation by the nuclear exosome. This process eliminates the mRNAs which failed to form normal mRNPs. In eukaryotes, this is catalysed by the exosome with nuclear exonuclease Rrp6p. The activity of the exosome is enhanced by a highly conserved TRAMP complex, which polyadenylates and recruits nuclear RNA to the exosome (Anderson and Wang, 2009). In yeast *S. cerevisiae*, two kinds of TRAMP complexes exist. These complexes contain similar components but with distinct substrate specificity (Paolo et al., 2009). At least two forms of TRAMP complexes exist in the cell, TRAMP4 and TRAMP5, which contain different poly(A)-polymerases, Trf4p and Trf5p. Recent studies show that the RNA binding proteins Air1p and Air2p are responsible for the substrate selection of different TRAMP complex (Schmidt et al., 2012).

Cytoplasmic surveillance The mRNAs that contain premature stop codon trigger the NMD pathway. Key players of this pathway are the Upf proteins in *S. cerevisiae* (He et al., 1997) and smgs in *Caenorhabditis elegans* (Page et al., 1999). The NMD pathway is a serial protein binding event that already begins in the nucleus. Upf3p is loaded onto the exon-junction complex (EJC), and Upf1p, an essential RNA helicase which is associated with translation release factors and Upf2p Upf3p, providing a link between translation termination and degradation (Kervestin and Jacobson, 2012; Lejeune and Maquat, 2005). If the mRNA molecules lack a stop codon, they will be subjected to non-stop decay (NSD). In this case, the mRNAs are targeted to the cytoplasmic exosome by a special factor, Ski7p. Another kind of cytoplasmic surveillance is the so-called no-go decay (NGD), which targets a broad range of ribosomal stalling events. This can be caused by mRNAs containing secondary structure, premature stop codon or rare codon (Doma and Parker, 2006). NGD triggers endonucleolytic cleavage of the mRNA. The mRNA is targeted by the proteins Dom34p (or Pelota) and Hbs1p. Structure analysis suggests that the Dom34p-Hbs1p resembles the structure of translation releasing factor eRF1:eRF3 (Becker et al., 2011). Dom34p-Hbs1p loose the translation machinery and this leads to peptidyl-tRNA releasing from ribosome. Subsequently, the mRNA is degraded by the cytosolic mRNA degradation pathway (Shoemaker et al., 2010).

1.3 Methods of investigating mRNA degradation

1.3.1 Dissecting the degradation events

mRNA degradation events have long intrigued scientists, but no suitable methodology existed to dissect the degradation events from the existing pool of mRNAs. The cellular mRNA pool is highly dynamic. Transcription constantly produces mRNAs and degradation diminishes mRNAs, which make it difficult to trace the degradation. The direct way to tackle this problem is to shut down the transcription. This is initially facilitated by *c-fos* induced promoters (Loflin et al., 1999). Using *c-fos* promoter, one can turn off the transcription of certain mRNAs for a defined time and monitor the degradation event of this transcript. Inducible promoter is also used in yeast using galactose controlled system (Decker and Parker, 1993). In yeast, one can take advantage of the heat inducible allele *rpb1-1* (Holstege et al., 1998), or more invasively to arrest RNA pol II by adding small molecule drugs (Grigull et al., 2004; Shalem et al., 2008). But all these methods introduce changes in the medium or temperature and are thus perturbing methods.

1.3.2 Monitoring mRNA metabolism using genome wide gene expression methods

Transcriptome analysis is a powerful tool to understand the function of the genome of a living organism. The microarray method is based on hybridization of nucleic acid. The first prototype of gene expression screening was published by Leonard H. Augenlicht and colleague in 1982 (Augenlicht and Kobrin, 1982), where they screened mouse colon tissue poly(A) mRNA using a nitrocellulose membrane with 378 genes spotted on it. The techniques developed by Schena and Shalon (Schena et al., 1995; Shalon et al., 1996) at Stanford University greatly changed the genetics community. They spotted the cDNAs on a coated glass slide and applied the hybridization to this slide. Because the spots are highly compact, one can get information from thousands of genes from one single glass slide. Nowadays, the experiments using gene chips are very well reproducible and reliable. Researchers have been using microarrays combined with methods mentioned in previous paragraph to measure the mRNA degradation rate globally (Grigull et al., 2004; Holstege et al., 1998). Non-invasive metabolic labeling methods enable the observation of mRNA synthesis and degradation without perturbing the

organisms. Combined with kinetic labeling, accurate synthesis and degradation rates can be calculated genome wide. This was first shown with 4-thiouridine (4sU) labeling in mammalian cells (Cleary et al., 2005; Dolken et al., 2008; Kenzelmann et al., 2007), and later translated to the yeast system (Miller et al., 2011; Munchel et al., 2011). The cells take up 4sU and phosphorylate it into 4sUTP. The transcription machinery can use this base analogue and build it into mRNA. The newly synthesized mRNAs bearing 4-thiouracile (4tU) can be biotinylated using biotin coupled with reactive sulfur. Purified newly synthesized mRNA represents the dynamic changes in synthesis and degradation.

1.3.3 Dynamic transcriptome analysis (DTA)

The uptake of 4sU in yeast was enabled by the expression of a human nucleoside transporter. *In vitro* transcription assays indicate that the incorporation rate of 4-thio-UTP by RNA pol II a has very similar kinetic as incorporation of UTP. *In vivo* cell growth is not affected by addition of 4sU. This results in a methods as an non-invasive method, and is able to monitor transcription and degradation. Dynamic transcriptome analysis developed previously by Miller et. al. in 2011 uses 4sU to label the cells for 6 min. This is short enough to meet the assumption of constant synthesis and decay rate during labeling, but sufficiently long to yield enough labeled RNA for robust measurements (Miller et al., 2011).

The normalization problem in transcriptome analysis Initially and still, cDNA samples in gene expression profiling are labeled by two fluorescence dyes. The samples are mixed in 1:1 ratio, and the signals are combined and normalized against the overall signal. In one color microarray system, the cDNA samples are only coupled to one dye. The signal normalization is applied to the median level of the total signal. In both cases, there is an assumption that is the overall level of gene expression hardly changes among experiments. Our observations and recently published work has shown that global changes can take place in certain perturbations or genetic changes (Lin et al., 2012; Sun et al., 2012). These changes in the transcriptome profile can only be monitored, if the data is properly normalized.

Normalization with external standard The idea of using external standard to monitor the global change of mRNA levels was first reported by Holstege and co-workers

in a genome wide study of artificial inactivation of RNA polymerase II (Holstege et al., 1998). The method was described in detail in another paper (van de Peppel et al., 2003). In this method, equal amounts of externally transcribed mRNAs are spiked with equal amounts of total RNA. The cell number is counted and the yield of total RNA is calculated in respect to the cell number. Similar normalization methods are also used in the study of RNA decay (Wang et al., 2002). Recently, Lin and co-workers in Richard Young’s lab counted the cell number and used a very small amount of cells. They used NanoString technology to determine the exact number of mRNAs (Lin et al., 2012). The method developed in this study (comparative dynamic transcriptome analysis, cDTA) deals with the normalization problem. cDTA takes cell numbers as a normalization baseline, and takes the cell lysis efficiency into account by using another distantly related yeast species as internal standard. cDTA ensures that the SRs and DRs are on the same scale, so that rates in different mutant strains can be compared.

1.4 Aims and scope of this work

The overall aims of this work were to (i) establish a protocol that allows for monitoring global synthesis rate of degradation rate; (ii) apply this protocol to study the degradation pathway in *S. cerevisiae*. As mentioned, cellular gene expression is controlled by mRNA levels, which are governed by the rates of nuclear mRNA synthesis and cytoplasmic mRNA degradation. The rates of mRNA synthesis are regulated during RNA polymerase (Pol) II transcription in the nucleus (Fuda et al., 2009), whereas bulk mRNA degradation occurs in the cytoplasm (Eulalio et al., 2007; Parker and Sheth, 2007; Wiederhold and Passmore, 2010). During transcription, the mRNA receives a 5’-cap and a 3’-poly(A) tail. The mature mRNA is then exported to the cytoplasm, translated, and eventually degraded co-translationally (Hu et al., 2009). Degradation of eukaryotic mRNAs has been extensively studied (Garneau et al., 2007; Parker and Sheth, 2007). mRNA degradation generally commences with a shortening of the 3’-poly(A) (pA) tail (deadenylation) (Collart, 2003; Yamashita et al., 2005), followed by removal of the 5’-cap (decapping) (Coller and Parker, 2004; Franks and Lykke-Andersen, 2008). mRNAs are then degraded in 5’ \rightarrow 3’ direction by the Xrn1 exonuclease (Houseley and Tollervey, 2009) and in 3’ \rightarrow 5’ direction by the exosome (Lebreton et al., 2008). When the pA tail reaches a critical length, mRNAs are subjected to decapping by Dcp2p (Muhlrad et al., 1994), which is promoted by Dcp1p and Edc3p

(Kshirsagar and Parker, 2004), the yeast-specific factors Edc1p and Edc2p (Dunckley et al., 2001), and the translation-repressing factors Dhh1p (Coller and Parker, 2005), Pat1p, and the Lsm complex (Chowdhury et al., 2007; Pilkington and Parker, 2008). Dedicated transcription- and translation-coupled quality surveillance pathways also contribute to mRNA degradation (Schmid and Jensen, 2010; Shoemaker and Green, 2012; Shyu et al., 2008). Cytoplasmic mRNA degradation generally begins with shortening of the poly(A)-tail by the Ccr4-Not complex that contains the deadenylases Ccr4p and Pop2p (Liu et al., 1998; Tucker et al., 2001). The mRNA is then decapped and degraded by exonucleases from both ends. Despite the spatial separation of mRNA synthesis and translation/degradation, there is evidence that these processes are coordinated (Harel-Sharvit et al., 2010; Lotan et al., 2005, 2007).

To investigate coordinated RNA synthesis and degradation, absolute changes in synthesis and decay rates must be measured after introducing a genetic perturbation that impairs either synthesis or degradation. Rates of mRNA synthesis and degradation can be measured by Dynamic Transcriptome Analysis (DTA) in yeast (Miller et al., 2011). Newly synthesized RNA is labeled with 4-thiouridine (4sU), which is taken up by cells that express a nucleoside transporter. After 6 minutes of labeling, total RNA is extracted and separated into newly synthesized (labeled) and pre-existing (unlabeled) fractions. Total, labeled, and unlabeled fractions are analyzed with microarrays and the data are fitted with a dynamic kinetic model to extract synthesis and decay rates. Whereas DTA accurately measures the relative rates for different RNAs within a single sample, it cannot compare rates from different samples, since the samples differ by an unknown global factor (Miller et al., 2011). In standard transcriptomics, comparison between samples with different mRNA levels may be achieved by counting cells and spiking RNA standards into the samples (Holstege et al., 1998; van de Peppel et al., 2003; Wang et al., 2002). However, such normalization does not take into account differences in cell lysis and RNA extraction efficiency, which can vary so strongly that no conclusions are possible.

To enable normalization between DTA measurements of different samples, we extended DTA to comparative DTA (cDTA). In cDTA, a defined number of labeled fission yeast *S. pombe* (*Sp*) cells is added to the budding yeast *S. cerevisiae* (*Sc*) sample before cell lysis and RNA preparation, and is used as an internal standard. Thereby, cDTA allows the absolute quantification and accurate comparison of mRNA synthesis and decay rates between samples. cDTA is a novel method that monitors absolute changes in

eukaryotic mRNA metabolism upon genetic perturbation. We applied cDTA to *S. cerevisiae* cells that are impaired in either mRNA synthesis or degradation. This revealed compensatory changes in degradation and synthesis, respectively, which indicates that a eukaryote can buffer mRNA levels to render gene expression robust. After our work was completed, an independent study appeared that postulates a similar compensation on an evolutionary scale (Dori-Bachash et al., 2011).

Along with our findings, evidences show that mRNA levels in eukaryotic cells are maintained close to normal values, i.e. buffered, when SRs or DRs are perturbed by mutations that impair nuclear mRNA synthesis or cytoplasmic mRNA degradation, respectively (Bregman et al., 2011; Pérez-Ortín et al., 2012; Sun et al., 2012; Trcek et al., 2011). In the yeast *S. cerevisiae*, a mutation in the transcribing enzyme RNA polymerase II (Pol II) leads to a global decrease of SRs that is compensated by a decrease in DRs, resulting in a buffering of mRNA levels. In another mutant strain, a decrease in DRs caused by the deletion of the gene encoding the mRNA degradation enzyme Ccr4 is compensated by a decrease in SRs (Sun et al., 2012). The mechanisms underlying the buffering of mRNA levels remain unknown. Kinetic modeling indicated that the buffering may depend on a putative factor that acts positively on mRNA degradation and negatively on mRNA synthesis (Sun et al., 2012). To search for such a factor, we further analyzed 46 mutant yeast strains that lacked mRNA degradation factor genes with the use of cDTA (Sun et al., 2012). Our factor search was based on the rationale that deletion of a degradation factor would result in changes in both DRs and SRs, and mRNA level buffering, unless the factor is required for buffering of mRNA levels.

In our analysis we included factors involved in deadenylation (Ccr4p, Pop2p, Caf40p, Not3p, Pan2p, and Pan3p) and exonucleases required for bulk mRNA degradation (Xrn1p and the exosome subunits Rrp6p, and Rrp47p). We also included factors that target decapping substrates (Lsm1p, Lsm6p, and Lsm7p), decapping enhancers (Edc1p, Edc2p, Edc3p, Dhh1p, Pat1p, and Scd6p), scavenger decapping factors (Dcs1p and Dcs2p), and exosome-associated factors (Ski2p, Ski3p, Ski8p, and Ski7p). We further included factors involved in transcription termination, nuclear RNA surveillance, and splicing (Rtt103p, Rai1p, Air1p, Air2p, Esc1p, and Bud13p), factors that bind RNA elements and regulate mRNA degradation (Puf1p, Puf2p, Puf3p, Puf4p, Puf5p, Puf6p, Pub1p, Tpa1p, and Cth1p), factors involved in mRNA export (Thp2p and

Tex1p), factors implicated in translation surveillance (Dom34p, Hbs1p, Upf2p, and Upf3p), and an endonuclease (Swt1p).

The resulting cDTA datasets for 46 yeast deletion strains each contain SRs and DRs for about 4300 mRNAs. All mutant strains showed a buffering of mRNA levels, with one marked exception, the strain lacking the exonuclease Xrn1p. We therefore analyzed mutants of Xrn1p to elucidate its role in the buffering of mRNA levels in more detail. Correlation analysis of DR changes in mutant strains recapitulated known interactions between degradation factors and unraveled new ones. Our results provide a rich resource for studying mRNA metabolism, and identify Xrn1p as a key factor required for the buffering of mRNA levels in a eukaryotic cell.

Chapter 2

Materials

2.1 List of Strains

Table 2.1: Strains used in the studies

ID	Name	Genotype	Source
1	BY4743	MATa/ α <i>his3</i> Δ 1/ <i>his3</i> Δ 1; <i>leu2</i> Δ 0/ <i>leu2</i> Δ 0; <i>LYS2/lys2</i> Δ 0; <i>MET15/met15</i> Δ 0; <i>ura3</i> Δ 0/ <i>ura3</i> Δ 0;	OpenBiosystems
2	BY4741	MATa <i>his3</i> Δ 1; <i>leu2</i> Δ 0; <i>met15</i> Δ 0; <i>ura3</i> Δ 0	OpenBiosystems
3	<i>air1</i> Δ	BY4741 MATa <i>his3</i> Δ 1; <i>leu2</i> Δ 0; <i>met15</i> Δ 0; <i>ura3</i> Δ 0; <i>yil079c::kanMX4</i>	OpenBiosystems
4	<i>air2</i> Δ	BY4741 MATa <i>his3</i> Δ 1; <i>leu2</i> Δ 0; <i>met15</i> Δ 0; <i>ura3</i> Δ 0; <i>ydl175c::kanMX4</i>	OpenBiosystems
5	<i>bud13</i> Δ	BY4741 MATa <i>his3</i> Δ 1; <i>leu2</i> Δ 0; <i>met15</i> Δ 0; <i>ura3</i> Δ 0; <i>ygl174w::kanMX4</i>	OpenBiosystems
6	<i>caf40</i> Δ	BY4741 MATa <i>his3</i> Δ 1; <i>leu2</i> Δ 0; <i>met15</i> Δ 0; <i>ura3</i> Δ 0; <i>ynl288w::kanMX4</i>	OpenBiosystems
7	<i>ccr4</i> Δ	BY4741 MATa <i>his3</i> Δ 1; <i>leu2</i> Δ 0; <i>met15</i> Δ 0; <i>ura3</i> Δ 0; <i>yal021c::kanMX4</i>	Generated in the lab
8	<i>cth1</i> Δ	BY4741 MATa <i>his3</i> Δ 1; <i>leu2</i> Δ 0; <i>met15</i> Δ 0; <i>ura3</i> Δ 0; <i>ydr151c::kanMX4</i>	OpenBiosystems
9	<i>dcs1</i> Δ	BY4741 MATa <i>his3</i> Δ 1; <i>leu2</i> Δ 0; <i>met15</i> Δ 0; <i>ura3</i> Δ 0; <i>ylr270w::kanMX4</i>	OpenBiosystems

Continued on next page

2. Materials

Table 2.1 Strains used in the studies

ID	Name	Genotype	Source
10	<i>dcs2</i> Δ	BY4741 MATa <i>his3</i> Δ 1; <i>leu2</i> Δ 0; <i>met15</i> Δ 0; <i>ura3</i> Δ 0; <i>yor173w</i> ::kanMX4	OpenBiosystems
11	<i>dhh1</i> Δ	BY4741 MATa <i>his3</i> Δ 1; <i>leu2</i> Δ 0; <i>met15</i> Δ 0; <i>ura3</i> Δ 0; <i>ydl160c</i> ::kanMX4	Generated in the lab
12	<i>dom34</i> Δ	BY4741 MATa <i>his3</i> Δ 1; <i>leu2</i> Δ 0; <i>met15</i> Δ 0; <i>ura3</i> Δ 0; <i>ynl001w</i> ::kanMX4	OpenBiosystems
13	<i>edc1</i> Δ	BY4741 MATa <i>his3</i> Δ 1; <i>leu2</i> Δ 0; <i>met15</i> Δ 0; <i>ura3</i> Δ 0; <i>ygl222c</i> ::kanMX4	OpenBiosystems
14	<i>edc2</i> Δ	BY4741 MATa <i>his3</i> Δ 1; <i>leu2</i> Δ 0; <i>met15</i> Δ 0; <i>ura3</i> Δ 0; <i>yer035w</i> ::kanMX4	Generated in the lab
15	<i>edc3</i> Δ	BY4741 MATa <i>his3</i> Δ 1; <i>leu2</i> Δ 0; <i>met15</i> Δ 0; <i>ura3</i> Δ 0; <i>yel015w</i> ::kanMX4	OpenBiosystems
16	<i>esc1</i> Δ	BY4741 MATa <i>his3</i> Δ 1; <i>leu2</i> Δ 0; <i>met15</i> Δ 0; <i>ura3</i> Δ 0; <i>ymer219w</i> ::kanMX4	OpenBiosystems
17	<i>hbs1</i> Δ	BY4741 MATa <i>his3</i> Δ 1; <i>leu2</i> Δ 0; <i>met15</i> Δ 0; <i>ura3</i> Δ 0; <i>ykr084c</i> ::kanMX4	OpenBiosystems
18	<i>lsm1</i> Δ	BY4741 MATa <i>his3</i> Δ 1; <i>leu2</i> Δ 0; <i>met15</i> Δ 0; <i>ura3</i> Δ 0; <i>yjl124c</i> ::kanMX4	OpenBiosystems
19	<i>lsm6</i> Δ	BY4741 MATa <i>his3</i> Δ 1; <i>leu2</i> Δ 0; <i>met15</i> Δ 0; <i>ura3</i> Δ 0; <i>ydr378c</i> ::kanMX4	OpenBiosystems
20	<i>lsm7</i> Δ	BY4741 MATa <i>his3</i> Δ 1; <i>leu2</i> Δ 0; <i>met15</i> Δ 0; <i>ura3</i> Δ 0; <i>ynl147w</i> ::kanMX4	OpenBiosystems
21	<i>not3</i> Δ	BY4741 MATa <i>his3</i> Δ 1; <i>leu2</i> Δ 0; <i>met15</i> Δ 0; <i>ura3</i> Δ 0; <i>yil038c</i> ::kanMX4	Generated in the lab
22	<i>not4</i> Δ	BY4741 MATa <i>his3</i> Δ 1; <i>leu2</i> Δ 0; <i>met15</i> Δ 0; <i>ura3</i> Δ 0; <i>yer068w</i> ::kanMX4	Generated in the lab
23	<i>pan2</i> Δ	BY4741 MATa <i>his3</i> Δ 1; <i>leu2</i> Δ 0; <i>met15</i> Δ 0; <i>ura3</i> Δ 0; <i>ygl094c</i> ::kanMX4	OpenBiosystems
24	<i>pan3</i> Δ	BY4741 MATa <i>his3</i> Δ 1; <i>leu2</i> Δ 0; <i>met15</i> Δ 0; <i>ura3</i> Δ 0; <i>ykl025c</i> ::kanMX4	OpenBiosystems
25	<i>pat1</i> Δ	BY4741 MATa <i>his3</i> Δ 1; <i>leu2</i> Δ 0; <i>met15</i> Δ 0; <i>ura3</i> Δ 0; <i>ycr077c</i> ::kanMX4	Generated in the lab
26	<i>pop2</i> Δ	BY4741 MATa <i>his3</i> Δ 1; <i>leu2</i> Δ 0; <i>met15</i> Δ 0; <i>ura3</i> Δ 0; <i>ynr052c</i> ::kanMX4	Generated in the lab

Continued on next page

2. Materials

Table 2.1 Strains used in the studies

ID	Name	Genotype	Source
27	<i>puf1</i> Δ	BY4741 MATa <i>his3</i> Δ 1; <i>leu2</i> Δ 0; <i>met15</i> Δ 0; <i>ura3</i> Δ 0; <i>ynl016w</i> ::kanMX4	OpenBiosystems
28	<i>puf1</i> Δ	BY4741 MATa <i>his3</i> Δ 1; <i>leu2</i> Δ 0; <i>met15</i> Δ 0; <i>ura3</i> Δ 0; <i>yjr091c</i> ::kanMX4	OpenBiosystems
29	<i>puf2</i> Δ	BY4741 MATa <i>his3</i> Δ 1; <i>leu2</i> Δ 0; <i>met15</i> Δ 0; <i>ura3</i> Δ 0; <i>ypr042c</i> ::kanMX4	OpenBiosystems
30	<i>puf3</i> Δ	BY4741 MATa <i>his3</i> Δ 1; <i>leu2</i> Δ 0; <i>met15</i> Δ 0; <i>ura3</i> Δ 0; <i>yll013c</i> ::kanMX4	OpenBiosystems
31	<i>puf4</i> Δ	BY4741 MATa <i>his3</i> Δ 1; <i>leu2</i> Δ 0; <i>met15</i> Δ 0; <i>ura3</i> Δ 0; <i>ygl014w</i> ::kanMX4	OpenBiosystems
32	<i>puf5</i> Δ	BY4741 MATa <i>his3</i> Δ 1; <i>leu2</i> Δ 0; <i>met15</i> Δ 0; <i>ura3</i> Δ 0; <i>ygl178w</i> ::kanMX4	OpenBiosystems
33	<i>puf6</i> Δ	BY4741 MATa <i>his3</i> Δ 1; <i>leu2</i> Δ 0; <i>met15</i> Δ 0; <i>ura3</i> Δ 0; <i>ydr496c</i> ::kanMX4	OpenBiosystems
34	<i>rai1</i> Δ	BY4741 MATa <i>his3</i> Δ 1; <i>leu2</i> Δ 0; <i>met15</i> Δ 0; <i>ura3</i> Δ 0; <i>ygl246c</i> ::kanMX4	OpenBiosystems
35	<i>rrp47</i> Δ	BY4741 MATa <i>his3</i> Δ 1; <i>leu2</i> Δ 0; <i>met15</i> Δ 0; <i>ura3</i> Δ 0; <i>yhr081w</i> ::kanMX4	Generated in the lab
36	<i>rrp6</i> Δ	BY4741 MATa <i>his3</i> Δ 1; <i>leu2</i> Δ 0; <i>met15</i> Δ 0; <i>ura3</i> Δ 0; <i>yor001w</i> ::kanMX4	Generated in the lab
37	<i>rtt103</i> Δ	BY4741 MATa <i>his3</i> Δ 1; <i>leu2</i> Δ 0; <i>met15</i> Δ 0; <i>ura3</i> Δ 0; <i>ydr289c</i> ::kanMX4	OpenBiosystems
38	<i>ski2</i> Δ	BY4741 MATa <i>his3</i> Δ 1; <i>leu2</i> Δ 0; <i>met15</i> Δ 0; <i>ura3</i> Δ 0; <i>ylr398c</i> ::kanMX4	Generated in the lab
39	<i>ski3</i> Δ	BY4741 MATa <i>his3</i> Δ 1; <i>leu2</i> Δ 0; <i>met15</i> Δ 0; <i>ura3</i> Δ 0; <i>ypr189w</i> ::kanMX4	OpenBiosystems
40	<i>ski7</i> Δ	BY4741 MATa <i>his3</i> Δ 1; <i>leu2</i> Δ 0; <i>met15</i> Δ 0; <i>ura3</i> Δ 0; <i>yor076c</i> ::kanMX4	OpenBiosystems
41	<i>ski8</i> Δ	BY4741 MATa <i>his3</i> Δ 1; <i>leu2</i> Δ 0; <i>met15</i> Δ 0; <i>ura3</i> Δ 0; <i>ygl213c</i> ::kanMX4	OpenBiosystems
42	<i>swt1</i> Δ	BY4741 MATa <i>his3</i> Δ 1; <i>leu2</i> Δ 0; <i>met15</i> Δ 0; <i>ura3</i> Δ 0; <i>yor166c</i> ::kanMX4	OpenBiosystems
43	<i>tex1</i> Δ	BY4741 MATa <i>his3</i> Δ 1; <i>leu2</i> Δ 0; <i>met15</i> Δ 0; <i>ura3</i> Δ 0; <i>ynl253w</i> ::kanMX4	OpenBiosystems

Continued on next page

Table 2.1 Strains used in the studies

ID	Name	Genotype	Source
44	<i>thp2</i> Δ	BY4741 MATa <i>his3</i> Δ 1; <i>leu2</i> Δ 0; <i>met15</i> Δ 0; <i>ura3</i> Δ 0; <i>yhr167w</i> ::kanMX4	OpenBiosystems
45	<i>tpa1</i> Δ	BY4741 MATa <i>his3</i> Δ 1; <i>leu2</i> Δ 0; <i>met15</i> Δ 0; <i>ura3</i> Δ 0; <i>yer049w</i> ::kanMX4	OpenBiosystems
46	<i>trf4</i> Δ	BY4741 MATa <i>his3</i> Δ 1; <i>leu2</i> Δ 0; <i>met15</i> Δ 0; <i>ura3</i> Δ 0; <i>yol115w</i> ::kanMX4	OpenBiosystems
47	<i>upf2</i> Δ	BY4741 MATa <i>his3</i> Δ 1; <i>leu2</i> Δ 0; <i>met15</i> Δ 0; <i>ura3</i> Δ 0; <i>yhr077c</i> ::kanMX4	OpenBiosystems
48	<i>upf3</i> Δ	BY4741 MATa <i>his3</i> Δ 1; <i>leu2</i> Δ 0; <i>met15</i> Δ 0; <i>ura3</i> Δ 0; <i>ygr072w</i> ::kanMX4	OpenBiosystems
49	<i>xrn1</i> Δ	BY4741 MATa <i>his3</i> Δ 1; <i>leu2</i> Δ 0; <i>met15</i> Δ 0; <i>ura3</i> Δ 0; <i>ygl173c</i> ::kanMX4	Generated in the lab
50	Y40343	W303 MAT α <i>tor1-1 fpr1::NAT RPL13A-2</i> \times <i>FKBP12::TRP1</i>	Euroscarf
51	XRN1AA	W303 MAT α <i>tor1-1 fpr1::NAT RPL13A-2</i> \times <i>FKBP12::TRP1 YGL173C::YGL173C-FRB-GFP-KanMX4</i>	Generated in the lab
52	<i>xrn1pm</i>	BY4741 MATa <i>his3</i> Δ 1; <i>leu2</i> Δ 0; <i>met15</i> Δ 0; <i>ura3</i> Δ 0; <i>ygl173c</i> ::pFA6a- <i>ygl173c-D206A,D208A-3HA-His3MX</i>	Generated in the lab
53	XRN1WT	BY4741 MATa <i>his3</i> Δ 1; <i>leu2</i> Δ 0; <i>met15</i> Δ 0; <i>ura3</i> Δ 0; <i>YGL173C</i> ::pFA6a- <i>YGL173C-3HA-His3MX</i>	Generated in the lab

2.2 List of Plasmids

Table 2.2: Plasmids

ID	Name	Insert	Selection Marker	Backbone	Source
23	pYMS14	XRN1orf	His3MX	pFA6A	This study
24	pYMS15	POP2orf	His3MX	pFA6A	This study
25	pYMS16	FRB-GFP	His3MX	pFA6a	Euroscarf
26	pYMS17	FRB-GFP	KanMX	pFA6a	Euroscarf
27	pYMS18	FRB	His3MX	pFA6a	Euroscarf
28	pYMS19	FRB	KanMX	pFA6a	Euroscarf
32	pYMS23	CCR4orf	His3MX	pFA6A	This study
33	YSC3869	Xrn1orf	Ura3	BG1805	ThermoScientific
34	YSC3867	Nrg1orf	Ura3	BG1805	ThermoScientific

2.3 List of important primers

Table 2.3: qPCR primers

Names	ID	Sequence	Length
spGpd1_fwr1	193	AGAGCTCTTAGGTGGTCAACTT- CT	24
spGpd1_rev1	194	GGAATTCATGAACATCCTTGG	21
spGdi1_fwr	197	TCAGTTATATGCTCTGTTTCGT- CCT	25
spGdi1_rev	198	CACCAGTCCCTATCTCGACCT	21

Table 2.4: Some primers for Knock-out and mutagenesis

Name	ID	Sequence	Length
Ccr4KOU _{p1}	250	CAGCAAGGGA ^{ACTCCGACTGACGTT-} ATCCCTGCAA ^{ACTACCGCTACGTAC-} GCTGCAGGTCGAC	63
Ccr4KOD _{n1}	251	GTAGTGTACAGAGAGGAGGGAGGG- AGTGGGATGAAAGTGTGCGGTATCG- ATGAATTCGAGCTCG	64
Ccr4KOU _{p2}	252	GAAGGTTCTCAAGCACAAGGGCACA- GCATAAGGGACACCAGCAAGGGAAC- TCCGACTGAC	60
Ccr4KOD _{n2}	253	AAGTGCGGTGAGATTGGGATCGTTT- CAATTTTATAATGAGGTAGTGTACA- GAGAGGAGGG	60
Ccr4C1	430	GAAGAAGAAGTCGACATGAACGACC- CTTCTTTACTAGGC	39
Ccr4C2	345	GAAGAAGAATTAATTAATACTTTCT- TACTGCCTGTGTTTGTC	42
Ccr4M1	321	GCTCATTTGTGGTGC GTTCAATTCA- TAC	28
Ccr4M2	322	GTATGAATTGAACGCACCACAAATG- AGC	28
Ccr4R1	323	AACTCCGACTGACGTTATCCCTGCA- AACTACCGCTAATGAACGACCCTTC- TTTACTAGGC	60
Ccr4R3	324	CTCAAGCACAAGGGCACAGCATAAG- GGACACCAGCAAGGGA ^{ACTCCGACT-} GACGTTATCC	60
Pop2KOU _{p1}	325	CAACTCAATTTTATAACATTTATAAA- GGGTCAAAAAGGATTCGTACGCTGC- AGGTCGAC	58

Continued on next page

Table 2.4 Some primers for Knock-out and mutagenesis

Name	ID	Sequence	Length
Pop2KODn1	326	AAACTTTTTTTTTTTTAAAATTGTGTA- TACATATAGTACATAAATGAATCGA- TGAATTCGAGCTCG	64
Pop2KOUp2	327	GTTTTTCATACTGGAAATACTTCGA- ACGATTAGAAACAGGCAACTCAATT- TTATACATTT	60
Pop2KODn2	328	TGTATTACTACATGTCCAATCATAA- GCTGATGTTGCTTTTAAACTTTTTT- TTTTAAAATTG	61
Pop2C1	329	GAAGAAGAAAAGCTTATGCAATCTA- TGAATGTACAACCG	39
Pop2C2	440	GAAGAAGAAGTCGACGTTGGTCCCC- ATCAATACCGTA	37
Pop2M1	331	CAATCGCTACTGCGTTTGTGGG	22
Pop2M2	332	CCCACAAACGCAGTAGCGATTG	22
Pop2R1	333	CAACTCAATTTTATACATTTATAAA- GGGTCAAAAAGGATTATGCAATCTA- TGAATGTACAACCG	64
Pop2R3	334	TCATACTGGAAATACTTCGAACGAT- TAGAAACAGGCAACTCAATTTTATA- CATTTATAAAG	61
Kem1KOUp1	335	CACTTGTAACAACAGCAGCAACAAA- TATATATCAGTACGGTCGCTGCAGG- TCGAC	55
Kem1KODn1	336	TAAAGTAACCTCGAATATACTTCGT- TTTTAGTCGTATGTTATCGATGAAT- TCGAGCTCG	59
Kem1KOUp2	337	CCTAGGACGATTTCGTGTACTATAAG- GAGAAAAAAAATCAACACTTGTAAC- AACAGCAGCAAC	62

Continued on next page

Table 2.4 Some primers for Knock-out and mutagenesis

Name	ID	Sequence	Length
Kem1KODn2	338	ATACAAATACCCCTCTTTATATAGG- TCTCAGATATACTATTAAAGTAACC- TCGAATATAC	60
Kem1C1	339	GAAGAAGAAGTCGACATGGGTATTC- CAAAATTTTTTCAGG	39
Kem1C2	346	GAAGAAGAATTAATTAAAGTAGATT- CGTCTTTTTTATTATCACGG	45
Kem1M1	341	CGGTCTTGCCGCAGCTTTGATTATGC	26
Kem1M2	342	GCATAATCAAAGCTGCGGCAAGACC- G	26
Kem1R1	343	ACTTGTAACAACAGCAGCAACAAAT- ATATATCAGTACGGTATGGGTATTC- CAAAATTTTTTCAGG	64
Kem1R3	344	TCCTAGGACGATTCGTGTACTATAA- GGAGAAAAAAAAATCAACACTTGTA- CAACAGCAGC	60
Kem1M1new	460	CATTGTATTTACGGTCTTGCCGCAG- CTTTGATTATGCTGGGTTTG	45
Kem1M2new	461	CAAACCCAGCATAATCAAAGCTGCG- GCAAGACCGTAAATACAATG	45

2.4 Growth media

Table 2.5: Growth media

Medium	Description	Species
YPD	1% (w/v) yeast extract; 2% (w/v) peptone; 2% (w/v) glucose (+2% (w/v) agar for plate)	<i>Sc</i>

Continued on next page

Table 2.5 Growth media

Medium	Description	Species
YES	0.5% (w/v) yeast extract; 3% (w/v) glucose; (+2% (w/v) agar for plate)	<i>Sp</i>
Synthetic complete (SC)	0.67% (w/v) yeast nitrogen base; 0.06% (w/v) complete synthetic mix of amino acids OR drop out as required; 2% (w/v) glucose; (+3% (w/v) agar for plate)	<i>Sc</i>
Over expression medium	0.67% (w/v) yeast nitrogen base; 0.06% (w/v) -URA drop out medium; 2% (w/v) galactose; +3% (w/v) agar for plate	<i>Sc</i>
LB	10g Bacto™ Tryptone; 5g Bacto™ Yeast Extract; 10g NaCl; add ddH ₂ O to 1L	<i>E. coli</i>
SOB	20g Bacto™ Tryptone; 5g Bacto™ Yeast Extract; 8.55mM (0.5g or 1.71ml 5M) NaCl; 2.5mM (2.5ml 1M) KCl; add ddH ₂ O to 1L (adjust pH to 7 with NaOH, add 10mM (5mL 2M) MgCl ₂ before use)	<i>E. coli</i>
SOC	add 20mM (20ml 1.1M 20%) glucose to SOB before use	<i>E. coli</i>

2.5 Buffers and Solutions

Table 2.6: Solutions

Name	Composition	Application
1×PBS	2 mM KH ₂ PO ₄ ; 4 mM Na ₂ HPO ₄ ; 140 mM NaCl; 3 mM KCl; pH 7.4 (25°C);	
6× Loading dye (Fermentas)	1.5 g/L Bromphenol blue; 1.5 g/L Xylene cyanol; 50% (v/v) Glycerol;	

Continued on next page

Table 2.6 Solutions

Name	Composition	Application
SDS gel staining solution	50% (v/v) Ethanol; 7% (v/v) Acetic acid; 0.125% (w/v); Coomassie Brilliant Blue R-250;	
SDS gel destaining solution	5% (v/v) Ethanol; 7.5% (v/v) Acetic acid;	
TELit	10 mM Tris-HCl, pH 8.0 at 25°C; 155 mM LiOAc; 1mM EDTA, pH 8.0;	
LitSorb	10 mM Tris-HCl, pH 8.0 at 25°C; 155 mM LiOAc; 1mM EDTA, pH 8.0; 18.2% (w/v) D-Sorbitol	
LitPEG	10 mM Tris-HCl, pH 8.0 at 25°C; 155 mM LiOAc; 1mM EDTA, pH 8.0; 40% (w/v) PEG 3350;	
Lyticase Buffer	1 M Sorbitol; 100 mM EDTA, pH 8.0; 14.3 mM -Mercaptoethanol;	
TE	50/100 Buffer 50 mM Tris-HCl, pH 7.5 at °C; 100 mM EDTA, pH8.0;	
WB transfer Buffer	25 mM Tris; 192 mM Glycine; 20% (v/v) Ethanol;	Western Blotting
WB blocking Buffer	2% (w/v) milk powder in 1× PBS;	Western Blotting
1× TBS	20 mM TrisHCl, pH 7.5 at 4°C; 150 mM NaCl;	
FA lysis Buffer	50 mM HEPESKOH, pH 7.5 at 4°C; 150 mM NaCl; 1 mM EDTA; 1% (v/v) Triton X100; 0.1% (v/v) Na deoxycholate; 0.1% (v/v) SDS; PI; PhI	
Protease inhibitor (PI)	1 mM Leupetin, 2 mM Pepstatin A, 100 mM Phenylmethylsulfonyl fluoride, 280 mM Benzamidine;	

Continued on next page

Table 2.6 Solutions

Name	Composition	Application
Phosphatase inhibitor (PhI)	1 mM NaN ₃ , 1 mM NaF, 0.4 mM Na ₃ VO ₄	
FA lysis buffer	FA lysis buffer with 500 mM NaCl instead of 150 mM NaCl	
ChIP wash Buffer	10 mM TrisHCl, pH 8.0 at 4°C; 0.25 M LiCl; 1 mM EDTA; 0.5% (v/v); NP40; 0.5% (v/v) Na deoxycholate	
TE Buffer	10 mM TrisHCl, pH 7.4 at 4°C; 1 mM EDTA;	
ChIP elution Buffer	50 mM TrisHCl, pH 7.5 at 25°C; 10 mM EDTA; 1% (v/v) SDS;	
RNase storage Buffer	10 mM HEPES, pH 7.5 at 25°C; 20 mM NaCl; 0.1% (v/v) Triton X-100; 1mM EDTA; 50% (v/v) Glycerol;	
Rnase free 10× biotinylation buffer	100 mM Tris pH 7.4; 10 mM EDTA	
Washing Buffer	100mM Tris pH7.5; 10mM EDTA; 1M NaCl; 0.1% Tween20	
Elution Buffer (DTT)	100 mM Dithiothreitol in H ₂ O	
Biotin-HPDP (Thermo Scientific)	1mg/ml in dimethylformamide(DMF)	

Chapter 3

Methods

3.1 Common Methods

3.1.1 Molecular cloning using *Escherichia coli*

Preparation of *E. coli* competent cell for electroporation This protocol is modified from Current protocol of molecular biology Unit 1.8 (Seidman et al., 2001). A single colony of *E. coli* cell was inoculated into 5mL SOB medium and let grown overnight at 37°C. On the next morning, 2.5mL or 5mL overnight culture was inoculated into 500mL or 1L SOB medium. When the culture reached 0.6OD₆₀₀, the flasks were chilled on ice. The chilled the culture was transferred into 1L centrifuge bottle. The cells were harvested by applying centrifugation at 4°C, 4000rpm in SLC-6000 rotor for 10min. The supernatant was discarded and the pellet was resuspended in 5 mL ice-cold water. Additional 500 mL ice-cold water was added and mixed well. The cells could be incubated at this stage for better efficiency. This step was repeated once. The cell was then resuspended in 40 mL ice-cold 10% glycerol and transferred to a 50mL falcon tube. The cell was again centrifuged resuspended in equal volume ice-cold 10% glycerol. The cells were placed in 50µL aliquots on dry ice and stored at -80°C.

Transformation An aliquot competent cell was thawed on ice. Proper amount DNA in maximum 5µL solution was pipetted onto competent cell. The samples were mixed gently, chilled 5 min on ice and transferred into 0.2cm electroporation cuvettes. Electroporation was applied in BioRad *E. coli* Pulser at 2.5kV. Immediately after pulse, 1mL ice cold SOC medium was added in the cuvette to resuspend the cell. The suspen-

sion was then transferred to a 1.5mL tube and incubated for 45-60min at 37°C 600rpm. Subsequently, the cell were spun down for 1min at 5000rpm in a table centrifuge, 850µL supernatant was taken using pipette. And the pellet was resuspended with the rest of medium. The suspension was then plated onto LB plate containing proper antibiotics and incubated overnight at 37°C.

Cloning with ligase PCR products or plasmids containing the inserts as well as the receiving plasmids are digested using restriction enzymes. Sequential or double digest was applied. After purification of the digest product use agarose gel, ligation using T4 ligase was applied at 16°C for 1 hour. 5µL ligation reaction was transformed to *E. coli* competent cell using the protocol above.

Plasmid preparation For plasmid miniprep, an *E. coli* overnight culture is grown in LB liquid medium and added proper antibiotica at 37°C 160rpm. On the second day, the bacteria is harvested by centrifugation at 4000rpm (Rotanta 46R) 4°C for 10min. The supernatant is then discarded and the plasmid is extracted using QIAprep Spin Miniprep Kit. The plasmid stored at -20°C for long term.

3.1.2 Cryo-stocks of yeast strains

Typicaly a single colony of desired strain was streaked from a solid culture on to a YPD plate(**Media**) and incubated for 2 days at 30°C. The cells were harvested from the plate and transferred to 1 mL sterile 50% v/v glycerol, vortexed and flash-frozen in liquid nitrogen. Cryo-stocks were stored at -80°C.

3.1.3 Generation of knock-out strains

The knock-out (KO) strains were generated by homologous recombination. A KanMX cassette was amplified by primer-extension PCR, resulting in a product contains KanMX cassette flanking with homologue sequence from 3'-UTR and 5'-UTR of the gene. This PCR product was transformed into *S. cerevisiae* competent cells. The complete open reading frame (ORF) was substituted by KanMX. The resulted KO strains were verified by colony PCR using KanMX specific and ORF specific primers. Yeast knock out strains were purchased from the YKO library (Thermo Scientific) or generated by substituting the target gene for a KanMX cassette using homologous recombination in the

same genetic background (Longtine et al., 1998). All knock out strains were validated by selective growth on G418 plates and PCR. Three primers were used to confirm the integration: forward primer A, which specifically binds to the region upstream of the ORF; reverse primer B, which binds to the ORF sequence; and reverse primer KanB, which binds to the sequence of the KanMX cassette. Correct knock-out strains gave rise to a PCR product with primers A and KanB, and a negative result with primers A and B. The length of the PCR products was subsequently compared to the theoretical length. The validated strains were stored in 50% glycerol at -80°C.

3.1.4 Colony PCR

Yeast solid culture from single colony was picked and solved in 100µL 20µM NaOH with approximately 50µL glass beads (0.5mm). The resulted mixture was incubated at 95°C exactly for 5min with vigorously shaking. After centrifugation for 15s at top speed, 5µL of the supernatant was used for PCR.

3.1.5 Generation of point mutants

The *S. cerevisiae* strains with point mutants were generated by homologous recombination. The target gene is first amplified by PCR on a genomic DNA template. This PCR product was then cloned into a yeast plamid using restriction enzyme and T4 ligase (**Methods**). Mutation was brought in via Quick change. Mutated region along with KanMX cassette was amplified by primer-extension PCR, resulting in a product contains the gene and KanMX cassette flanking with homologue sequence from 3'-UTR and 5'-UTR of the gene. This PCR product was transformed into *S. cerevisiae* competent cells contains the knockout of the target gene. The complete open reading frame (ORF) was substituted by mutated gene with KanMX. The resulted mutant strains were verified by colony PCR and sequencing.

3.1.6 Molecular cloning of tagged protein

The *S. cerevisiae* strains containing epitope tag were also generated by homologous recombination. A epitope sequence with KanMX cassette was amplified by primer-extension PCR from plamid, resulting in a product contains the epitope and KanMX cassette flanking with homologue sequence from 5'-end and 5'-UTR of the gene. The PCR primer is so designed, in order to delete the stop codon. This PCR product was

transformed into *S. cerevisiae* competent cells. The PCR product was inserted in frame directly after the last codon. The resulted mutant strains were verified by colony PCR and sequencing.

3.2 comparative Dynamic Transcriptomic Analysis (cDTA)

3.2.1 Metabolic labeling of the cells

Because of instability of some of the genetical engineered strains, the cells were maintained as cryo-stocks (**Common Methods**), and streaked out on YPD plates before experiments. Generally, the yeast cells *S. cerevisiae* or *S. pombe* were inoculated into 20mL YPD liquid medium from a single colony on solid medium. The preculture was then grown overnight. On the early next day, the OD₆₀₀ of the overnight culture was measured and proper volume of the preculture was then inoculated to 50 mL YPD liquid medium and grown to desired OD₆₀₀. The cells were harvested by centrifugation at 2465×g at 30°C for 1 min. The supernatant was discarded and the cells were resuspended in RNAlater solution (Life technologies™). The suspension was then transformed to a 1.5mL eppendorf tube and flash-frozen in liquid nitrogen. The cell concentration was determined by Cellometer N10 (Nexus) before flash-freezing in liquid nitrogen. *S. pombe* cells were grown in YES liquid medium (**Media**) overnight, diluted to OD₆₀₀ = 0.1, and grown to OD₆₀₀ = 0.8. 4sU was solved in ddH₂O (50 mM) and added to a final concentration of 500 mM, and cells were labeled for 6 min. Cells were harvested by centrifugation at 2465×g for 3 min. Other steps were applied as above. A 4-liter-culture of *S. pombe* cells was labeled to generate a stock and eliminate errors by variations in the standard. Cells were counted as above.

3.2.2 Microarray procedure

0.75×10^8 *S. pombe* cells were mixed with 2.25×10^8 *S. cerevisiae* cells resulting in a 1:3 ratio. A total RNA was extracted by RiboPure™-Yeast Kit (Life technologies™). The cell lysis procedure was replaced by adding acid washed glass beads and using FastPrep-24. The cell lysis protocol is eight times 6.5m/s for 45 seconds. The cells were put on ice for 1 minutes between runs. Total RNA was stored in RNase free water at -20°C or -80°C for longer time. (Miller et al., 2011).

3.2.3 Brief about data analysis

Data was preprocessed arraywise using `expresso` (R/Bioconductor) with the RMA background correction method. We created our own probe annotation environment (`cdf`), which excludes probes in probesets that show cross-hybridization between *S. cerevisiae* and *S. pombe*. A total of 8708 annotated *S. cerevisiae* probes and 13,317 annotated *S. pombe* probes out of a total of 120,855 probes showed cross-hybridization when a conservative intensity cut-off of 4.5 (log intensity values after preprocessing) was used. Cross-hybridizing probes were excluded from further analysis. This included 16 whole probe sets (Figure 4.3). Note that the standard GC-RMA method is not suitable for our purposes since its bias model cannot handle bimodal intensity distributions, as caused by the simultaneous hybridization of *S. cerevisiae* and *S. pombe* transcripts with global differences in RNA abundance (Figure 4.4). Labeling bias estimation and correction was done as described in (Miller et al., 2011). Between-array normalization of arrays containing mixed *S. cerevisiae* and *S. pombe* total RNA was done by proportional rescaling, such that the median *S. pombe* gene expression level was 1 (Figure 4.5A). Accordingly, between-array normalization of arrays containing mixed *S. cerevisiae* and *S. pombe* labeled RNA was done by proportionally scaling the array to a median-labeled *S. pombe* gene expression level of c (Figure 4.5B). The constant c scales the median half-life of all experiments. We calibrated c in a way that the resulting median *S. cerevisiae* wild-type mRNA half-life equaled that observed previously (Miller et al., 2011). Now, all *S. cerevisiae* RNA levels, no matter whether total or labeled, no matter from which experiment, can be compared on an absolute level. Decay rates and synthesis rates were obtained as described (Miller et al., 2011). We assume that the labeled RNA fraction is subject to degradation from the very time it is synthesized. In contrast, (Rabani et al., 2011) (see Supplemental Methods therein) assume that the labeled RNA fraction is mostly nuclear and not degraded at all. We compared the synthesis rate estimates resulting from both alternatives. Given our labeling time, the differences of both approaches are negligible. The whole analysis workflow has been carried out using the open source R/Bioconductor package DTA (Schwalb et al., 2012).

3.3 Other biochemical methods

3.3.1 Flow cytometry analysis

FACS analysis 20mL YPD were inoculated with a saturated overnight culture and incubated at 30°C until OD₆₀₀ reached 0.8. Then a 1mL sample was taken and 2.5mL ethanol was added. Cells were then washed with 50 mM sodium citrate pH 7.0 and RNA was digested at 37°C overnight with 0.1mg/mL RNase A (Fermentas). Cells were washed with citrate buffer and subjected to protease K digestion at 50°C for two hours. After washing, cells were resuspended in 50 mM sodium citrate buffer containing 1µM Sytox Green (Invitrogen). To avoid cell clustering, we sonified cells four times for 30 sec in a Biorupter (DIAGENODE). The measurement was carried out on a BD FACS Calibur machine. The data were analyzed use the FCS Express software (De Novo™ Software).

3.3.2 *in vitro* transcription assay

Nuclear extracts of BY4741 and *xrn1*Δ were prepared from 3Lof yeast culture as described (Ranish et al., 1999; Seizl et al., 2011b). Endogenous Xrn1p and *xrn1*pm were purified from 4L C-terminally TAP-tagged strains using protein A coupled IgG-Dynabeads. Activator-dependent *in vitro* transcription assays were carried out using 200 ng of recombinant full-length Gcn4p (Seizl et al., 2011a). The transcript was detected by primer extension using the 5'-Cy5-labelled oligonucleotide 5'-TTCACC-AGTGAGACGGGCAAC-3' (Seizl et al., 2011b). The resulting gel was scanned on a typhoon scanner FLA9400 and the data were analyzed with ImageQuant Software (GE Healthcare).

3.3.3 RT-qPCR

The yeast cells were grown to OD₆₀₀ = 0.8, harvested and flash-frozen in liquid nitrogen. Total RNA was extracted using RT-qPCR was carried out as described (Miller et al., 2011). 500 ng RNA was used to reverse transcribe cDNA using the iScript cDNA Synthesis Kit (BioRad). Primers were designed with the ProbeFinder online tool (<http://qpcr.probefinder.com/organism.jsp>, Roche Applied Science). The primer-pair efficiency was tested individually and ranged between 97 and 100%. PCR reactions contained 1 µL DNA template, 2 µL of 10 µM primer pairs, and 12.5 µL

SsoFast™ EvaGreen Supermix (BioRad). qPCR was performed on a Bio-Rad CFX96™ Real-Time System (Bio-Rad) using a 30 sec denaturing step at 95°C, followed by 40 cycles of 1 s at 95°C, 4 s at 63°C. Data analysis was performed with the software Bio-Rad CFX Manager™ 1.6.

Chapter 4

Results

4.1 cDTA analysis reveals a mutual feedback loop between mRNA transcription and degradation

4.1.1 Establishment of cDTA based on DTA

In order to measure global changes in mRNA synthesis and decay rates between different strains of budding yeast (*S. cerevisiae*), it is crucial to include an internal standard (**Introduction**). Here we included the distantly related fission yeast (*S. pombe*) in our DTA protocol as an internal standard (Figure 4.1). We counted *S. cerevisiae* sample cells and *S. pombe* control cells and mixed them in a defined ratio (**Methods**). The resulting cell mixture was lysed, total mRNA extracted, labeled RNA purified, and microarrays were hybridized as described (Miller et al., 2011). The RNA mixture was quantified on a microarray that contains probes for both *S. cerevisiae* and *S. pombe* transcripts (Affymetrix[®] GeneChip[®] Yeast Genome 2.0 Array) (Miller et al., 2011). We used 4-thiouracil (4tU) instead of 4sU for *S. cerevisiae* RNA labeling, because it is taken up by *S. cerevisiae* (Munchel et al., 2011) without expression of a nucleoside transporter as previously done (Miller et al., 2011). 4tU labeling did not affect normal cell physiology (Figure 4.2) and allowed growth of yeast in YPD instead of selective medium. We quantified only labeled and total RNA, because the unlabeled fraction was not required for rate extraction. We refer to this protocol as comparative DTA (cDTA).

We first tested whether the *S. cerevisiae* sample showed cross-hybridization to *S. pombe* array probes and *vice versa*. When either a *S. cerevisiae* or *S. pombe* sample

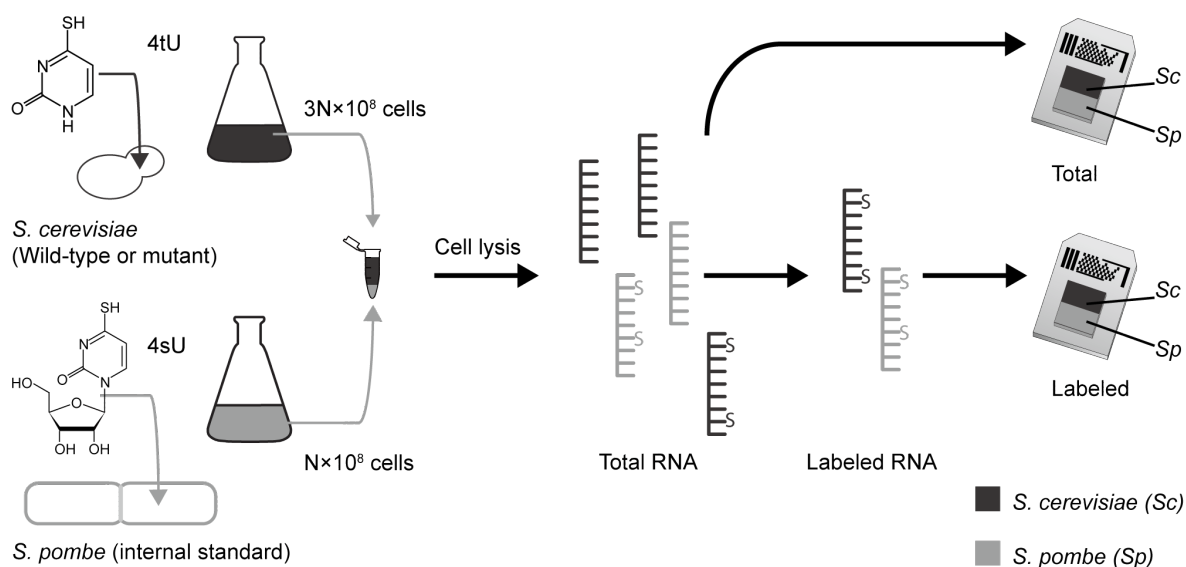


Figure 4.1: **Schematic diagram of the procedure of cDTA experiment** The *S. cerevisiae* cells are labeled by adding 4tU into the media whereas *S. pombe* cells are labeled by adding 4sU. The cells are then counted. *S. cerevisiae* cells from different experiments are mixed with always the same amount of labeled *S. pombe* cells from a single batch. Cells are then lysed, RNA is extracted, biotinylated, and labeled RNA separated. Microarrays containing probes against both *S. cerevisiae* and *S. pombe* transcripts are then used to quantify both total and labeled RNA.

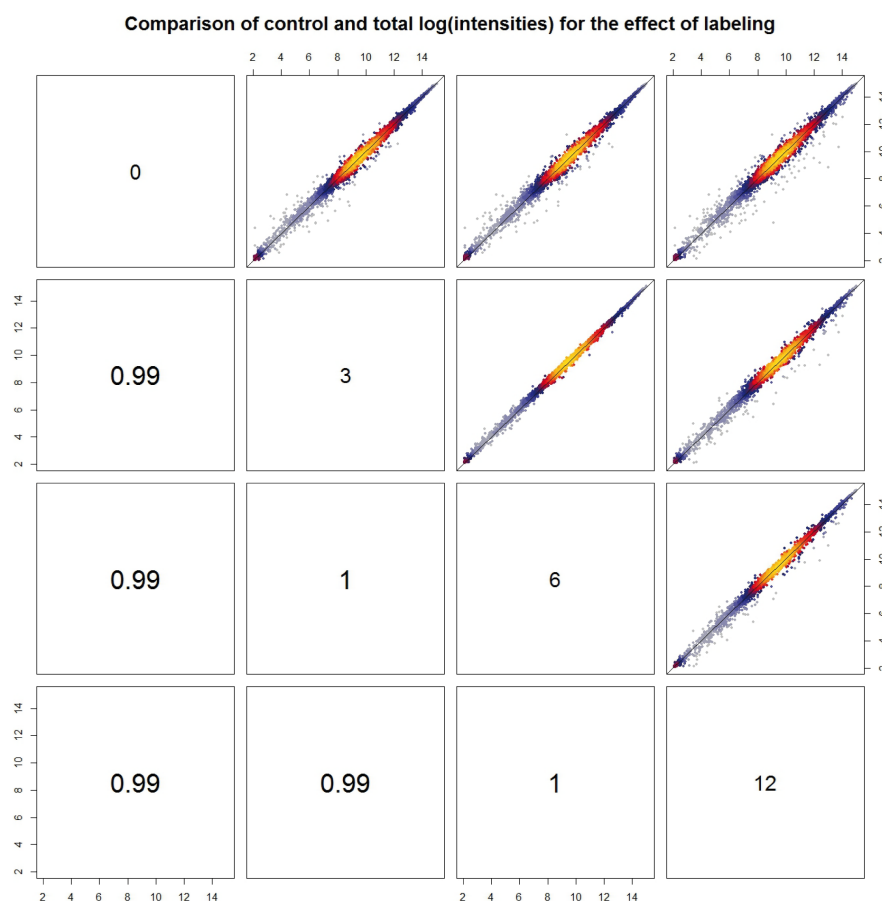


Figure 4.2: Comparison of control and total log intensities for the effect of labelling
 We compared RNA intensities of wild type cells against the total RNA intensities of cells after 3, 6 and 12 min of 4tU labeling (all cells were grown in YPD media). Almost no significant folds above a factor of 2 (below a factor of 0.5) were detected, and the distributions were almost identical to that of replicate wild type measurements. Pairwise scatterplots of log-intensities. The lower panel shows the respective Spearman correlations. The diagonal gives the length of the labeling period in minutes. Compared fractions are obtained by taking the gene-wise median over all intensities of replicate measurements.

was hybridized to the array, cross-hybridization occurred for a minor fraction of the probes (**Methods**) when a conservative intensity cut-off of 4.5 (log intensity values after preprocessing) was used (Figure 4.3). Cross-hybridizing probes were excluded

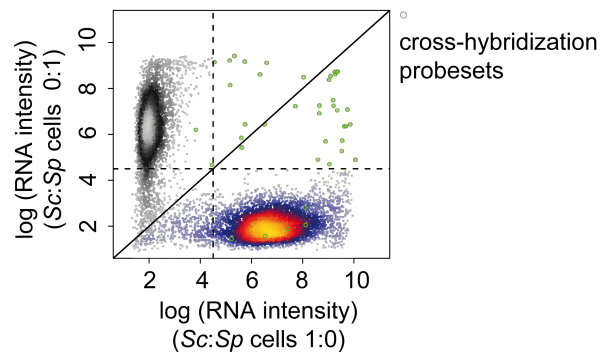


Figure 4.3: **Assessment of cross-hybridization** Scatterplot of log intensities of 10,928 Affymetrix probe sets. The values on the x- resp. y-axis are obtained as the mean of two pure *S. cerevisiae* resp. *S. pombe* replicate samples that were hybridized to the arrays. *S. cerevisiae* and *S. pombe* probe sets (heat-colored and grey-scaled, respectively) can be separated almost perfectly. 23 out of 5,771 *S. cerevisiae* probe sets show intensities above a (log) background intensity threshold of 4.5 in the *S. pombe* sample, whereas 8 out of 5,028 *S. pombe* probe sets were above background in the *S. cerevisiae* sample. These 31 probe sets are regarded as affected by cross-hybridization (green circles). Of these, 16 probe sets were excluded from analysis because all probes were affected by cross-hybridization (**Methods**)

from further analysis, leading to loss of only 16 out of 10,799 probe sets (**Methods**). The mixing ratio between *S. cerevisiae* and *S. pombe* cells was tuned to 3:1, to maximize the overlap of the *S. cerevisiae* and *S. pombe* expression intensity distributions (Figure 4.4). This ensured that after calibration most *S. cerevisiae* and *S. pombe* probe intensities were in the linear measurement range of the microarray, an important prerequisite for our calculations. The analysis was restricted to RNAs with log intensity signals above 4.5 and below 8 (Figure 4.4).

4.1.2 Rate extraction from cDTA data

To obtain absolute synthesis and decay rates for *S. cerevisiae* and *S. pombe*, we derived the ratios of labeled to total RNA intensities c_{Sc} and c_{Sp} for *S. cerevisiae* and *S. pombe*, respectively. These ratios set the global median level of synthesis and decay rates and rely on a robust previous estimate of the median *S. cerevisiae* half-life (Miller et al.,

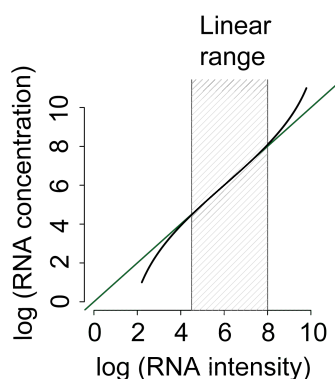


Figure 4.4: **Linear measurement range** Exemplary illustration showing that the relation of mRNA concentration (real amount) and mRNA intensity (fluorescent scanner readout) follows the Langmuir adsorption model (Hekstra et al., 2003; Held et al., 2003, 2006; Skvortsov et al., 2007). The green line indicates linearity. The black line shows sigmoidal behavior, resulting from noise at low hybridization levels and saturation effects at high hybridization levels. The grey stripe indicates the linear measurement range that we defined as an intensity range of 4.5-8 (natural log basis) based on noise signals below 4.5, for example for probes that detect transcripts of genes that were knocked out, and based on observed saturation effects above 8.

2011) for which labeled, total, and unlabeled RNA fractions were available. Once C_{Sp} is known, the measured levels of the *S. pombe* standard can be used to calibrate the *S. cerevisiae* data (Figure 4.5A). This new normalization method allows rate estimation from labeled and total quantities alone (**Methods**). Our published median half-life for *S. cerevisiae* mRNAs (Miller et al., 2011) enabled determination of the median *S. pombe* half-life relative to *S. cerevisiae* (Figure 4.6A,B). We measured growth curves, and obtained a doubling time of 90 minutes for *S. cerevisiae* in YPD medium at 30°C and 116 minutes for *S. pombe* in YES medium at 32°C. These doubling times were used in kinetic modeling (Miller et al., 2011). We confirmed that the rates obtained by cDTA are essentially the same as the ones previously obtained by DTA (Table 4.1, Figure 4.6).

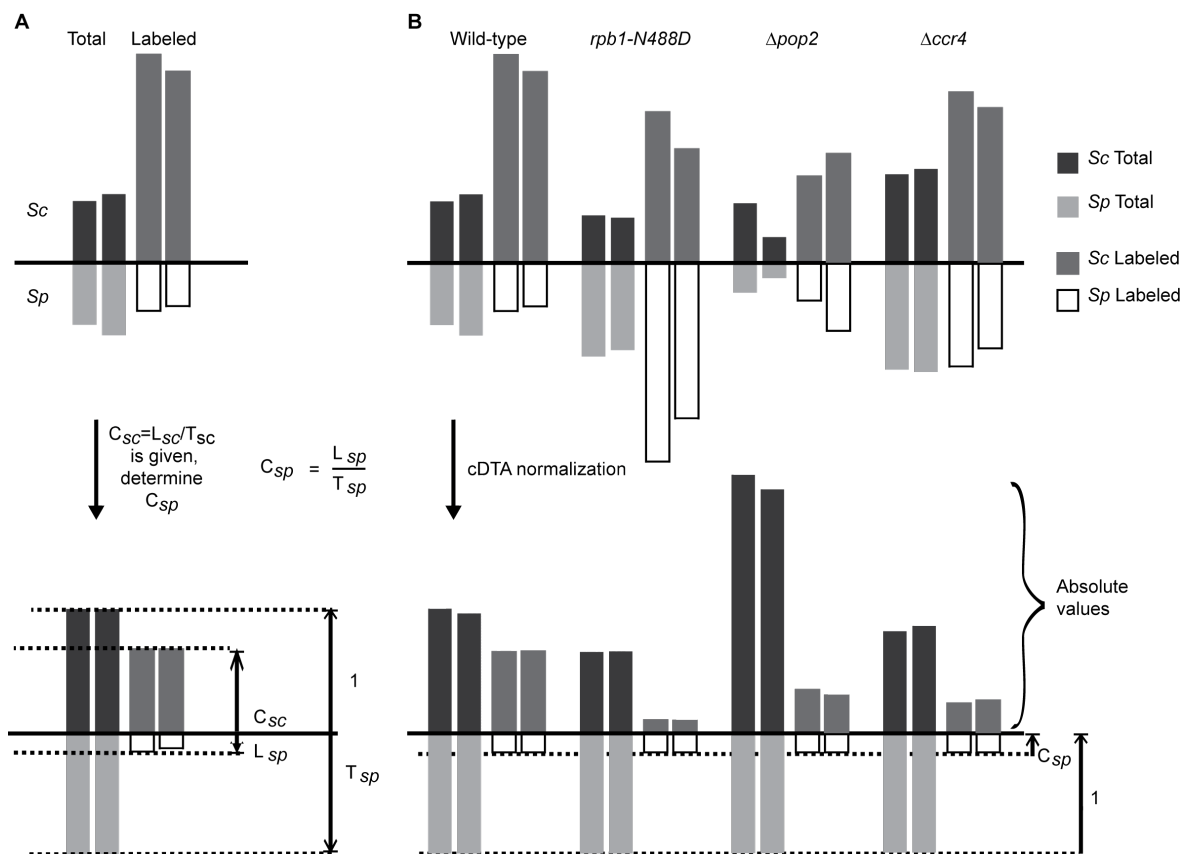


Figure 4.5: **Schematic diagram of cDTA normalization procedure A.** Determination of c_{Sp} , the ratio of labeled over total *S. pombe* mRNA. To obtain absolute synthesis and decay rates for *S. cerevisiae* and *S. pombe*, we derived ratios of labeled to total RNA c_{Sc} and c_{Sp} for *S. cerevisiae* and *S. pombe*, respectively. The c_{Sc} ratio was obtained in our previous study (Miller et al., 2011). To determine c_{Sp} , L_{Sc} and T_{Sc} are set to c_{Sc} and 1, respectively. L_{Sp} and T_{Sp} are then linearly rescaled. The resulting L_{Sp}/T_{Sp} is defined as c_{Sp} and then used in the further experiments as global cDTA normalization factor. **B.** cDTA normalization uses *S. pombe* signals as internal standard. The bars indicate the median intensities of the array probe sets. Due to our experimental design, the ratio of labeled to total *S. pombe* RNA ($c_{Sp} = L_{Sp}/T_{Sp}$) must be the same in all experiments. To correct for differences in cell lysis, RNA extraction efficiency, and RNA purification efficiencies, the levels of *S. pombe* total and labeled mRNA are rescaled to the same values in all experiments. The *S. cerevisiae* RNA levels are then corrected by median centering of *S. pombe* RNA levels. This normalization allows for a direct comparison of Sc data between experiments. Shown are both replicates for each of the four cDTA experiments.

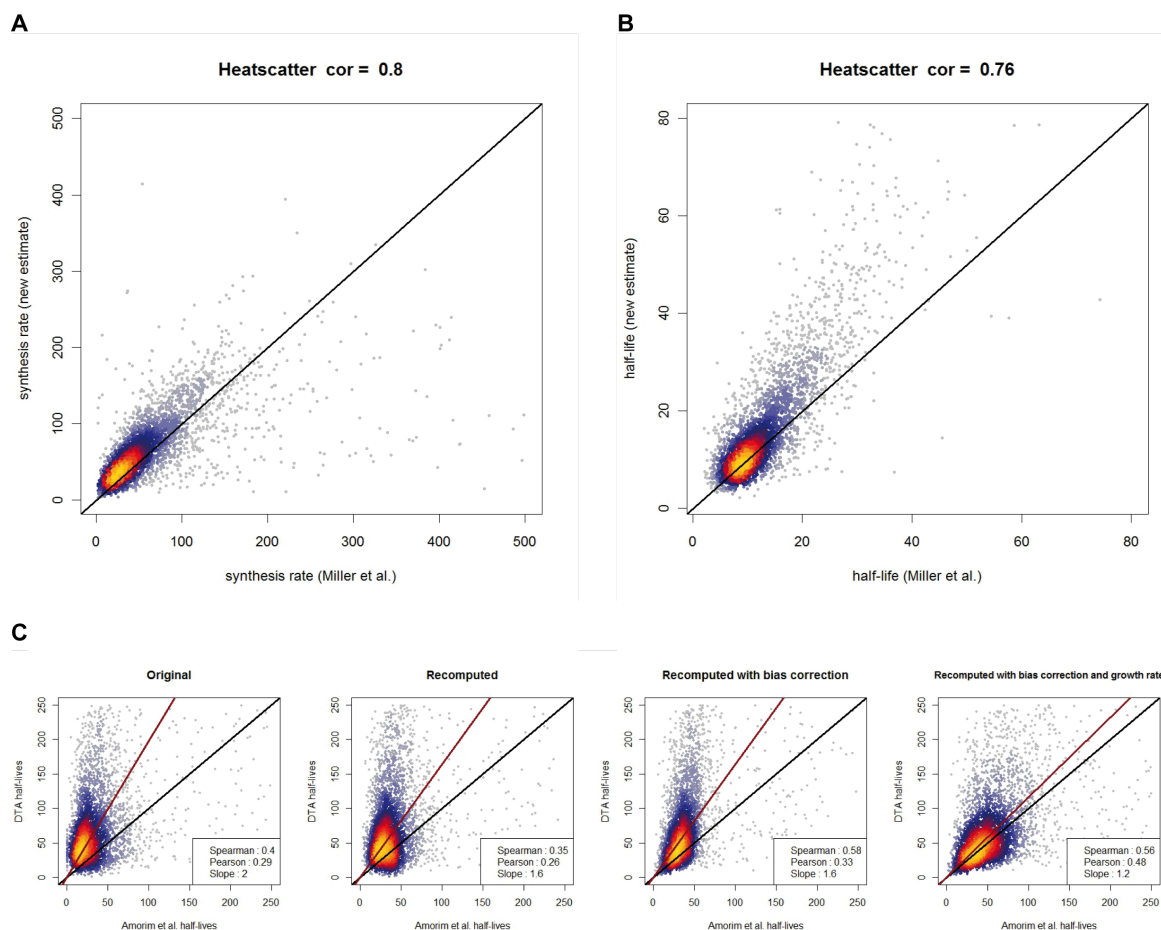


Figure 4.6: **Scatter plots comparing data from these and other studies** The scatter plots compare the *S. cerevisiae* synthesis (**A**) and half-lives (**B**) as obtained by cDTA (y-axis) and those obtained from our data using the method from (Miller et al., 2011). Spearman correlations are 0.8 and 0.76 respectively. (**C**) Comparison of the *S. pombe* transcript half-lives as obtained by us (y-axis; median half-life 59 min) and by (Amorim et al., 2010) (x-axis). Spearman and Pearson correlation coefficients are given in the legends. From left to right: comparison of our data to original estimates (Amorim et al., 2010), to recomputed estimates, to recomputed estimates with labeling bias correction and to recomputed estimates with labeling bias and growth rate correction.

Table 4.1: Median mRNA half-lives and synthesis rates of *S. cerevisiae* and *S. pombe* transcripts.

			Species	cDTA ¹	DTA
Median mRNA half-life [min]			<i>Sc</i>	12	11.5
			<i>Sp</i>	59	<i>N. A.</i>
Median mRNA synthesis rate [mRNAs per cell and cell cycle time] ²			<i>Sc</i>	53 ²	18 (72) ²
			<i>Sp</i>	44	<i>N. A.</i>

RNA half-lives that were recently determined by 4tU pulse-chase labeling in *S. cerevisiae* are 1.5-fold longer (Munchel et al., 2011), likely because a very long labeling time was used that allowed for thio-nucleotide re-incorporation after mRNA decay. We calculated mRNA synthesis rates as the number of complete transcripts made per cell and per 90 minutes (the cell cycle time for wild type *S. cerevisiae*), using a new estimate of 60,000 transcripts per yeast cell (Zenklusen et al., 2008), instead of the previously used, four-fold lower estimate (Hereford and Rosbash, 1977). For *S. pombe*, we estimated the number of transcripts from the observed 2.51-fold cumulative total RNA level to be 150,801. Our rate estimates were unaffected by the efficiency of 4tU labeling, which varied between strains and experiments (Figure 4.7). For normalization between different *S. cerevisiae* samples, we linearly rescaled all array intensities such that the total and labeled *S. pombe* fractions have a median intensity of 1 or C_{Sp} (Figure 4.5B). We assessed the accuracy of the cDTA procedure by estimating the intensity ratios of *Sc:Sp* cells that were mixed at 1:1, 3:1, and 10:1. The correct values were recovered with an accuracy of 95% (Figure 4.8). Selected mRNA levels of

¹The cDTA contains the estimates obtained from using the labeled:total ratio of the complementary strain and the known total and labeled *Sc:Sp* ratios to calculate the missing labeled:total ratio, i.e.,. The DTA column shows the *S. cerevisiae* half-life estimate obtained from (Miller et al., 2011). Note that the *S. cerevisiae* estimates are virtually identical to ours, although we used a different labeling technique (4tU instead of 4sU) and had spiked-in *S. pombe* controls in the sample.

²Please note we previously used in our calculations a total number of transcripts per cell of 15,000, according to an old estimate (Hereford and Rosbash, 1977), whereas we now used a recent estimate of 60,000 (Zenklusen et al., 2008). If the same number of transcripts is used, the median synthesis rate obtained by DTA would be 72, comparable to our new estimate obtained by cDTA, despite the difference in media and cell cycle time (Miller et al., 2011)

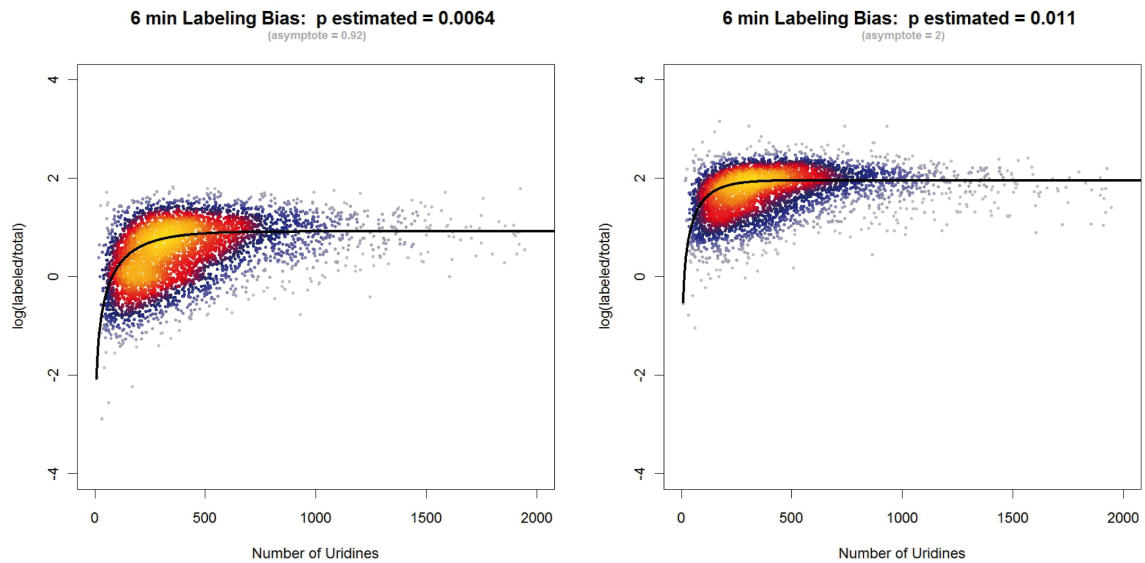


Figure 4.7: **Scatter plot showing labeling bias** The number of uridines is plotted versus the log-ratio of L and T. The black line shows that the labeling bias curve estimated as in (Jimeno-González et al., 2010). Left: labeling bias plot for the slow Pol II mutant. $p_{lab} = 0:0064$ means that approximately every 156th uridine residue is replaced by 4tU and afterwards attached to a biotin molecule. Right: labeling bias plot for the wild-type. $p_{lab} = 0:011$ means that approximately every 90th uridine residue is replaced by 4tU and afterwards attached to a biotin molecule. The shifted asymptotes indicate the observed fold of the decay rate comparing these two conditions. Note that differences in labeling efficiency p_{lab} do not affect decay and synthesis rate measures, as these efficiency biases only occur for transcripts with less than 500 uridine residues. Though these transcripts make up two thirds of all mRNAs, biases can be accurately removed. Therefore, different labeling biases estimated as in (Jimeno-González et al., 2010) can only adopt different curvatures, whereas altered synthesis and decay rates can only lead to shifted asymptotes of the respective curves.

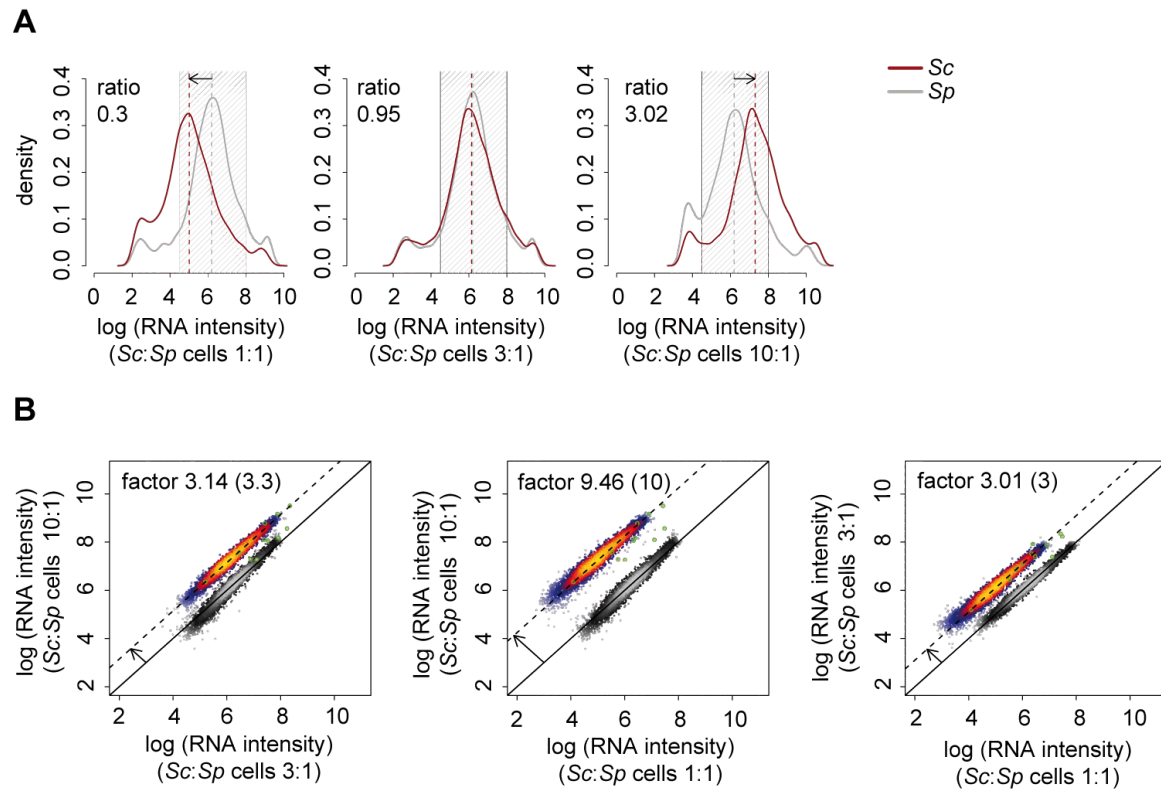


Figure 4.8: **Determination of the mixing ratio** (A) Calibration of *Sc:Sp* cell mixture ratio. The optimal cell mixture ratio has been chosen to maximize the number of probes for both *S. cerevisiae* and *S. pombe* that fall into the linear measurement range (Figure 4.4). *S. cerevisiae* and *S. pombe* cells were mixed in *Sc:Sp* ratios of 1:1, 3:1, and 10:1. The respective median mRNA level ratios are 0.3, 0.95, and 3.02. Log (RNA intensity) distributions of *Sc* (red) and *Sp* (grey) are shown. The median intensity level of *S. pombe* is approximately three times higher than that of *S. cerevisiae*. As a consequence, a *Sc:Sp* cell mixture ratio of 3:1 was used. (B) Comparison of the three different cell mixtures of (A) in pairwise log-log scatter plots. All arrays are normalized to a common median of 4,052 *S. pombe* probe sets (grey-scaled). 4,475 *S. cerevisiae* probe sets (those in the linear measurement range) are shown in heat colors. The parallel offset of the *S. cerevisiae* probe sets from the main diagonal measures the mRNA level differences of *S. cerevisiae* in the three cell mixtures. The differences should be 3.3, 10, and 3 when we plot *Sc:Sp* ratios of 10:1 vs. 3:1, 10:1 vs. 1:1, and 3:1 vs. 1:1, respectively. The corresponding measured offsets are 3.14, 9.46, and 3.01, and thus in very good agreement.

the 1:1 and 10:1 ratio mixtures were additionally quantified by RT-qPCR (Methods). The expected ratio of the four tested *S. cerevisiae* transcripts was recovered within a relative error of 9% when normalized to two housekeeping *S. pombe* genes (not shown). In summary, cDTA normalization removes the major sources of experimental differences between samples in RNA labeling efficiency, cell lysis, RNA extraction, RNA biotinylation and labeled RNA purification, and array hybridization. cDTA detects global changes between *S. cerevisiae* samples, in contrast to standard normalization procedures that eliminate global changes because they assume constant median RNA levels.

4.1.3 cDTA supersedes conventional methods

Conventional methods measure mRNA half-lives by inducing transcription arrest and following changes in mRNA levels over time. Transcription arrest has been achieved by adding the transcription inhibitor 1,10-phenanthroline (Dori-Bachash et al., 2011), or by shifting the temperature-sensitive mutant strain *rpb1-1*, which carries a point mutations in the largest subunit of Pol II (Nonet et al., 1987), to the restrictive temperature (Grigull et al., 2004; Holstege et al., 1998; Shalem et al., 2008; Wang et al., 2002). To investigate whether the latter method yields reliable data or whether it perturbs mRNA metabolism, we re-generated the *rpb1-1* strain and analyzed it with cDTA using published growth parameters (Holstege et al., 1998) (**Methods**). This revealed that mRNA synthesis rates were decreased globally by a factor of 2.7 already at the permissive temperature of 30°C (Figure 4.9A). After 24 minutes at the restrictive temperature, mRNA synthesis rates had decreased further by a factor of 3.4, but recovered essentially to the rates measured at permissive temperature after 66 minutes (Figure 4.9A). These observations indicated that the mRNA metabolism in the *rpb1-1* strain was already perturbed at the permissive temperature, and that the temporary changes in mRNA metabolism observed at the restrictive temperature were mainly due to a heat shock response. To test this, we conducted a corresponding heat shock experiment on wild type cells. We analyzed the total mRNA from this experiment together with the data from the *rpb1-1* mutant by conventional decay time series analysis (Grigull et al., 2004; Holstege et al., 1998; Shalem et al., 2008; Wang et al., 2002). The obtained mRNA half-lives during heat shock correlated very well with data derived from the *rpb1-1* mutant strain, and with published half-lives obtained with this strain (Figure 4.9B). The obtained half-lives were longer than the half-lives

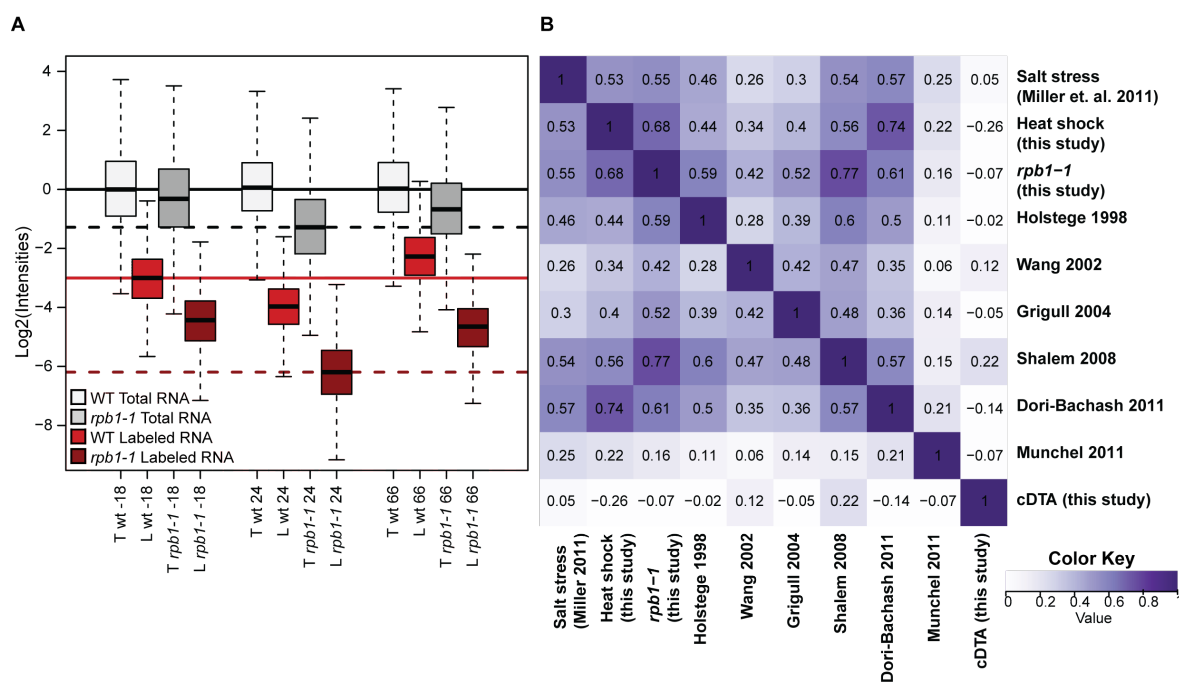


Figure 4.9: **Study of *rpb1-1* strain transcription and degradation** (A) Box plots of the expression distributions of the total and the labeled (newly synthesized) mRNA after cDTA normalization, obtained from the wild type and the *rpb1-1* mutant before and 24 and 66 minutes after the shift to restrictive temperature. Transcriptional activity is roughly restored in both strains after 66 minutes. The global shifts in labeled expression are only slightly more pronounced in the *rpb1-1* mutant, indicating a dominant role of heat shock in the profiles of *rpb1-1*. (B) Correlation analysis of mRNA half-life measurements. The heatmap shows pair wise Spearman correlation coefficients of half-life measurements (white: negative or zero correlation; purple: perfect correlation). The published half-life estimates except for (Munchel et al., 2011) were obtained by experiments using transcriptional arrest. The estimates of (Holstege et al., 1998), Wang et al. (Wang et al. 2002), Grigull et al. (Grigull et al. 2004) and Shalem et al. (Shalem et al. 2008) were obtained using a yeast strain containing the Pol II temperature sensitive mutant *rpb1-1*. Dori-Bachash et al. (Dori-Bachash et al. 2011) used the transcription inhibitor 1,10-phenanthroline.

measured in unperturbed cells, likely because mRNA degradation was down-regulated during the stress response. There was also a good correlation with half-lives obtained after adding 1,10-phenanthroline, and even with our previous data obtained during the osmotic stress response (Miller et al., 2011), if processed in the conventional way. This indicates that all these data are dominated by perturbations in mRNA metabolism that result from a general stress response. In contrast, published half-lives derived from metabolic RNA labeling (Munchel et al., 2011) and our cDTA-derived half-lives do not correlate with data obtained by perturbing conventional methods. We conclude that conventional methods for estimating mRNA half-lives using the *rpb1-1* mutant strain or transcription inhibition cannot be used to obtain reliable half-life estimations.

4.1.4 Comparison of mRNA metabolism in distant yeast species

As an immediate result, cDTA reveals similarities and differences in the mRNA metabolism of *S. cerevisiae* and *S. pombe*. First, the median mRNA synthesis rates are very similar in *S. cerevisiae* and *S. pombe*. The median synthesis rate was 53 mRNAs per cell and 90 minutes for wild type *S. cerevisiae* and 44 mRNAs per cell and 90 minutes for *S. pombe*. Second, *S. pombe* mRNAs have about five-fold longer half-lives on average than *S. cerevisiae* mRNAs, with a median of 59 minutes (Figure 4.10A, Figure 4.11), compared to 12 minutes for *S. cerevisiae*. As expected, the cDTA-derived *S. pombe* half-lives show a fair correlation with half-lives obtained by another non-perturbing metabolic labeling (Amorim et al., 2010). Furthermore, reprocessing the data of Amorim et al. with our cDTA algorithm, which takes into account the labeling bias and an additional parameter to correct for cell growth, increases the correlation to our results and leads to a median half-live of 50 minutes, in good agreement with an estimate of 59 minutes in our study (Figure 4.6C). Third, the overall mRNA levels in *S. pombe* were about 3.1-fold higher than in *S. cerevisiae*. Since the haploid *S. cerevisiae* cells with a median volume of $42\mu\text{m}^3$ are approximately two- to three-fold smaller than *S. pombe* cells with a median cell volume of approximately $115\mu\text{m}^3$ (Jorgensen et al., 2002; Neumann and Nurse, 2007), the higher mRNA levels apparently lead to similar cellular mRNA concentrations. The change in mRNA levels is mainly a global multiplicative change ($R^2=0.82$, Figure 4.11C). Taken together, these data suggest that *S. pombe* cells generally contain more stable mRNAs than *S. cerevisiae* cells to reach similar mRNA concentrations at similar mRNA synthesis rates despite their larger volume.

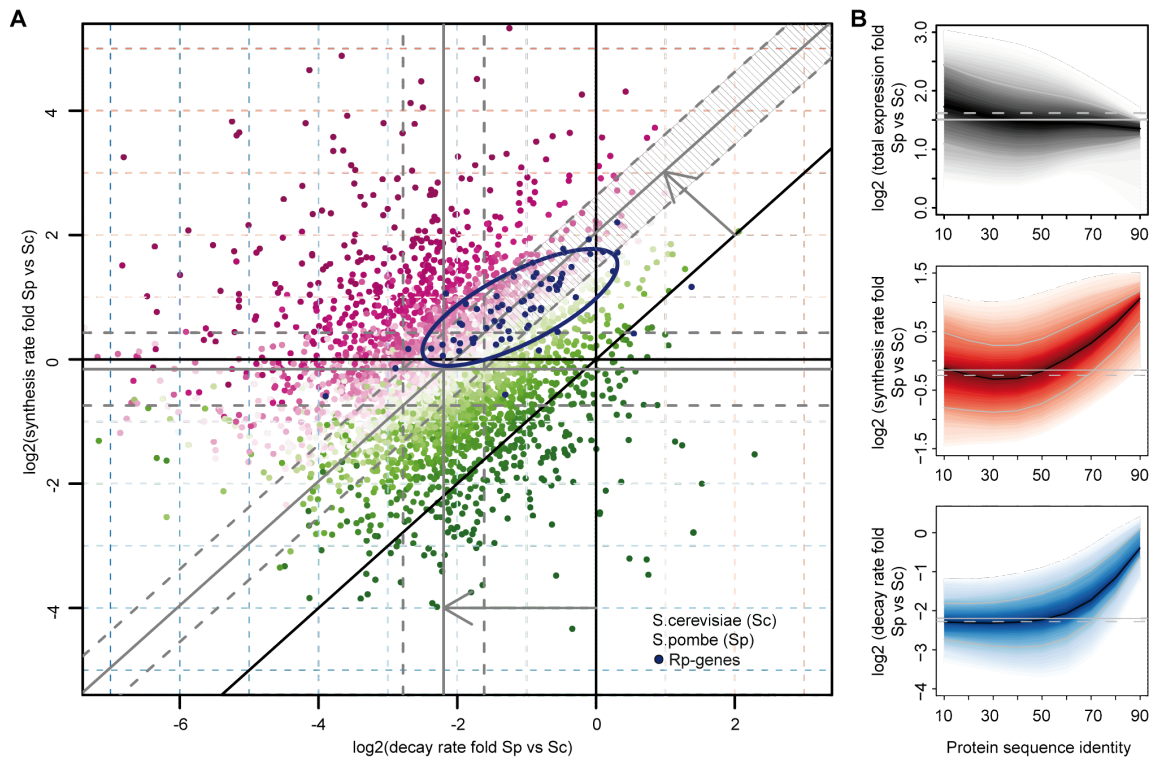


Figure 4.10: (**Comparison of the decay rate and expression rate of *S. cerevisiae* and *S. pombe*** **A**) Scatter plot comparing mRNA decay rate folds versus synthesis rate folds of *Sp* and *Sc* transcripts encoding protein orthologs (>25% amino acid sequence identity). The offset of grey lines to parallel black lines indicate *Sp:Sc* ratios of median decay rates, synthesis rates, or total mRNA (0.20/0.83/2.72). Dashed grey lines indicate 1.5-fold changes from the median (grey lines). Color scheme corresponds to folds in total mRNA (magenta, positive log fold; green, negative log fold). A set of genes that show higher decay and synthesis rates (1.5-fold & adjusted P-value 0.5%) but almost unchanged (<1.5-fold) total mRNA (93 transcripts, striped area) was selected and tested with a Bayesian network-based gene set analysis (MGSA)(Bauer et al., 2010). In this gene set, the ribosomal protein genes were enriched (blue dots; ellipse shows the 75% region of highest density). (**B**) Plots show \log_2 fold distributions of total mRNA (grey), synthesis rate (red) and decay rate (blue) of *Sp* versus *Sc* transcripts encoding orthologous proteins as a function of amino acid sequence identity (%). Transcripts encoding highly conserved proteins such as ribosomal proteins are located on the right. They show more rapid turnover (synthesis and decay) in *S. pombe*, resulting in similar mRNA levels. The solid black lines represent the median \log_2 fold, the shaded bands are the central 80% regions. The solid/dashed grey lines indicate the median \log_2 fold of all orthologs/all genes.

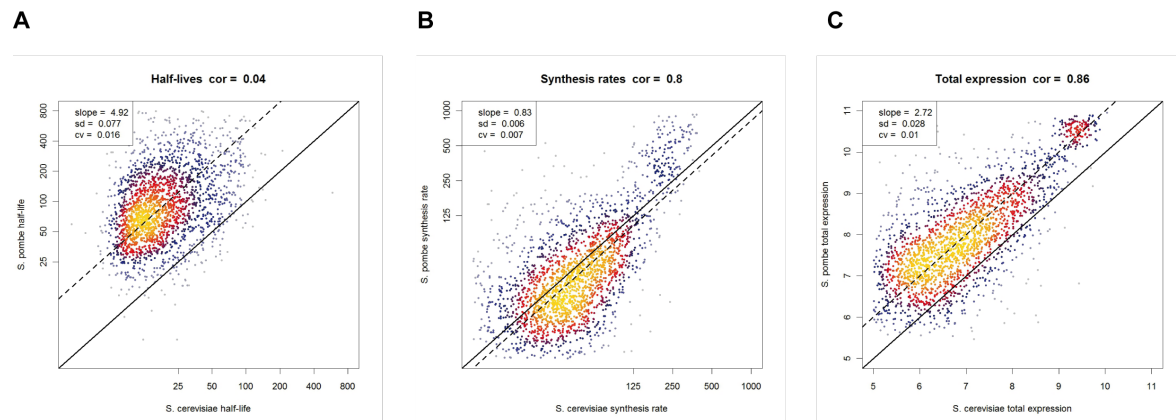


Figure 4.11: **Scatter plot comparing mRNA half-life (A), synthesis rate (B) and total expression (C) of *S. pombe* against *S. cerevisiae* orthologs (>25% protein sequence identity).** The offset of dashed lines to (parallel) black lines indicate ratios of median half-life resp. synthesis rate resp. total mRNA of *S. pombe* to *S. cerevisiae* (4.92/0.83/2.72).

We investigated whether mRNA sequence conservation correlates with a conservation of total RNA levels, synthesis rates, or decay rates (Figure 4.10B, Figure 4.11). This analysis revealed a conservation of the relative total levels of mRNAs that encode orthologous proteins in *S. cerevisiae* and *S. pombe*. The levels of mRNAs that encode proteins with an amino acid sequence identity of at least 25% (2568 mRNAs) show a high Spearman correlation of 0.69. Synthesis rates correlate well between both species (Spearman correlation 0.61), but the half-lives show only a fair correlation (Spearman correlation 0.4). Although the data suggest that *S. pombe* cells have globally shifted decay rates, to reach similar cellular mRNA concentrations, there is a minor fraction of transcripts that behave exceptionally. In particular, 93 *S. pombe* transcripts show almost unchanged mRNA levels (< 1.5 fold), but significantly higher synthesis and decay rates (> 1.5 fold), and are enriched for ribosomal protein genes (Figure 4.10A). More generally, transcripts that encode highly conserved proteins show similar levels, but a faster turnover in *S. pombe* (Figure 4.10B). We also assessed the correlation of synthesis rates with transcript lengths, and revealed a substantially higher Pol II drop-off rate in *S. pombe* (Figure 4.12).

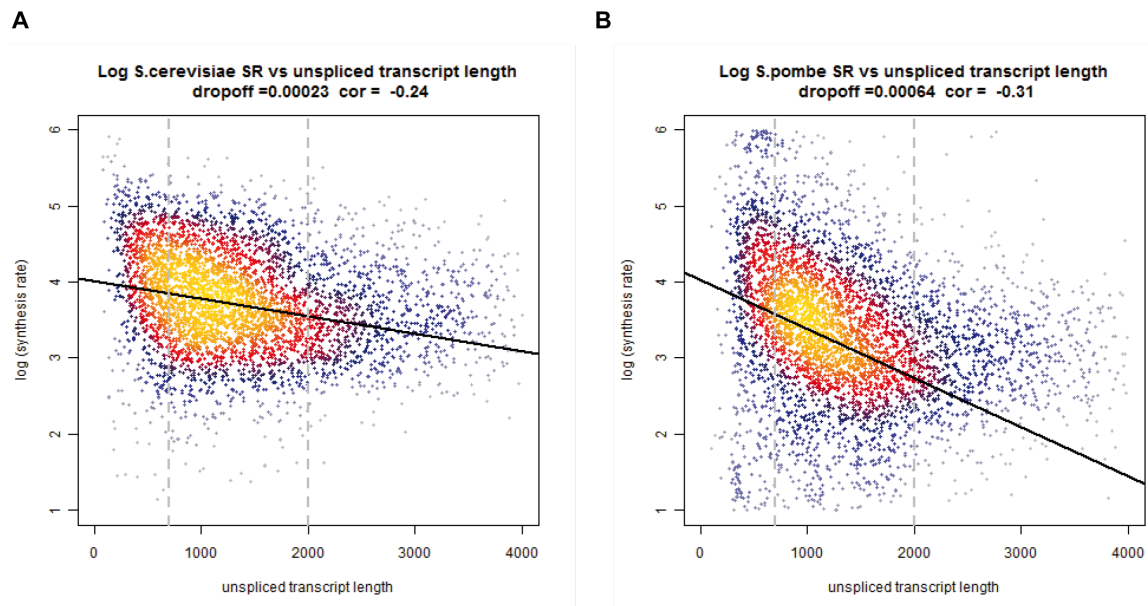


Figure 4.12: **Correlation of log synthesis rates with transcripts length (A)** for *S. cerevisiae* and **(B)** for *S. pombe*. The linear regression and the Pearson correlation were calculated for the transcripts with a length between 700 and 2000 nucleotides.

4.1.5 Impaired mRNA synthesis is compensated by decreased degradation

We applied cDTA to the question of whether the speed of Pol II is relevant for setting the cellular rates of mRNA synthesis. We used a yeast strain that carries the non-disruptive point mutation N488D in the largest Pol II subunit Rpo21 (also known as Rpb1) (*rpb1-N488D*). This mutation slows down Pol II speed in RNA elongation assays *in vitro* (Malagon et al., 2006) and is located near the active site (Cramer et al., 2001). We subjected this strain and an isogenic wild type strain to cDTA, and collected two biological replicates, which showed a Spearman correlation of 0.99 for total and labeled RNA (Figure 4.13). We measured cell-doubling times, and used these in the kinetic modeling, to correct synthesis rates for a change in doubling time (Table 4.2). In the *rpb1-N488D* mutant strain, mRNA synthesis rates were globally decreased 3.9-fold (Figure 4.14A,B). This is consistent with the observed 2- to 4.5-fold decrease in Pol II speed measured *in vitro* (Malagon et al., 2006). We observed a Pol II drop-off rate similar to that described previously (Jimeno-González et al., 2010), but

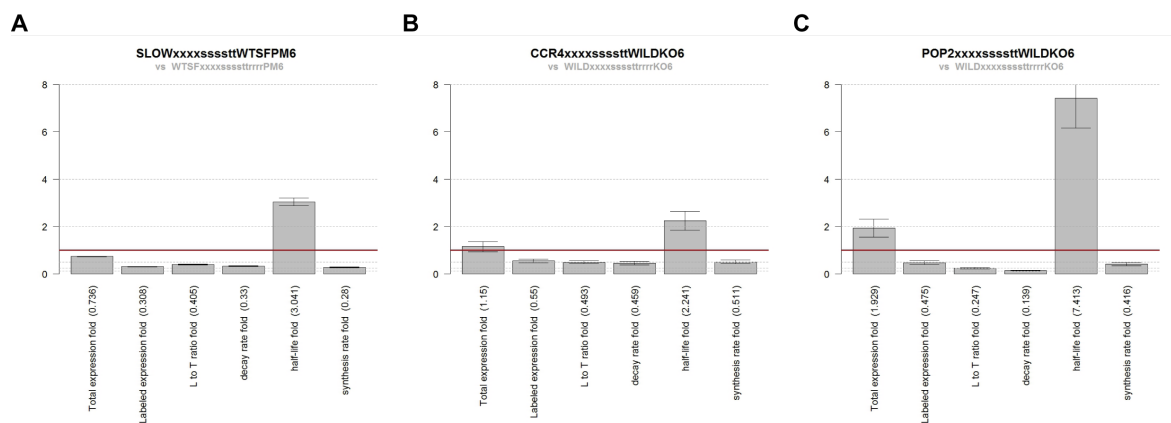


Figure 4.13: **Barplot of measured global shifts** Total expression, labeled expression, labeled to total ratio (decay proxy), decay rate, half-life and synthesis rate are showing here. (A) slows Pol II mutant against its isogenic wild-type; (B) *ccr4* Δ against wild type; (C) *pop2* Δ against wild-type in log scale. Error bars indicate the standard deviation of pairwise comparison of respective replicates.

Table 4.2: Growth rate of the mutants studied

Mutants	Doubling time/min
wild-type	90
<i>ccr4</i> Δ	219
<i>pop2</i> Δ	126
<i>rpb1-N488D</i>	150

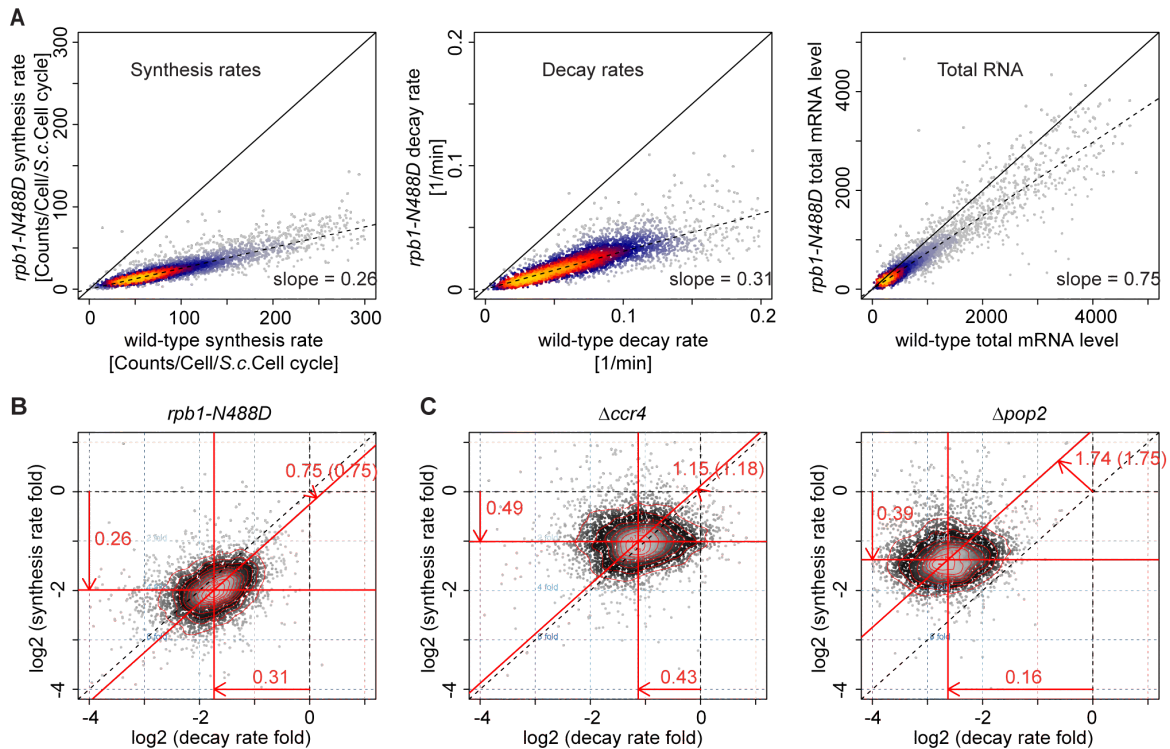


Figure 4.14: **cDTA reveals changes in mRNA metabolism upon genetic perturbation** (A) Linear scatter plots (heat-colored) of mRNA synthesis rates, decay rates, and total mRNA levels in wild type and mutant *rpb1-N488D* yeast strains as measured by cDTA. Slopes indicate global shift ratios of median synthesis rates, decay rates, and total mRNA of the *rpb1-N488D* mutant strain compared to wild type (0.26/0.31/0.75). (B) Alternative representation of the data from panel A in a single scatter plot comparing the changes in mRNA synthesis rates (log folds, x-axis) and decay rates (log folds, y-axis) in the *rpb1-N488D* mutant strain compared to the wild type strain. Each point corresponds to one mRNA. The density of points is encoded by their brightness (grey scale). Contour lines define regions of equal density. The center of the distribution is located at (-1.8, -1.6), indicating that there is a global shift in the median synthesis rate by a factor of 0.26 (shift of the horizontal red line relative to the dashed x-axis line), and a global shift in the median decay rate by a factor of 0.31 (shift of the vertical red line relative to the dashed y-axis line). The global change in total mRNA levels is predicted by the offset of the diagonal red line from the dashed main diagonal, which corresponds to a change by a factor of 0.75. The number in brackets following this number (0.75) is the global change as it has been observed in the total mRNA measurements, which agrees well with the predicted number. The changes in total RNA levels do not exactly equal the quotient of synthesis and decay rate changes, due to an additional parameter for cell growth. (C) Scatter plots as in (B) comparing synthesis rates, decay rates, and total mRNA levels of *ccr4Δ* and *pop2Δ* mutant strains to wild type yeast. Ratios of median synthesis rates, decay rates, and total mRNA of the *ccr4Δ/pop2Δ* mutant strain compared to wild type are 0.49/0.39, 0.43/0.16, and 1.15/1.74, respectively.

quantitative modeling excludes drop-off of Pol II during elongation as the cause for the decreased synthesis rates (Figure 4.15, Table 4.3). Despite the lower synthesis

Table 4.3: Pol II drop off rate

	<i>S. cerevisiae</i>	<i>S. pombe</i>	Slow PolIII	<i>ccr4</i> Δ	<i>pop2</i> Δ
Drop of rate per nucleotide	2.3×10^{-4}	6.4×10^{-4}	2.9×10^{-4}	3.7×10^{-4}	2.3×10^{-4}
Pol II drop off per 1000 nucleotides	21%	47%	26%	31%	21%

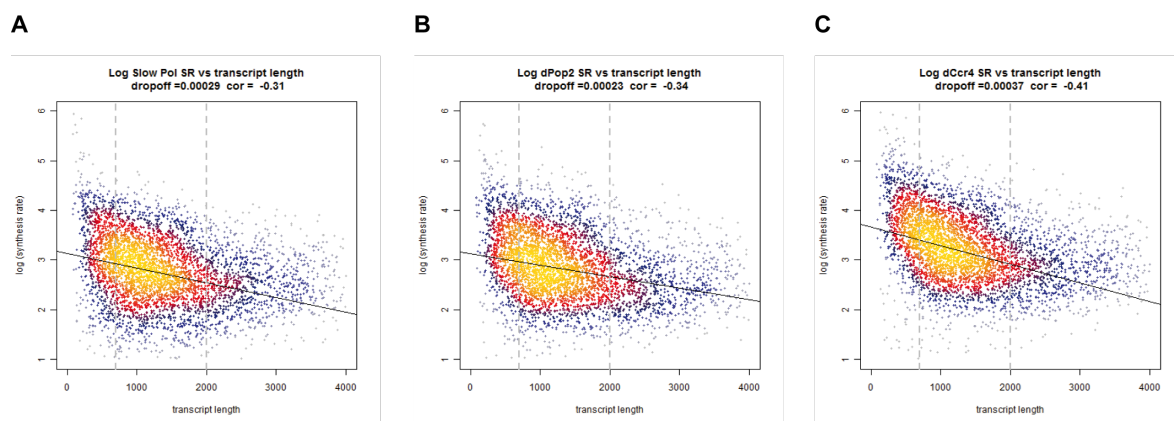


Figure 4.15: **Comparison of the synthesis rate and transcript length in the mutants**

The discovery of a global regulation of mRNA transcription activity raises the question about the responsible mechanism. A straightforward hypothesis is that transcription inhibition is achieved by increasing the abort rate of Polymerase during transcription elongation. However, the abort rate of Pol II (Figure 4.12) in all three mutants (slow Pol II mutant, deadenylation mutants *ccr4* Δ and *pop2* Δ) is comparable to that of *S. cerevisiae* wild type. It is thus likely that the feedback mechanism does not intervene at the elongation stage, but rather at the stage of transcription initiation or during the transition from transcription initiation to elongation. Figure shows the dependence of synthesis rates on transcript length for the slow (A) Pol II mutant, the deadenylation mutants (B) *ccr4* Δ and (C) *pop2* Δ .

rates, global mRNA levels were not changed very much in the slow Pol II mutant strain (Figure 4.14A). This resulted from a strong decrease in mRNA decay rates of 3.2-fold on average. Synthesis and decay rates of all mRNAs were shifted by approximately the same factor, independent of their wild type expression level, synthesis rate, or

decay rate. The globally increased mRNA half-lives apparently compensated for the decreased mRNA synthesis rates, to buffer cellular mRNA levels, which were decreased 1.3-fold only. The measured total RNA levels agreed well with total mRNA levels calculated from the changed synthesis and decay rates (not shown). These results show that cells with a strong defect in mRNA synthesis can maintain nearly normal mRNA levels by compensatory changes in mRNA decay rates.

4.1.6 Impaired degradation is compensated by decreased synthesis

The observed synthesis-decay compensation implies that cells buffer total mRNA levels. If true, cells should also be able to compensate for a mutation that impairs mRNA degradation with a change in mRNA synthesis rates. To investigate this, we applied cDTA to mutant yeast strains with global defects in mRNA degradation. The choice of mutant was difficult, since RNA degradation involves multiple enzymes in the nucleus and cytoplasm (Houseley and Tollervey, 2009). We decided to use mutant strains that lack either one of the two catalytic subunits of the Ccr4-Not complex, Ccr4p or Pop2p, which show a defect in mRNA deadenylation, a rate-limiting step in mRNA degradation (Tucker et al., 2002). As predicted, mRNA decay rates were globally decreased in the *ccr4* Δ and *pop2* Δ strains, and changed on average by a factor of 0.43 and 0.16, respectively (Figure 4.14C). This suggests that Ccr4p and Pop2p mRNA degradation factors are used globally.

In both degradation-deficient knock-out strains, an unexpected decrease in mRNA synthesis rates was observed (Figure 4.14C). Synthesis rates were changed by a factor of 0.49 and 0.38 in the *ccr4* Δ and *pop2* Δ strains, respectively, limiting the increase in total mRNA levels due to highly defective degradation to a factor of only 1.18 and 1.75, respectively (Figure 4.14C). This effect could be observed directly in the labeled fractions of the *ccr4* Δ and *pop2* Δ strains. Only 62% or 46% of the RNA was labeled within the same labeling time, indicating lower synthesis rates. Thus the defects in RNA degradation in these strains are at least partially compensated by decreased mRNA synthesis rates, to buffer mRNA levels. This mutual compensation cannot be explained by measurement variance. A variation analysis for the estimation of the median synthesis and decay rates (Figure 4.16) shows that the 95% confidence regions of the median synthesis and decay rate estimates are clearly disjoint.

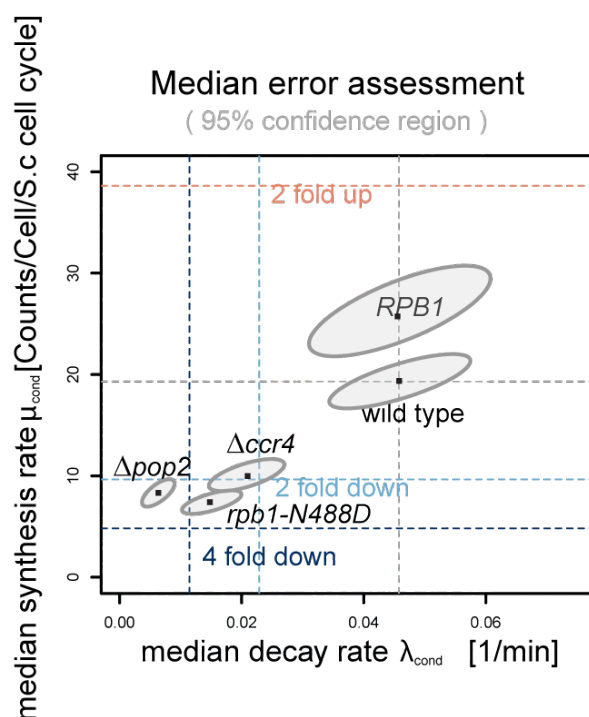


Figure 4.16: **Coupling of synthesis and decay rates on the absolute level.** For each condition, the median synthesis rate (y-axis) and degradation rate (x-axis) is shown (dark dots). Dashed lines indicate fold induction/repression relative to wild-type. The dots lie approximately on a line with positive slope, indicating synthesis-decay compensation. A variation analysis for the estimation of the median synthesis and decay rates with cDTA has been performed. The ellipses show the 95% bootstrap confidence regions in each condition. The main axes of the ellipses reveal that the errors in the estimation of synthesis and decay rates are not independent, yet small enough to prove that the coupling is not due to estimation variance.

4.1.7 A transcription inhibitor and degradation enhancer may buffer mRNA levels

The above data show that yeast cells can compensate for impaired mRNA synthesis with decreased mRNA decay rates, and for impaired degradation by decreased mRNA synthesis rates. Yeast cells thus have mechanisms to at buffer mRNA levels by mutual negative feedback between nuclear mRNA synthesis and cytoplasmic mRNA decay. To explore this further, we extended our model for mRNA turnover under steady state conditions. The mRNA of a gene G is synthesized at a gene-specific constant rate μ_g , and is degraded at a gene-specific rate $g \cdot \lambda_g$, with g being the mRNA amount resulting from gene G . We assume that there is a transcription modulator S and a degradation modulator D that globally affect the synthesis rate (SR) and decay rate (DR) by factors $f(s)$ and $h(d)$, respectively 4.1:

$$\frac{dg}{dt} = SR(g, s) - DR(g, d) = \mu_g \cdot f(s) - g \lambda_g \cdot h(d) \quad (4.1)$$

The important and plausible assumption of this model is that f and h are monotonic functions. We do however not assume that mRNA levels translate linearly into protein levels, or that the degree of modulation is a linear function of the underlying mRNA concentrations of S and D . One might think of S and D as proteins, whose activity is a function of their mRNA concentrations s and d .

From the model 4.1, we inferred the regulatory logic of the observed feedback, as outlined below. A rigid derivation and an extensive discussion of the models assumptions are given in Methods. We compare here synthesis and decay rates of a gene between two conditions C and C.

$$\frac{SR'(g', s')}{SR(g, s)} = \frac{\mu'_g f(s')}{\mu_g f(s)} \quad (4.2)$$

$$\frac{DR'(g', s')}{DR(g, s)} = \frac{\lambda'_g h(d')}{\lambda_g h(d)} \quad (4.3)$$

The left hand sides of equations 4.2 and 4.3 can be evaluated by cDTA. The left hand side of equation 4.2 is substantially smaller than 1 for virtually all measurements g , g and for both deadenylation mutants (Figure 4.14B). For these mutants, we also know that $\mu_g = \mu_g$, and consequently $f(s) < f(s)$. We also observe generally that $g > g$ and $s > s$, from which we conclude that f is monotonically decreasing. This implies that S acts as a transcription inhibitor. In the slow Pol II mutant, we observe $\lambda_g = \lambda_g$

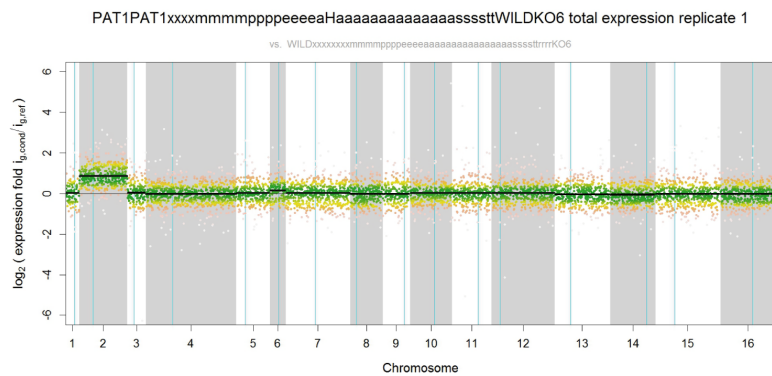
. Using a similar argument as above and equation 4.3 and cDTA data of the slow Pol II mutant, we conclude that h is monotonically increasing, implying that D is a degradation enhancer. These conclusions could only be derived because cDTA enables the comparison of global synthesis and decay rates. The results would be identical if S and D were the same molecule. Thus, the most simple explanation of our observations is the existence of a factor that serves as an inhibitor of transcription and an enhancer of degradation, and shuttles between the nucleus and cytoplasm.

4.2 Global analysis of eukaryotic mRNA degradation reveals Xrn1-dependent buffering of transcript levels

4.2.1 Global analysis of mRNA degradation

We gathered cDTA data from *S. cerevisiae* BY4741 strains during logarithmic growth in YPD media (Table 2.1). Strains were verified by PCR and growth on selective media (**Methods**). cDTA was carried out as described (Sun et al., 2012). Briefly, RNA was metabolically labeled with 4sU for 6 minutes and 2.25×10^8 cells were mixed with 0.75×10^8 cells from labeled *Schizosaccharomyces pombe* culture that provided an internal standard. Strain ploidy was analyzed by plotting the levels of total RNA per chromosome (Figure 4.17). This uncovered nine aneuploid mutant strains, six of which we could regenerate with normal ploidy, whereas the others had to be excluded. For strains that showed more than a two-fold difference in total RNA, chromosome copy number was analyzed by FACS and polyploid strains were excluded. From each strain, at least two biological replicates were measured. The Spearman correlation of replicate measurements was always close to 1. With the use of our previously described algorithm (Sun et al., 2012), we obtained a high quality dataset including for each strain the median SR and DR, the total mRNA levels, the SRs based on labeled mRNA, and the DRs, which will be deposited in ArrayExpress after publication.

A



B

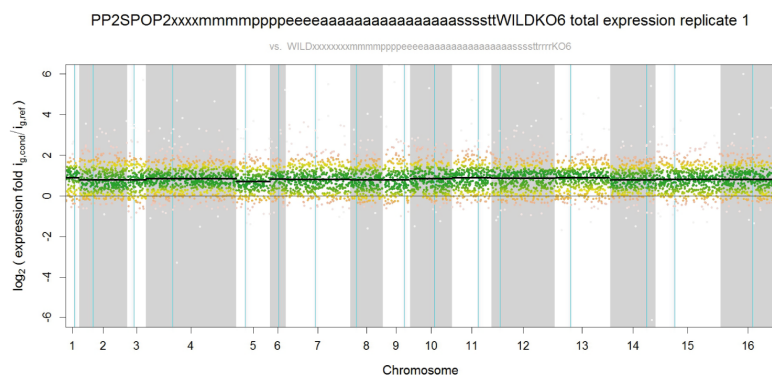


Figure 4.17: **Scatter plots show the aneuploidy of mutant** The expression level of genes in *pat1Δ* is plotted to their position in chromosomes. **(A)** shows that the aneuploid strain has two folds overexpression of genes on Chr II compared to the median level of all other genes. **(B)** is the strain used in this study. The the strain *pop2Δ* in previous section was checked by this procedure and found to have a chromosome IIX aneuploidy. A new knock-out strain was generated by homologous recombination and measured by cDTA. The new data does not change any of the conclusions in the previous section

4.2.2 Generality of mRNA level buffering

When we plotted the changes in median SRs against changes in median DRs for each mutant strain, the data points scattered along the main diagonal (Figure 4.18). Thus changes in DRs that were induced upon mutation were generally compensated by changes in SRs. To assign a significance level to these changes, we fitted a bivariate Gaussian distribution to the pooled median SR and DR estimates of a total of 228 *S. cerevisiae* samples after normalization to their *S. pombe* references, including 18 biological wild-type replicates. Data points outside the resulting 95% confidence region (grey ellipse in Figure 4.18) indicate significant changes in global SR and/or DR, since they do not result from random fluctuations. The high precision of our measurements revealed even mild effects of most mutations under optimum growth conditions (standard deviation for changes in SR is 0.22, and for changes in DR is 0.24). Of the 46 strains analyzed, 7 showed strong effects with median SR or DR changes above two-fold, whereas 16 strains did not show significant rate changes. Most strains maintained similar mRNA levels (Figure 4.19A) demonstrating the generality of mRNA level buffering.

4.2.3 mRNA level buffering requires Xrn1p activity

The analysis revealed a single strong outlier, the strain lacking the exonuclease Xrn1p (Figure 4.18). In this strain, the median DR was decreased by 2-fold relative to wild type, but the median SR was increased by 1.6-fold. As a result, mRNA levels increased 3.2-fold (Figure 4.19A), showing that the buffering mechanism was defective. Thus Xrn1p stimulates global mRNA degradation as expected, but its absence showed an unexpected positive effect on mRNA synthesis, rather than a negative effect that would be required for buffering. The apparent repression of mRNA synthesis cannot be explained by stabilization of labeled RNAs, since our SR estimator accounts for the degradation of labeled RNA. To quantify the mRNA buffering capacity of mutant strains, we introduced the buffering index (BI), which is calculated as follows:

$$BI = 1 - \frac{T_{mutant} - T_{wt}}{T_{theoretical} - T_{wt}} \quad (4.4)$$

In this equation, T_{mutant} and T_{wt} are the measured median total mRNA levels of the mutant and the wild type, respectively. $T_{theoretical}$ is the theoretically obtained total

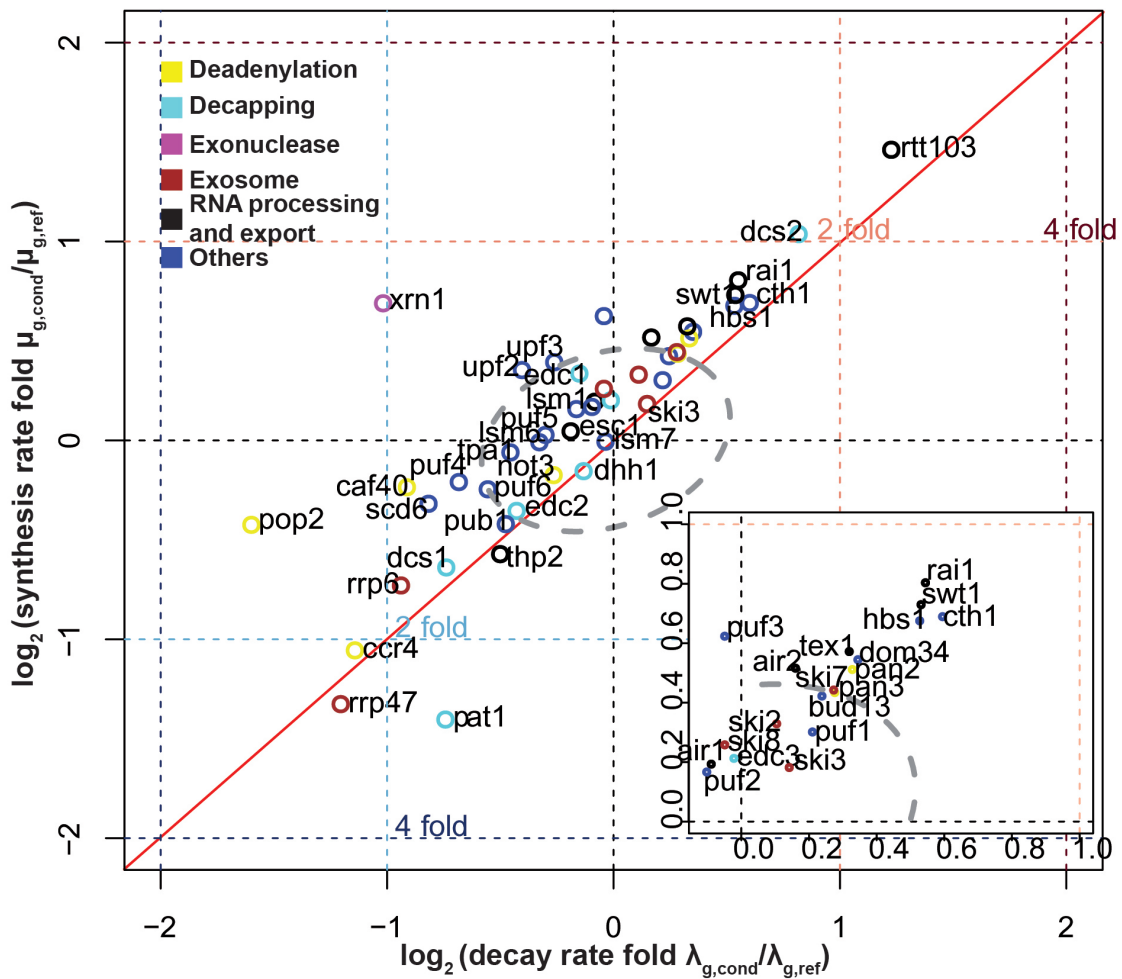
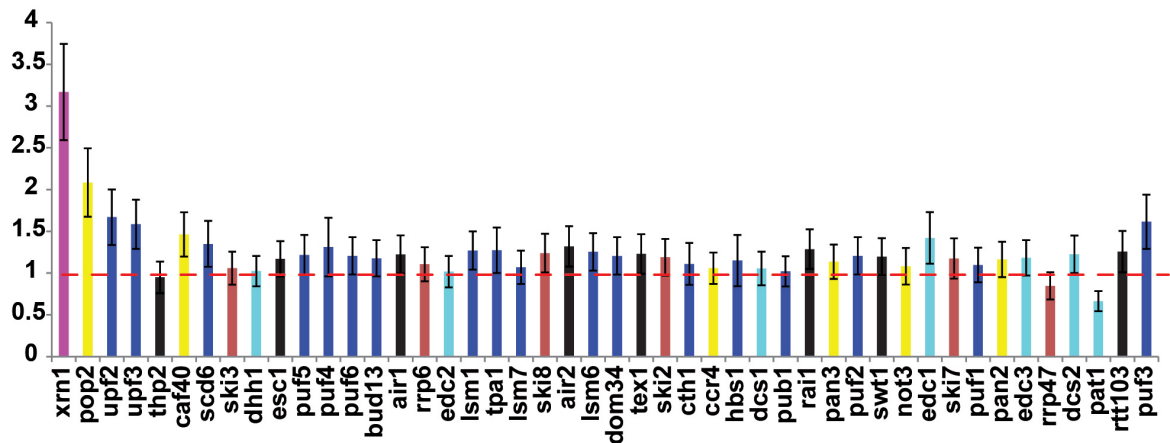


Figure 4.18: **Global view of changes in mRNA DRs and SRs** Scatter plot showing global changes in mRNA DRs (log fold of median mRNA decay rates in mutant versus wild type, x-axis) and SRs (log fold of median mRNA synthesis rates in mutant versus wild type, y-axis) in 46 yeast deletion strains. The centre of each circle is determined by the median DR and SR of the strain. The grey ellipse indicates the 95% confidence region.

A Total mRNA fold changes



B Buffering index

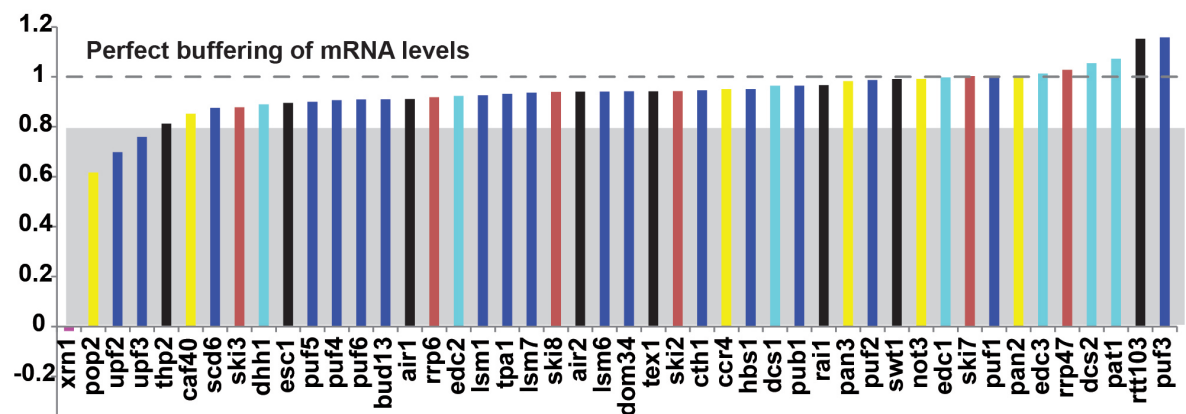


Figure 4.19: **The ability of mutants to keep its total mRNA level (A)** Bar plot depicting changes in global mRNA level in 46 yeast deletion strains. A mRNA level change of 1 indicates that global mRNA levels of the mutant and wild-type strains are the same. **(B)** Bar plot depicting the buffering index (BI). BI is 1 when mRNA level buffering is perfect. BI is between 0 and 1 when mRNA level buffering is partial. BI of 0 or below 0 indicates that there is no mRNA level buffering.

RNA level that would result from impaired degradation but unaffected synthesis, i.e. in the absence of buffering. The ratio $(T_{mutant}-T_{wt})/(T_{theoretical}-T_{wt})$ measures the change in total mRNA relative to the expected change assuming no buffering. Thus the BI measures the fraction of the expected total mRNA change that has been buffered. A BI of 1 indicates perfect buffering, i.e. changes in DR are entirely compensated by changes in SR. Out of the 46 mutant strains, 42 showed a BI above 0.8, three showed a BI between 0.6 and 0.8, and only the *xrn1* Δ mutant had a BI close to zero (Figure 4.19B). Xrn1 thus exhibits the features predicted for a factor involved in mRNA buffering; it is an mRNA degradation factor with a negative effect on mRNA synthesis (Sun et al., 2012). To investigate the role of Xrn1p in the buffering mechanism, we prepared a yeast strain (*xrn1pm*) with two point mutations in the Xrn1p active site (D206A, D208A) that abolish exonuclease activity (Solinger et al., 1999). We collected a cDTA profile for the *xrn1pm* strain and compared it to an isogenic wild-type strain (Methods). The median DR was decreased to 36%, similar as in the *xrn1* Δ strain, but the median SR remained unchanged, leading to a 2.6-fold increase in total mRNA levels (Figure 4.20). These results demonstrate that the catalytic activity of Xrn1p is responsible for the decrease in DRs and is required for mRNA level buffering.

4.2.4 Xrn1p represses mRNA synthesis indirectly

The median SR differed between the *xrn1* Δ strain and the *xrn1pm* strain (Figure 4.20), suggesting that Xrn1p represses mRNA synthesis and that this function is independent of its catalytic activity. To investigate this, we depleted Xrn1p from the nucleus using the anchor-away technique (Haruki et al., 2008) and monitored changes in SR and DR. We generated an Xrn1p anchor away (*XRN1-AA*) strain in which Xrn1p was fused with a FKBP-rapamycin binding (FRB) domain in a strain containing the ribosomal protein RPL13A fused to the FKBP12 receptor of rapamycin (Haruki et al., 2008). Upon rapamycin addition, the Xrn1-FRB fusion protein was pulled out of the nucleus. When the *XRN1-AA* strain was grown in media supplemented with rapamycin the median SR was increased 1.5-fold during mid-log growth phase (Figure 4.21), in agreement with a 1.6-fold increase in the *xrn1* Δ strain. The median DR was increased 1.9-fold, possibly due to increased cytoplasmic Xrn1 levels.

These results were consistent with a nuclear function of Xrn1p in repressing mRNA synthesis, and with reports that Xrn1p interacts with nuclear proteins such as histones (Gilmore et al., 2012; Lambert et al., 2009) and the Nrd1-complex (Gavin et al.,

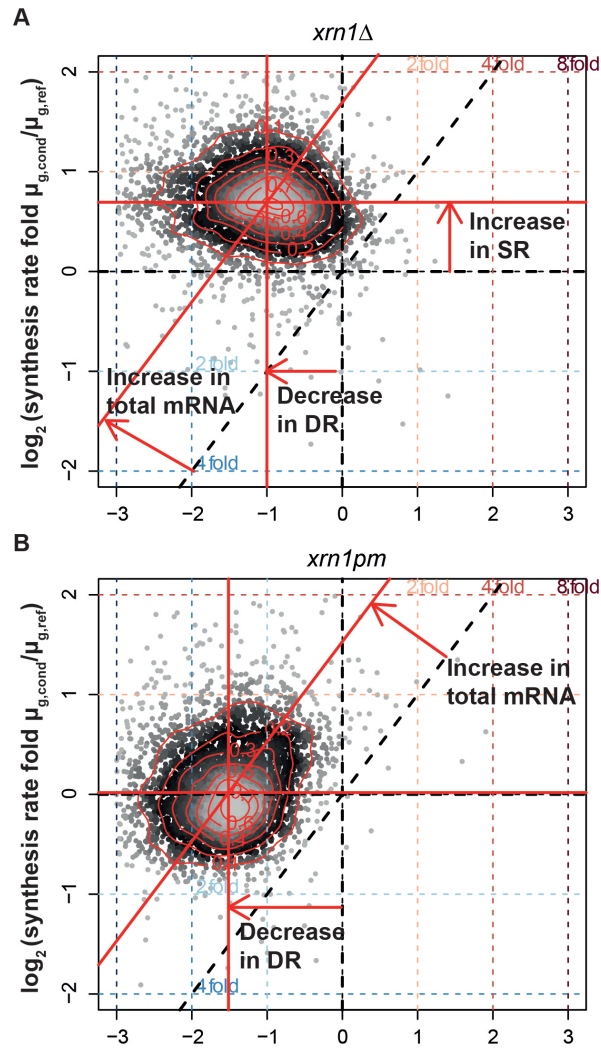


Figure 4.20: *xrn1Δ* strain show anti-compensation effect (A) Scatter plot with changes in mRNA SRs (log fold, y-axis) and DRs (log fold, x-axis) in the *xrn1Δ* deletion strain. Each point corresponds to one mRNA. The density of points is encoded by their brightness (grey scale). Contour lines define regions of equal density. A global shift in the median DR is indicated by the shift of the horizontal red line relative to the dashed x-axis line. Arrows indicate change in global SR (vertical), DR (horizontal), and mRNA level (diagonal). (B) Scatter plot as in (A) but for the *xrn1pm* strain relative to its isogenic wild-type strain *XRN1*.

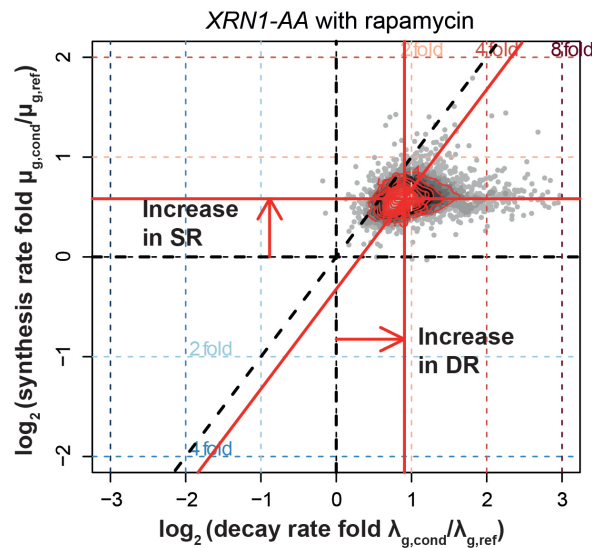


Figure 4.21: Scatter plot as in (Figure 4.20) but showing the changes in the *XRN1AA* strain after treatment with rapamycin compared to the untreated strain.

2006). However, we did not detect association of Xrn1p with the constitutively transcribed genes *ADH1*, *ILV5*, and *RPS11A* by means of chromatin immunoprecipitation *in vivo*. Also, Xrn1 was not required for activator- and promoter-dependent transcription *in vitro*, since nuclear extracts from *xrn1Δ* cells were active in transcription assays (Methods, Figure 4.22). In these assays, addition of TAP-purified Xrn1p protein or the catalytically inactive Xrn1pm variant did not change the activity of transcription. These results indicated that Xrn1p has a nuclear function, but argue against a direct function in mRNA synthesis.

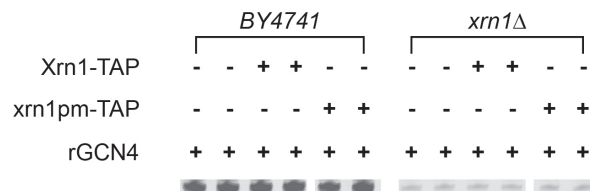


Figure 4.22: **Purified Xrn1p cannot inhibit transcription *in vitro*** The *in vitro* transcription assay carried out using nuclear extract from BY4741 (left column) and *xrn1Δ* (right column). TAP purified Xrn1p and xrn1pm has added to the assay separately. RNase inhibitor was added to inhibit the interior RNase and the RNase activity of Xrn1p. No difference was observed in the Gcn4p activator dependent transcription activity *in vitro* from *HIS4* promoter.

4.2.5 Induction of transcription repressor Nrg1p

Since Xrn1p does not directly affect transcription, we searched for nuclear factors that may inhibit mRNA synthesis in an Xrn1p-dependent manner. We investigated DR-dependent changes in SRs of transcription repressors. We observed that the SRs for the gene encoding the transcription repressor Nrg1p (Vyas et al., 2005) were increased in the *xrn1* Δ strain and in several other strains with decreased global DR (*xrn1pm*, *ccr4* Δ , *pop2* Δ , *pat1* Δ , *dhh1* Δ , Figure 4.23). Vice versa, the SR of *NRG1* mRNA was

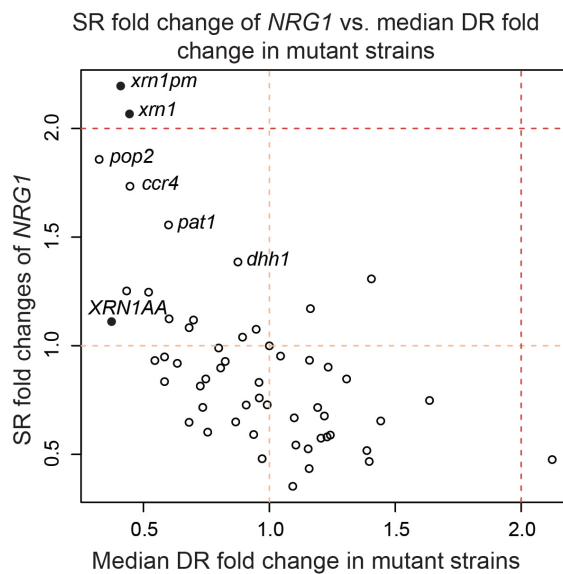


Figure 4.23: **The SR of the transcription repressor *NRG1* is anti-correlated with the median DR of the yeast deletion strains** The x-axis represents the median DR fold changes of the strains compared to BY4741. The y-axis represents the SR fold changes of the transcription repressor *NRG1* in the strains compared to BY4741

repressed in mutants with increased median DR such as *dcs1* Δ and *rtt103* Δ . The general significance of these changes is revealed by an anti-correlation between changes in SR of *NRG1* mRNA with the median DR of the mutant strain (Spearman's correlation -0.61 , $R^2 = 0.41$) (Figure 4.23). These results suggested that Nrg1p could be part of the buffering machinery. To investigate the relationship between Xrn1p and Nrg1p, we induced overexpression of Nrg1p in wild-type and *xrn1* Δ mutant yeast cells (Figure 4.24). Overexpression of Nrg1p in wild-type cells led to a slow-growth phenotype, as expected for a transcription repressor. However, there was no additive effect observed when Nrg1p was overexpressed in *xrn1* Δ cells, indicating that repression of transcrip-

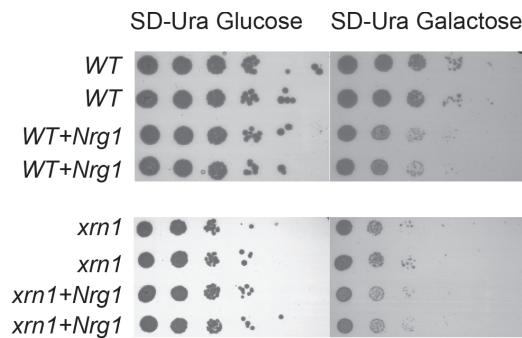


Figure 4.24: **Nrg1p overexpression leads to a slow-growth phenotype** Cultures of wild-type and *xrn1* Δ transformed with pRS316 or *GAL-NRG1* were grown in SD-URA medium at 30°C overnight and diluted to an OD₆₀₀ of 1 with fresh medium. The same amount of cells was spotted on plates in 10-fold serial dilutions. Plates were incubated for 4 days at 30°C and inspected daily.

tion by Nrg1p requires Xrn1p, and consistent with the model that Xrn1p is part of the buffering machinery.

4.2.6 Delayed mRNA buffering upon degradation inhibition

These results suggested that down-regulation of mRNA degradation triggers the expression of transcription repressor Nrg1p that subsequently down-regulates mRNA synthesis and establishes mRNA level buffering. If true, mRNA level buffering would occur in a time-delayed manner after conditionally impairing mRNA degradation. To test this, we down-regulated mRNA degradation with the use of cycloheximide, a translation elongation inhibitor that impairs mRNA degradation (Hu et al., 2009). We added cycloheximide to cells during the mid-log growth phase at a low concentration of 0.1 $\mu\text{g}/\text{mL}$, which has almost no effect on cell growth, and used cDTA to quantify changes in SRs and DRs after 10 and 60 minutes of treatment.

The median DR was decreased to 65% after ten minutes of cycloheximide treatment, and to 12% after 60 minutes (Figure 4.25). This confirmed the generality of translation-coupled mRNA degradation (Hu et al., 2009). The median SR remained essentially unchanged after 10 minutes of cycloheximide treatment, but was strongly decreased to about 37% after 60 minutes (Figure 4.25). This demonstrated for the first time that mRNA level buffering occurs in wild-type cells. Remarkably, the SR for NRG1 mRNA showed a dramatic 7.1-fold increase after 60 minutes of cyclohex-

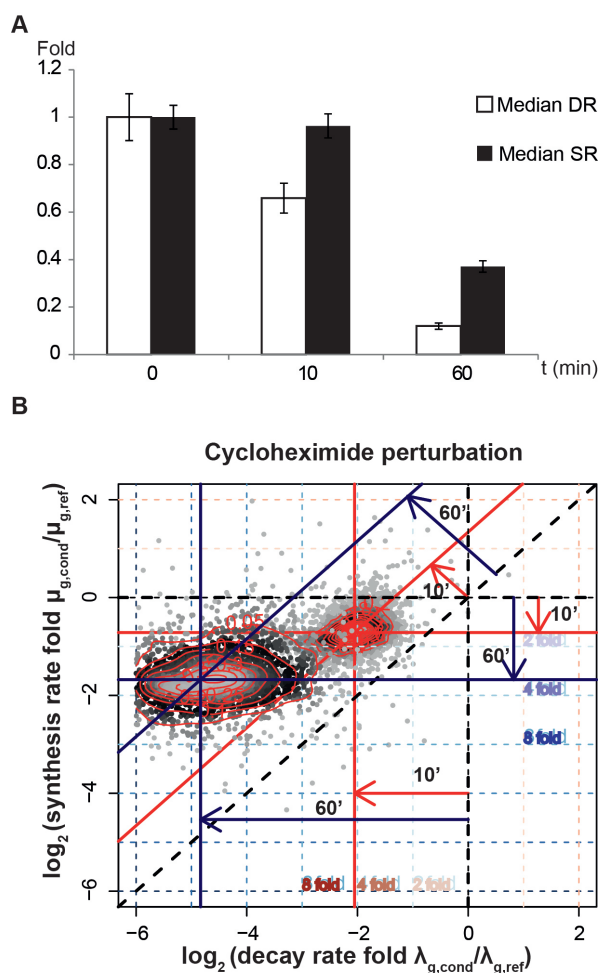


Figure 4.25: **Cycloheximide perturbation lead to synthesis compensation (A)** Time-dependent changes in median DRs and SRs upon cycloheximide perturbation. **(B)** Scatter plot comparing changes in SRs (log fold, y-axis) and DRs (log fold, x-axis) upon degradation inhibition by cycloheximide perturbation in wild-type yeast after 10 minutes (red lines) and 60 minutes (blue lines) (depicted as in Figure 4.20). The center of the distribution of 10 minutes treatment is located at (-0.62, -0.054), indicating that there is a global shift in the median DR by 0.28-fold, and a global shift in the median SR by 0.61-fold. The total mRNA levels change 2.22-fold globally. The center of the distribution of 60 minutes treatment is located at (-3.06, -1.43), indicating that there is a global shift in the median DR by 0.06-fold, and a global shift in the median SR by 0.35-fold. The total mRNA levels change globally by 2.68-fold.

imide treatment, in contrast to the general decrease in SRs observed for most mRNAs. These results demonstrate time-delayed mRNA level buffering and synthesis induction of transcription repressor Nrg1p upon inhibition of mRNA degradation, and are consistent with the indirect role of Xrn1p in the buffering mechanism.

4.2.7 Rapid buffering upon mRNA synthesis inhibition

The above results indicated that mRNA level buffering following impaired mRNA degradation is delayed, due to transcription repressor induction. To test whether mRNA buffering following impaired mRNA synthesis is also delayed, we treated wild-type cells with 1,10-phenanthroline, an inhibitor of mRNA synthesis, and monitored changes in SRs and DRs. We added 1,10-phenanthroline to cells at mid-log growth at a concentration of 25 $\mu\text{g}/\text{mL}$, which is typically used to arrest transcription (Dori-Bachash et al., 2011), and carried out cDTA after 18 minutes of treatment. The median SR was decreased to 38% of the untreated level, as expected after transcription inhibitor treatment (Figure 4.26). The median DR was also strongly decreased to 29% after 18

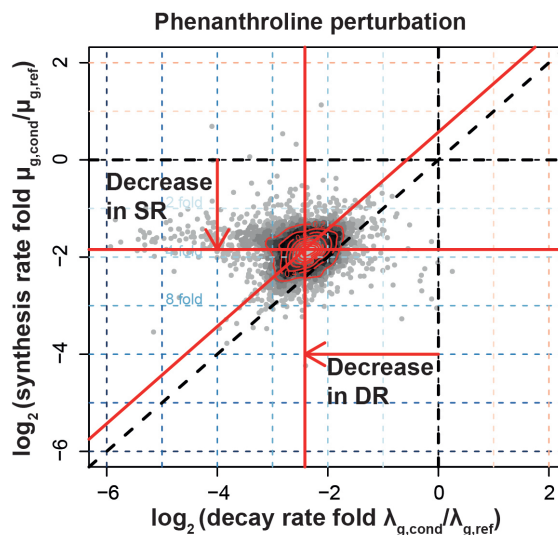


Figure 4.26: **Phenanthroline perturbation leads to decay compensation** Scatter plot as in (Figure 4.25B) but upon mRNA synthesis inhibition by phenanthroline perturbation after 18 minutes. There is a global shift in the median DR by 0.29-fold, and in the median SR by 0.378-fold. The total mRNA levels are essentially unchanged.

minutes. This demonstrated that conditional inhibition of mRNA synthesis leads to a

rapid decrease in mRNA degradation rates and mRNA level buffering.

4.2.8 Cluster analysis reveals mRNA degradation complexes

Our data not only led to the key discovery of Xrn1p as a factor for mRNA level buffering, but also provide a wealth of information on interactions between mRNA degradation factors and on their general and gene-specific functions (Figures 4.27). Cluster analysis of the mutant strains based on their DR changes (Figures 4.27), was

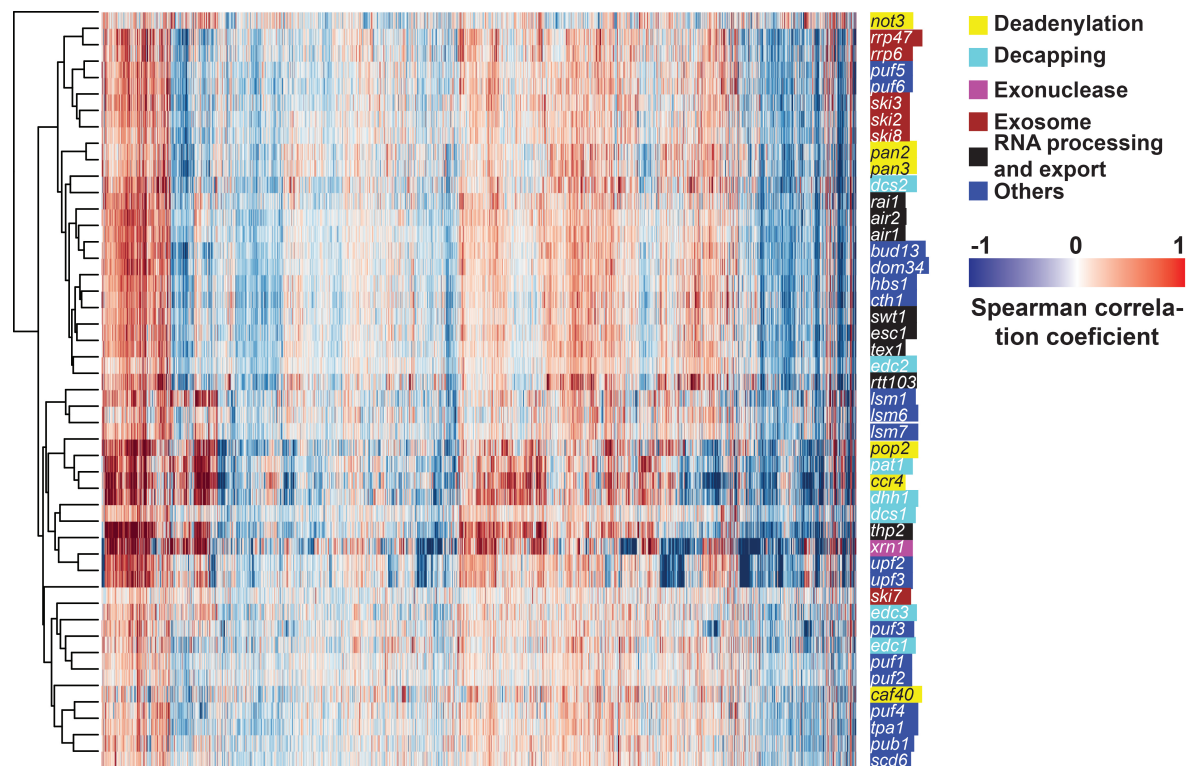


Figure 4.27: **Cluster analysis of DR profiles of the 46 deletion strains** The pairwise Spearman correlation was used for average-linkage, Euclidean distance-based hierarchical clustering of the mutants (rows) and 2761 genes (columns) with highest variance (> 0.01). The color code indicates DR changes from red (increased DR) to blue (decreased DR).

translated into a two dimensional network plot (Figures 4.28), in which the distances between nodes are given by the Spearman correlation coefficient ($R_{\zeta 0.5}$). This revealed known functional relationships between factors. Mutants cluster together when

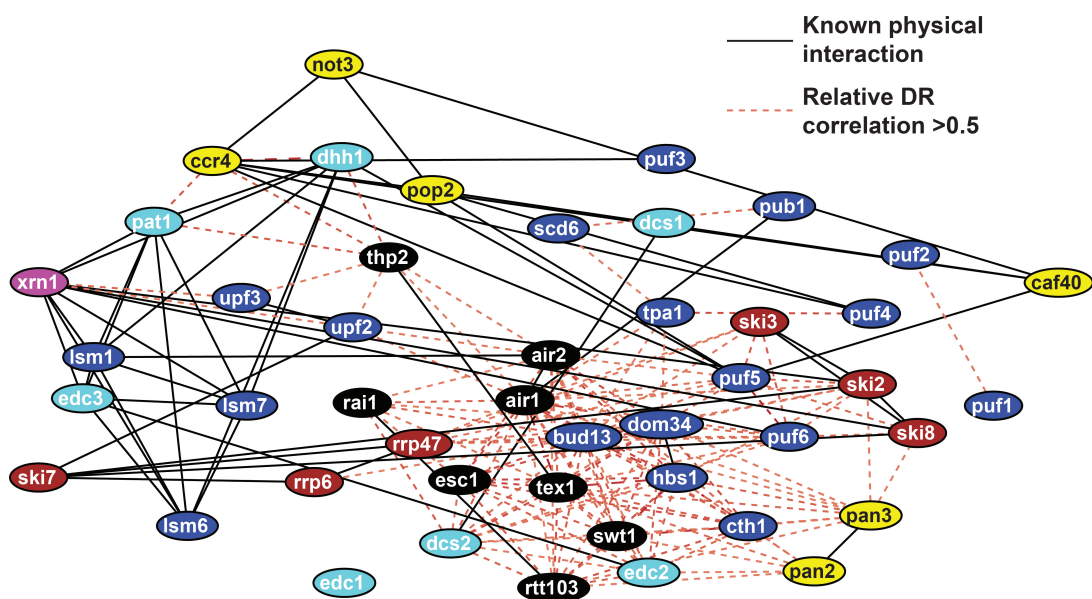


Figure 4.28: **Two-dimensional network representation of correlation analysis of deletion strains reveals functional interactions** Two-dimensional network representation of the correlations in (Figures 4.27) (1-Spearman correlation coefficients) used as a distance metric. Proximity of nodes indicates strong positive correlation (Spearman correlation coefficients >0.5). The black solid lines represent known physical interactions (STRING database) and the red dashed lines represent positive correlations.

they lack subunits of a known physical multisubunit complex, such as the Ccr4-Not complex (Ccr4p and Pop2p Spearman correlation coefficient, $R=0.67$), the Lsm complex (Lsm1p, Lsm6p and Lsm7p, $R>0.5$), the Ski complex (Ski2p, Ski3p and Ski8p, $R>0.62$), the exosome (Rrp6p and Rrp47p, $R=0.75$), components in the TRAMP complex, the zinc-knuckle orthologs Air1p and Air2p ($R=0.66$), the No-Go mRNA decay complex (Hbs1p and Dom34p, $R=0.67$) (Becker et al., 2011), and the UPF-EJC complex involved in nonsense-mediated decay (Upf2p and Upf3p, $R=0.80$). Factors with similar cellular functions build up sub-clusters, such as the deadenylase subunits Pan2p and Pan3p ($R=0.78$) and the decapping enhancers Dhh1p and Pat1p ($R=0.70$). Cluster analysis also recovers known genetic interactions between factors, for example between Swt1p, Ecs1p, and Tex1p ($R > 0.60$) (Skružný et al., 2009) (Figures 4.27). Thus the cluster analysis reliably reveals known interactions between degradation factors in functional complexes, and can be used to detect novel interactions.

4.2.9 General mRNA degradation machinery

We observe correlations of DR changes in strains with deletions of the Ccr4-Not complex subunits, Xrn1p, Pat1p, Dhh1p, the Lsm complex (Figures 4.27, 4.28, and 4.29). This indicates that the general mRNA degradation machinery that has been identified biochemically is responsible for global mRNA turnover and comprises the Ccr4-Not deadenylase complex, the Xrn1p 5'-exonuclease, and the decapping activator Pat1p, and thus apparently the decapping complex Dcp1-Dcp2, which we could not include in our analysis due to its essential nature. Our cluster analysis additionally indicates that the THO transcription elongation complex and the scavenger decapping factor Dcs2p are components of a general degradation machinery. The Ski complex subunits Ski2p, Ski3p and Ski8p cluster, consistent with formation of a stable complex (Synowsky and Heck, 2008; Wang et al., 2005) that cooperates with the exosome (Araki et al., 2001). In contrast, the Ski7p subunit deletion results in a different profile (Spearman correlation < 0.15 to Ski2p, Ski3p, and Ski8p), suggesting a peripheral location and functional differences for this subunit (Araki et al., 2001). The three Edc proteins apparently have gene-specific functions.

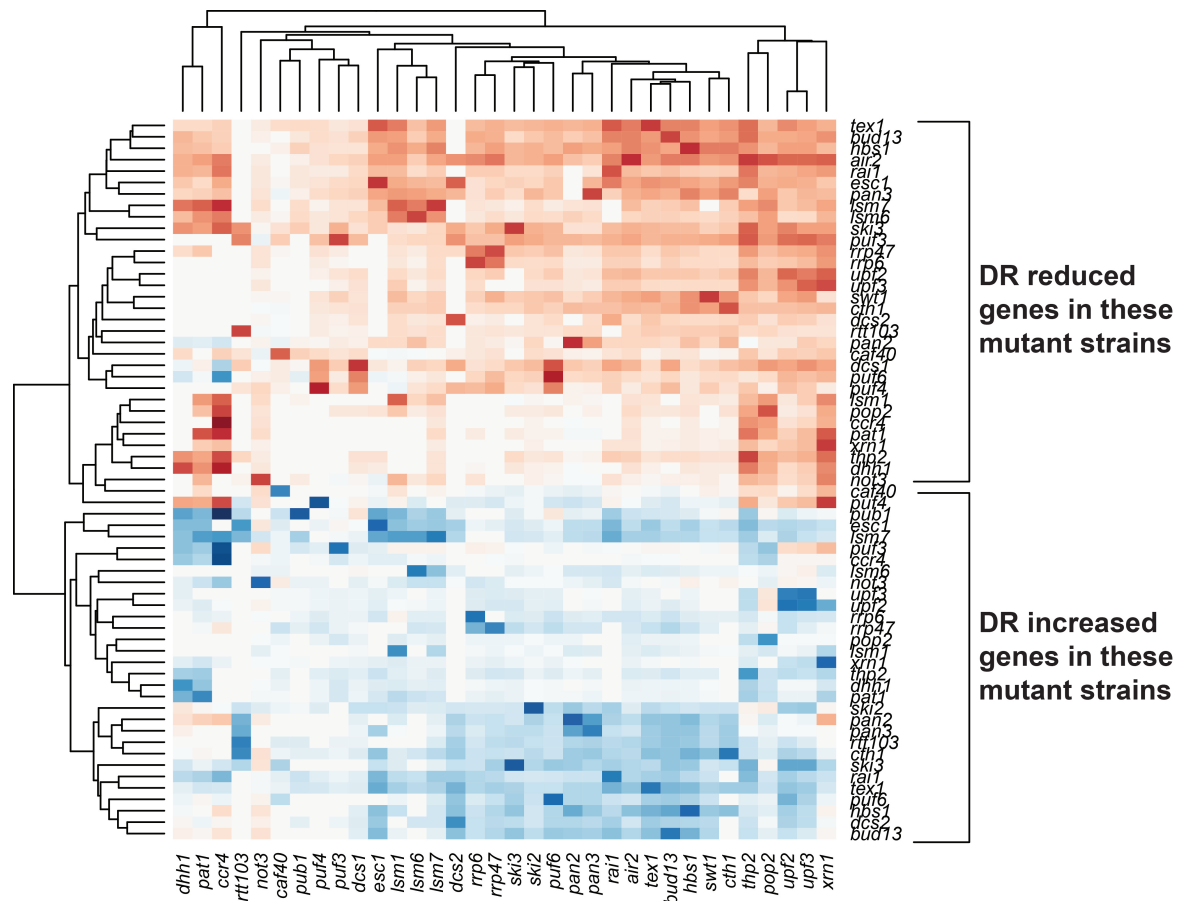


Figure 4.29: **Cluster analysis provides evidence for a general mRNA degradation machinery.** The plot shows the color-coded median t-statistics of DRs of mRNAs that show significantly decreased or increased DRs in the gene deletion strains shown on the x-axis. The t-statistics gives the ratio of the difference in mean DR and its standard errors as a measure for differential stabilization (decreased/increased DR). Destabilization (increased DR) is shown in red, stabilization (decreased DR) in blue. The overall directionality of perturbed degradation indicates a general mRNA degradation machinery.

4.2.10 Deadenylase complexes differ in substrate preference

The cluster analysis also reveals differences between the two mRNA deadenylase complexes Ccr4-Not and Pan2-Pan3. Deletion of Ccr4-Not complex subunits leads to strong degradation defects, whereas deletion of Pan2p or Pan3p has mild effects (Figures 4.18). In addition, the DR changes are not correlated ($R < 0.05$ between Ccr4p and Pan2/3p), indicating different mRNA substrate preferences of the two complexes. The mRNAs that show a decreased DR in *pan2* Δ and *pan3* Δ strains are not strongly influenced by deletion of Ccr4-Not complex subunits, or their DR is even higher (Figure 4.27 and 4.29). The deadenylation mechanism may be different in human, where Pan2-Pan3 initiates deadenylation (Boeck et al., 1996; Yamashita et al., 2005), whereas the bulk of the tail is digested by the Ccr4-Not complex (Bai et al., 1999; Collart, 2003). The analysis further showed that DR changes observed upon deletion of the Caf40p subunit of the Ccr4-Not complex do not correlate with other complex subunits ($R < 0.07$ between Caf40p and Ccr4p/Not3p), in agreement with a previous description of functional modules in the Ccr4-Not complex (Cui et al., 2008). The analysis also reveals a functional interaction of the Pan2-Pan3 complex with the Tex1p subunit of the TREX complex ($R > 0.55$), which is involved in mRNA export (Str  ber et al., 2002).

4.2.11 Scavenger decapping factors Dcs1p and Dcs2p are global antagonists

For mRNA molecules that were not decapped but degraded from the 3'-end by the exosome complex, the scavenger decapping enzyme clears up the residual 5'-portion of the RNA (Liu et al., 2002; Muhlr  d et al., 1995). Our data show that the *S. cerevisiae* scavenger decapping enzyme Dcs1p and its inhibitor Dcs2p function globally, since all DRs are changed, and that their function is globally antagonistic (Figure 4.30). In the *dcs1* Δ strain, the median DR is decreased 1.7-fold, whereas it is increased 1.8-fold in the *dcs2* Δ strain (Figure 4.30). This is consistent with a general role of Dcs1 in mRNA degradation (Liu and Kiledjian, 2005), and reveals a general role of Dcs2p in inhibiting Dcs1p that is not restricted to stress conditions (Malys and McCarthy, 2006). The DR profiles of *dcs1* Δ and *dcs2* Δ mutant strains were slightly correlated (Figure 4.27), consistent with the fact that Dcs2p does not contribute to the substrate specificity, and only globally represses the enzymatic activity of Dcs1p.

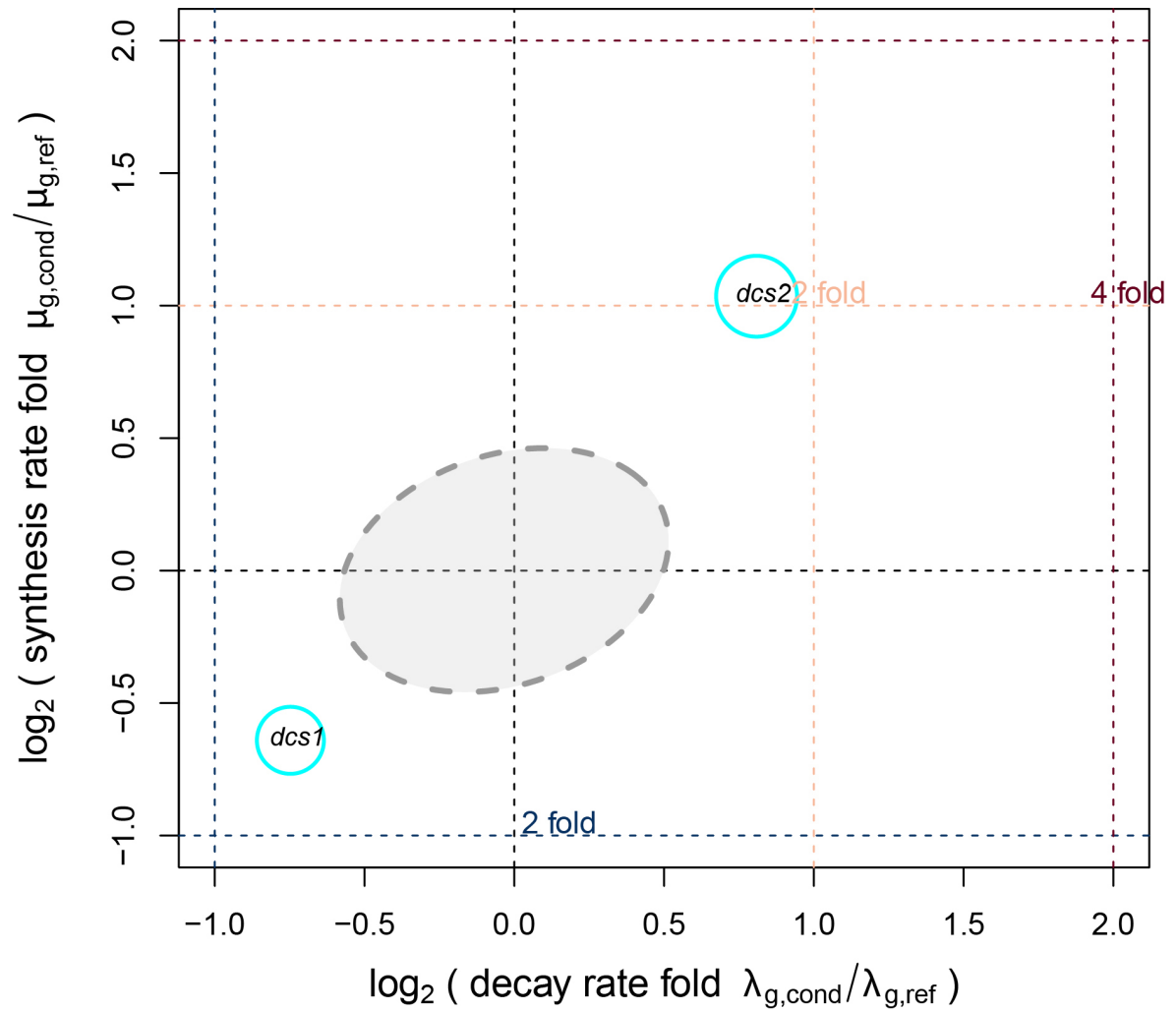


Figure 4.30: **Antagonistic effect in *dcs1* Δ and *dcs2* Δ .** Scatter plots show global changes in mRNA DRs (log fold, x-axis) against the global changes in SRs (log fold, y-axis). The global changes of *dcs1* Δ and *dcs2* Δ are plotted. The coordinate of the center of each circle is determined by the median DR and SR of the mutant. The diameters of the circles represent the relative comparison of the fold of RNA amount over wild-type level.

4.2.12 An interwoven mRNA surveillance network

In the nucleus, aberrant RNAs are recognized by TRAMP complexes, which add a poly(A) tail to enable exosome-dependent degradation (Vaňáčová et al., 2005). The subunits Air1p and Air2p are part of two distinct TRAMP complexes, and determine the substrate specificity of the nuclear exosome (Paolo et al., 2009; Schmidt et al., 2012). In the cytoplasm, an mRNA that causes the ribosome to stall is subjected to No-Go decay (Shoemaker and Green, 2012), which involves the factors Dom34p and Hbs1p, and mRNAs that contain a nonsense codon are subjected to nonsense-mediated decay (NMD), which involves the factors Upf2p and Upf3p.

Aberrant nascent RNAs with an incomplete cap structure are degraded by the 5'-exonuclease Rat1 and its cofactor Rai1 (Schmid and Jensen, 2010). Rai1p and its associated factor Rtt103p cluster with Air1p, Air2p, Esc1p, Tex1p, and Bud13p ($R > 0.5$). This cluster involves the TRAMP-dependent perinuclear mRNP surveillance system (Skružný et al., 2009), the mRNA export complex (Sträßer et al., 2002), and factors involved in pre-mRNA splicing and retention.

Our cluster analysis suggests a functional interaction between Air1-Air2 and Dom34-Hbs1 ($R > 0.65$) and Upf2-Upf3 ($R > 0.46$), but factors involved in No-Go decay and NMD do not correlate. Air1-Air2 and Hbs1-Dom34 cluster with Tpa1p, a putative translation termination factor (Keeling et al., 2006), indicating Tpa1p as a translation termination factor for No-Go decay. The Tpa1p DR profile resembles those of the poly(A)-binding protein Pub1p ($R = 0.49$) and the inhibitor of translation initiation Scd6p ($R = 0.51$) (Rajyaguru et al., 2012; Ruiz-Echevarría and Peltz, 2000). Surprisingly, the mRNA-binding factor Cth1p, which plays an important role in iron response (Sanvisens et al., 2011), also show high correlation to Dom34p, Hbs1p and Swt1p ($R > 0.65$), suggesting a role in mRNA surveillance. Upf2p and Upf3p cluster with Pub1p, which is involved in NMD (Ruiz-Echevarría and Peltz, 2000), and with Puf6p, one of six Puf proteins in yeast, Puf1-Puf6, which have distinct functions (Gerber et al., 2004; Goldstrohm et al., 2007; Miller and Olivas, 2011) and show differences in mRNA substrate preference. These findings suggest a redundant mRNA surveillance system with interconnected activities.

Chapter 5

Discussion

5.1 cDTA reveals mutual feedback loop of transcription and degradation of mRNA

A systemic investigation of gene expression requires quantitative monitoring of cellular mRNA metabolism. In particular, a technique is required to quantify absolute mRNA synthesis and decay rates on a genome scale upon genetic perturbation. Here we provide such a technique that we refer to as comparative Dynamic Transcriptome Analysis (cDTA). cDTA is based on non-perturbing metabolic RNA labeling in mutant and wild type budding yeast cells, and the use of fission yeast cells as an internal standard. cDTA is a non-perturbing method for monitoring mRNA turnover and supersedes conventional methods, which require transcription inhibition, resulting in a stress response and perturbation of mRNA metabolism.

cDTA improves our previous DTA protocol (Miller et al., 2011) in several respects. First, cDTA provides reliable estimates of the absolute synthesis and decay rates, thereby allowing for a direct comparison of rates between different yeast strains. Second, cDTA uses 4tU instead of 4sU for RNA labeling, allowing for standard media and abolishing the need for a nucleoside transporter. Third, cDTA requires only two instead of three microarray measurements per rate estimation. As an immediate result, cDTA revealed that *S. pombe* and *S. cerevisiae* cells have similar synthesis rates, but Sp RNAs have about five-fold longer mRNA half-lives, leading to similar cellular mRNA concentrations despite a different cell volume.

Application of cDTA to Sc cells expressing a Pol II point mutant that elongates mRNA

slowly in vitro showed that mRNA elongation is a critical determinant for mRNA synthesis in growing cells in vivo. It also revealed that cells compensate for low synthesis rates by lowering decay rates, thus stabilizing mRNAs and buffering their levels. Application of cDTA to two mutant strains that lack either one of the two catalytic subunits of the mRNA deadenylase complex Ccr4-Not showed not only the expected defect in mRNA degradation but also a compensatory decrease in mRNA synthesis, also leading to a buffering of mRNA levels. This indicated the existence of a feedback loop that connects mRNA synthesis and degradation, and serves to buffer mRNA levels. These results support published evidence for a global control of mRNA levels in dependence of cell size (Zhurinsky et al., 2010). This global control of mRNA levels occurs despite the separation of mRNA synthesis and degradation into nuclear and cytoplasmic compartments.

The mechanisms underlying the synthesis-decay feedback loop and the buffering of mRNA levels are unclear. The feedback loop may be a result of a physical and functional coupling between the various parts of mRNA metabolism. Transcription is coupled to mRNA processing and export (Maniatis and Reed, 2002), and translation is coupled to mRNA degradation (Bregues et al., 2005; Coller and Parker, 2004, 2005; Hu et al., 2009). There is also evidence that nuclear and cytoplasmic mRNA metabolism are linked. The Pol II subcomplex Rpb4/7p shuttles between the nucleus and cytoplasm (Selitrennik et al., 2006), and is involved in transcription (Edwards et al., 1991) and mRNA translation and degradation (Harel-Sharvit et al., 2010; Lotan et al., 2005, 2007). The Ccr4-Not complex is involved in mRNA degradation (Tucker et al., 2002), but also in transcription (Collart, 2003; Collart and Timmers, 2004; Kruk et al., 2011; Liu et al., 1998). From an extension of our kinetic model of mRNA turnover, we propose that the feedback loop is established by a factor that acts as degradation enhancer and a transcription inhibitor. It is thus unlikely that factors that act positively on transcription, such as Rpb4/7p and the Ccr4-Not complex, are the feedback factors, although the validity of our model's assumptions remains to be shown. This question was addressed in my subsequent work.

5.2 Global analysis of mRNA degradation indicates Xrn1p as a buffering factor

We present a global analysis of changes in cellular mRNA synthesis and degradation rates upon deletion of 46 factors involved in eukaryotic mRNA turnover. The significance of the obtained data set is twofold. First, it demonstrates the generality of mRNA level buffering in a eukaryotic cell and implicates the exonuclease Xrn1p and the transcription repressor Nrg1p in the buffering mechanism. Second, it is a resource providing a wealth of information on the global and gene-specific function of factors involved in mRNA degradation and related processes, and the functional interactions between these factors.

This study shows that Xrn1-dependent mRNA level buffering is contributing to the robustness of genome expression, and elucidates the mechanisms underlying this phenomenon. Our results suggest a simple model that may explain mRNA level buffering (Figure 5.1). A simple feedback loop may link the level of XRN1 mRNA with its

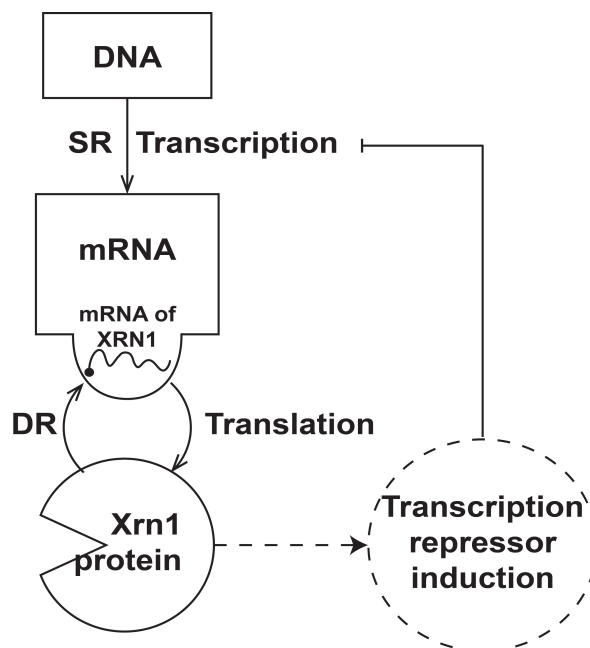


Figure 5.1: **Model for the cellular mechanism of mRNA level buffering.** The mRNA levels are controlled by feedback regulation of XRN1 mRNA levels. Xrn1p protein level is maintained by translation and degradation of XRN1 mRNA. The global SR is controlled by Xrn1p-dependent transcription repressor induction.

product, the Xrn1p exonuclease protein. When XRN1 mRNA levels rise, Xrn1p level rises, leading to a subsequent decrease of its mRNA levels. When XRN1 mRNA levels fall, Xrn1p protein levels fall, leading to mRNA stabilization and thus an increase of the mRNA level. Since Xrn1p acts globally on all mRNA, this simple feedback loop can control all mRNA levels.

The model explains mRNA level buffering upon perturbation. When mRNA synthesis is impaired, XRN1 mRNA and protein levels decrease, leading to slower global mRNA degradation. When mRNA degradation is impaired, transcription repressors such as Nrg1p are induced, leading to a time-delayed down-regulation of mRNA synthesis. Transcription repression involves a nuclear function of Xrn1p, since *XRN1* deletion or nuclear depletion lead to induction of Nrg1p, but not to complete mRNA level buffering. It is likely that the C-terminal region of Xrn1p outside the catalytic domain (Chang et al., 2011) is responsible for this function because its overexpression inhibits cell growth (Page et al., 1998).

The model apparently requires that Xrn1p levels control decapping, because otherwise non-functional decapped messages would accumulate during mRNA level buffering. Such Xrn1p-dependent decapping is consistent with genetic and physical interactions of Xrn1p with the Dcp1/2p complex and the decapping activators Lsm1-7p and Pat1p (Bouveret et al., 2000; Braun et al., 2012; Hatfield et al., 1996; Nissan et al., 2010), with co-localization of these proteins (Parker and Sheth, 2007), and with the recent demonstration that Xrn1p interacts with decapping activators (Braun et al., 2012). Xrn1p may thus act as a universal sensor of cellular mRNA levels and controls homeostatic mRNA level maintenance.

In addition to these insights, interactions between factors involved in mRNA metabolism were detected by cluster analysis of our data. This defined a general mRNA degradation machinery that acts globally and apparently includes the Ccr4-Not complex, the Dcp2p decapping machinery, Xrn1p, and the exosome, consistent with a large body of published results (Harigaya and Parker, 2012). Cluster analysis also confirmed many known interactions between degradation factors in functional complexes, and revealed new functional interactions between factors. Selected new findings include mRNA substrate preferences for the deadenylase complexes Ccr4-Not and Pan2-Pan3, and their putative interaction with the two decapping scavenger proteins that act antagonistically. Further, the data indicate an involvement of Esc1p, Puf1p, Cth1p and Swt1p in nuclear mRNA surveillance, of Cth1p and Swt1p in mRNA No-Go decay, and of

Tpa1p, Pub1p and Puf6p in NMD.

5.3 Outlook

This study provided a method to investigate the global changes of mRNA synthesis and degradation rate. cDTA takes advantage of the Affymetrix Yeast array, which contains probes from two distinct yeast species, *S. cerevisiae* and *S. pombe*. Using this method, we provided a profound resource of genome wide analysis of mRNA degradation pathway in yeast *S. cerevisiae*. We not only confirmed the known interaction of the factors, e.g. the polyadenylation factors and decapping factors, but also provided new insights into this complex pathway. A novel discovery of the global analysis of mRNA degradation pathway is that it revealed factors that are responsible for mRNA level buffering.

However, the majority of this dataset was obtained from the yeast knock out library and thus only the non-essential genes were studied. Exosome, decapping enzymes, which are essential and important were not studied during my work. The essential genes can only be investigated by proper conditional depletion method. We used anchor away strains to observe the nuclear function of Xrn1p. But this method can only be applied to the essential proteins which function in the nucleus. We used the temperature sensitive strain *rpb1-1* in the first part of the study to investigate the buffering effect when mRNA synthesis is impaired. However, as we have shown, the profile of temperature sensitive strain is dominated by heat shock. Non invasive conditional system exist, e.g. the auxin inducible degron system. A peptide of the auxin response protein is cloned to the target protein and plant ubiquitin E3 ligase Tir1p is overexpressed in the cell. Upon addition of auxin hormone, target protein is degraded by protease. This system does not affect the host metabolism. But preliminary trials show that this method cannot deplete protein effectively and mutations of Tir1p can easily accumulated and thus disrupt the system.

Second, we have shown the Xrn1p along with Nrg1p buffers the mRNA level, but detailed mechanism is unknown. Overexpression of Nrg1p show repression of growth rate. cDTA analysis of deletion and overexpression of Nrg1p could give further insight into the global function of Nrg1p.

Third, the global analysis of mRNA degradation pathway uncovers multiple interac-

tions that were unknown. Cth1p profile shows its possible function in mRNA surveillance pathway but little is known about this protein. Interaction experiments can be carried out to find the binding partners of Cth1p, RIP-ChIP or PAR-CLIP can identify its binding motif. Deep sequencing of the mRNAs in the *Cth1* Δ strain could show whether loss of Cth1p will cause defect of mRNAs.

We can now only apply cDTA to *S. cerevisiae* or *S. pombe* strains, because this method is limited to Affymetrix Yeast 2.0 arrays, which contains the probes from these two species. An expansion of this method to other species and using deep sequencing is possible, when the major issue is solved. In this study, we use *S. pombe* as a pool of spike-ins. It could be substituted by using a set of mRNAs. As Lin and co-workers did in the recent published work (Lin et al., 2012), they counted the cells and added spike-ins to certain amount of cells. Later they could define the global shift of the transcriptome with the help of the amount of spike-ins. Here, if we want to monitor the dynamic changes in transcriptome, we label the cell, and pull down the newly synthesized transcripts. So the spike-ins we will use must contain unlabeled RNAs and labeled RNAs with certain ratio. These could be generated *in vitro* using *in vitro* transcription with modified UTP, but the production of spike-ins need to be optimized.

References

- Thomas K. Albert, Hiroyuki Hanzawa, Yvonne I. A. Legtenberg, Marjolein J. de Ruwe, Fiona A. J. van den Heuvel, Martine A. Collart, Rolf Boelens, and H. Th. Marc Timmers. Identification of a ubiquitin-protein ligase subunit within the CCR4-NOT transcription repressor complex. *EMBO J*, 21(3):355–364, February 2002. ISSN 0261-4189. 4
- Maria J. Amorim, Cristina Cotobal, Caia Duncan, and Juan Mata. Global coordination of transcriptional control and mRNA decay during cellular differentiation. *Mol Syst Biol*, 6, 2010. 40, 46
- James Anderson and Xuying Wang. Nuclear RNA surveillance: no sign of substrates tailing off. *Critical reviews in biochemistry and molecular biology*, 44(1):16–24, 2009. 9
- Yasuhiro Araki, Shinya Takahashi, Tetsuo Kobayashi, Hiroaki Kajiho, Shin ichi Hoshino, and Toshiaki Katada. Ski7p G protein interacts with the exosome and the ski complex for 3'-to-5' mRNA decay in yeast. *EMBO J*, 20(17):4684–4693, September 2001. ISSN 0261-4189. 70
- Leonard H. Augenlicht and Diane Kobrin. Cloning and screening of sequences expressed in a mouse colon tumor. *Cancer Research*, 42(3):1088–1093, March 1982. 10
- V Badarinarayana, Y Chiang, and C Denis. Functional interaction of CCR4-NOT proteins with TATAA-binding protein (TBP) and its associated factors in yeast. *Genetics*, 2000. 5
- Yongli Bai, Christopher Salvatore, Yueh-Chin Chiang, Martine A. Collart, Hai-Yan Liu, and Clyde L. Denis. The Ccr4 and Caf1 Proteins of the CCR4-NOT Complex Are Physically and Functionally Separated from Not2, Not4, and Not5. *Mol Cell Biol*, 19(10):6642–6651, 1999. 4, 5, 72

REFERENCES

- Jérôme Basquin, Vladimir V. Roudko, Michaela Rode, Claire Basquin, Bertrand Séraphin, and Elena Conti. Architecture of the Nuclease Module of the Yeast Ccr4-Not Complex: the Not1-Caf1-Ccr4 Interaction. *Molecular Cell*, 48(0):207–218, 2012. ISSN 1097-2765. 5
- Sebastian Bauer, Julien Gagneur, and Peter N. Robinson. GOing bayesian: model-based gene set analysis of genome-scale data. *Nucleic Acids Res*, 38(11):3523–3532, 2010. 47
- Thomas Becker, Jean-Paul Armache, Alexander Jarasch, Andreas M Anger, Elizabeth Villa, Heidemarie Sieber, Basma Abdel Motaal, Thorsten Mielke, Otto Berninghausen, and Roland Beckmann. Structure of the no-go mRNA decay complex Dom34-Hbs1 bound to a stalled 80S ribosome. *Nat Struct Mol Biol*, 18(6):715–720, June 2011. ISSN 1545-9993. 9, 70
- Ronald Boeck, Salvador Jr. Tarun, Michael Rieger, Julie A. Deardorff, Silke Müller-Auer, and Alan B. Sachs. The Yeast Pan2 Protein Is Required for Poly(A)-binding Protein-stimulated Poly(A)-nuclease Activity. *Journal of Biological Chemistry*, 271(1):432–438, January 1996. 72
- Mark S. Borja, Kirill Piotukh, Christian Freund, and John D. Gross. Dcp1 links coactivators of mRNA decapping to Dcp2 by proline recognition. *RNA*, 17(2):278–290, 2011. 7
- Emmanuelle Bouveret, Guillaume Rigaut, Anna Shevchenko, Matthias Wilm, and Bertrand Séraphin. A Sm-like protein complex that participates in mRNA degradation. *EMBO J*, 19(7):1661–1671, April 2000. ISSN 0261-4189. 78
- Joerg E Braun, Vincent Truffault, Andreas Boland, Eric Huntzinger, Chung-Te Chang, Gabrielle Haas, Oliver Weichenrieder, Murray Coles, and Elisa Izaurralde. A direct interaction between DCP1 and XRN1 couples mRNA decapping to 5' exonucleolytic degradation. *Nat Struct Mol Biol*, 19(12):1324–1331, December 2012. ISSN 1545-9993. 78
- Almog Bregman, Moran Avraham-Kelbert, Oren Barkai, Lea Duek, Adi Guterman, and Mordechai Choder. Promoter elements regulate cytoplasmic mRNA decay. *Cell*, 147(7):1473–1483, 2011. ISSN 0092-8674. 14

REFERENCES

- Muriel Brengues, Daniela Teixeira, and Roy Parker. Movement of eukaryotic mRNAs between polysomes and cytoplasmic processing bodies. *Science*, 310(5747):486–489, October 2005. 76
- Christine E. Brown and Alan B. Sachs. Poly(A) tail length control in *saccharomyces cerevisiae* occurs by message-specific deadenylation. *Molecular and Cellular Biology*, 18(11):6548–6559, November 1998. 4
- G Caponigro and R Parker. Multiple functions for the poly(A)-binding protein in mRNA decapping and deadenylation in yeast. *Genes & Development*, 9(19):2421–2432, October 1995. 2, 7
- Jeong Ho Chang, Song Xiang, Kehui Xiang, James L Manley, and Liang Tong. Structural and biochemical studies of the 5→3′ exoribonuclease Xrn1. *Nat Struct Mol Biol*, 18(3):270–276, March 2011. ISSN 1545-9993. 78
- Chyi-Ying A. Chen and Ann-Bin Shyu. Mechanisms of deadenylation-dependent decay. *Wiley Interdisciplinary Reviews: RNA*, 2(2):167–183, 2011. ISSN 1757-7012. 4
- J Chen, YC Chiang, and CL Denis. CCR4, a 3′-5′ poly(A) RNA and ssDNA exonuclease, is the catalytic component of the cytoplasmic deadenylase. *EMBO J*, 21(6):1414–26–, March 2002. 4
- Alan C. M. Cheung and Patrick Cramer. Structural basis of RNA polymerase II backtracking, arrest and reactivation. *Nature*, 471(7337):249–253, March 2011. ISSN 0028-0836. 3
- Aleksander Chlebowski, Micha Lubas, Torben Jensen, and Andrzej Dziembowski. RNA decay machines: The exosome. *Biochimica et biophysica acta*, 2013. 8
- Ashis Chowdhury, Jaba Mukhopadhyay, and Sundaresan Tharun. The decapping activator Lsm1p-7p-Pat1p complex has the intrinsic ability to distinguish between oligoadenylated and polyadenylated RNAs. *RNA*, 13(7):998–1016, July 2007. 13
- Michael D. Cleary, Christopher D. Meiering, Eric Jan, Rebecca Guymon, and John C. Boothroyd. Biosynthetic labeling of RNA with uracil phosphoribosyltransferase allows cell-specific microarray analysis of mRNA synthesis and decay. *Nat Biotech*, 23(2):232–237, 2005. 11

REFERENCES

- Diana F. Colgan and James L. Manley. Mechanism and regulation of mRNA-polyadenylation. *Genes & Development*, 11(21):2755–2766, 1997. 2
- Martine A. Collart. Global control of gene expression in yeast by the Ccr4-Not complex. *Gene*, 313:1–16, August 2003. ISSN 0378-1119. 4, 12, 72, 76
- Martine A. Collart and H. Th. Marc Timmers. The eukaryotic Ccr4-Not complex: A regulatory platform integrating mRNA metabolism with cellular signaling pathways? *Progress in Nucleic Acid Research and Molecular Biology*, Volume 77:289–322, 2004. ISSN 0079-6603. 76
- J. M. Collier, N. K. Gray, and M. P. Wickens. mRNA stabilization by poly(A) binding protein is independent of poly(A) and requires translation. *Genes Dev*, 12(20):3226–3235, October 1998. 2
- J. M. Collier, M. Tucker, U. Sheth, M. A. Valencia-Sanchez, and R. Parker. The DEAD box helicase, Dhh1p, functions in mRNA decapping and interacts with both the decapping and deadenylase complexes. *RNA*, 7(12):1717–1727, December 2001. 7
- Jeff Collier and Roy Parker. Eukaryotic mRNA decapping. *Annu Rev Biochem*, 73(1):861–890, 2004. 6, 12, 76
- Jeff Collier and Roy Parker. General translational repression by activators of mRNA decapping. *Cell*, 122(6):875–886, September 2005. 7, 13, 76
- Katrina Cooper, Matthew Scarnati, Elizabeth Krasley, Michael Mallory, Chunyan Jin, Michael Law, and Randy Strich. Oxidative-stress-induced nuclear to cytoplasmic relocalization is required for not4-dependent cyclin C destruction. *Journal of cell science*, 125(Pt 4):1015–1026, 2012. 5
- Patrick Cramer, David A. Bushnell, and Roger D. Kornberg. Structural basis of transcription: RNA polymerase II at 2.8 ngstrom resolution. *Science*, 292(5523):1863–1876, 2001. 49
- Yajun Cui, Deepti Ramnarain, Yueh-Chin Chiang, Liang-Hao Ding, Jeffrey McMahon, and Clyde Denis. Genome wide expression analysis of the CCR4-NOT complex indicates that it consists of three modules with the NOT module controlling SAGA-responsive genes. *Molecular Genetics and Genomics*, 279:323–337, 2008. ISSN 1617-4615. 10.1007/s00438-007-0314-1. 4, 5, 72

REFERENCES

- C J Decker and R Parker. A turnover pathway for both stable and unstable mRNAs in yeast: evidence for a requirement for deadenylation. *Genes & Development*, 7(8):1632–1643, August 1993. 2, 10
- Cécile Deluen, Nicole James, Laurent Maillet, Miguel Molinete, Grégory Theiler, Marc Lemaire, Nicole Paquet, and Martine Collart. The Ccr4-Not complex and yTAF1 (yTaf(II)130p/yTaf(II)145p) show physical and functional interactions. *Molecular and cellular biology*, 22(19):6735–6749, 2002. 5
- Mandar Deshmukh, Brittnee Jones, Quang-Dang, Duc-Uy, Jeremy Flinders, Stephen Floor, Candice Kim, Jacek Jemielity, Marcin Kalek, Edward Darzynkiewicz, and John Gross. mRNA decapping is promoted by an RNA-binding channel in Dcp2. *Molecular cell*, 29(3):324–336, 2008. 6
- L. Dolken, Z. Ruzsics, B. Radle, C. C. Friedel, R. Zimmer, J. Mages, R. Hoffmann, P. Dickinson, T. Forster, P. Ghazal, and U. H. Koszinowski. High-resolution gene expression profiling for simultaneous kinetic parameter analysis of RNA synthesis and decay. *RNA*, 14(9):1959–72, 2008. 11
- Meenakshi K. Doma and Roy Parker. Endonucleolytic cleavage of eukaryotic mRNAs with stalls in translation elongation. *Nature*, 440(7083):561–564, March 2006. ISSN 0028-0836. 9
- Mally Dori-Bachash, Efrat Shema, and Itay Tirosh. Coupled evolution of transcription and mRNA degradation. *PLoS Biol*, 9(7):e1001106, 2011. 14, 44, 67
- T. Dunckley, M. Tucker, and R. Parker. Two related proteins, Edc1p and Edc2p, stimulate mRNA decapping in *Saccharomyces cerevisiae*. *Genetics*, 157(1):27–37, 2001. 13
- Travis Dunckley and Roy Parker. The Dcp2 protein is required for mRNA decapping in *Saccharomyces cerevisiae* and contains a functional MutT motif. *EMBO J*, 18(19):5411–5422, October 1999. ISSN 0261-4189. 6
- A M Edwards, C M Kane, R A Young, and R D Kornberg. Two dissociable subunits of yeast RNA Polymerase II stimulate the initiation of transcription at a promoter *in vitro*. *J Biol Chem*, 266(1):71–75, 1991. 76

REFERENCES

- Ana Eulalio, Isabelle Behm-Ansmant, and Elisa Izaurralde. P bodies: at the crossroads of post-transcriptional pathways. *Nat Rev Mol Cell Biol*, 8(1):9–22, 2007. 10.1038/nrm2080. 12
- Nicole Fischer and Karsten Weis. The DEAD box protein Dhh1 stimulates the decapping enzyme Dcp1. *EMBO J*, 21(11):2788–2797, 2002. 7
- Tobias M. Franks and Jens Lykke-Andersen. The control of mRNA decapping and P-body formation. *Mol Cell*, 32(5):605–615, 2008. 12
- Nicholas J. Fuda, M. Behfar Ardehali, and John T. Lis. Defining mechanisms that regulate RNA polymerase II transcription *in vivo*. *Nature*, 461(7261):186–192, 2009. 1, 12
- Nicole L. Garneau, Jeffrey Wilusz, and Carol J. Wilusz. The highways and byways of mRNA decay. *Nat Rev Mol Cell Biol*, 8(2):113–126, February 2007. ISSN 1471-0072. 1, 12
- Anne-Claude Gavin, Patrick Aloy, Paola Grandi, Roland Krause, Markus Boesche, Martina Marzioch, Christina Rau, Lars Juhl Jensen, Sonja Bastuck, Birgit Dumpelfeld, Angela Edelmann, Marie-Anne Heurtier, Verena Hoffman, Christian Hoefert, Karin Klein, Manuela Hudak, Anne-Marie Michon, Malgorzata Schelder, Markus Schirle, Marita Remor, Tatjana Rudi, Sean Hooper, Andreas Bauer, Tewis Bouwmeester, Georg Casari, Gerard Drewes, Gitte Neubauer, Jens M. Rick, Bernhard Kuster, Peer Bork, Robert B. Russell, and Giulio Superti-Furga. Proteome survey reveals modularity of the yeast cell machinery. *Nature*, 440(7084):631–636, March 2006. ISSN 0028-0836. 61
- Andr P. Gerber, Daniel Herschlag, and Patrick O. Brown. Extensive association of functionally and cytotopically related mRNAs with Puf family RNA-binding proteins in yeast. *PLoS Biol*, 2(3):e79, 2004. 74
- Joshua M. Gilmore, Mihaela E. Sardi, Swaminathan Venkatesh, Brent Stutzman, Allison Peak, Chris W. Seidel, Jerry L. Workman, Laurence Florens, and Michael P. Washburn. Characterization of a highly conserved histone related protein, Ydl156w, and its functional associations using quantitative proteomic analyses. *Molecular & Cellular Proteomics*, 11(4), 2012. 61

REFERENCES

- Aaron C. Goldstrohm, Daniel J. Seay, Brad A. Hook, and Marvin Wickens. PUF protein-mediated deadenylation is catalyzed by Ccr4p. *J Biol Chem*, 282(1):109–114, 2007. 74
- Carlos I González, Anirban Bhattacharya, Weirong Wang, and Stuart W Peltz. Nonsense-mediated mRNA decay in *Saccharomyces cerevisiae*. *Gene*, 274(1):15–25, August 2001. ISSN 0378-1119. 3
- Jorg Grigull, Sanie Mnaimneh, Jeffrey Pootoolal, Mark D. Robinson, and Timothy R. Hughes. Genome-wide analysis of mRNA stability using transcription inhibitors and microarrays reveals posttranscriptional control of ribosome biogenesis factors. *Mol Cell Biol*, 24(12):5534–5547, 2004. 10, 44
- Liat Harel-Sharvit, Naama Eldad, Gal Haimovich, Oren Barkai, Lea Duek, and Mordechai Choder. RNA Polymerase II subunits link transcription and mRNA decay to translation. *Cell*, 143(4):552–563, November 2010. ISSN 0092-8674. 13, 76
- Yuriko Harigaya and Roy Parker. Global analysis of mRNA decay intermediates in *Saccharomyces cerevisiae*. *Proceedings of the National Academy of Sciences*, 109(29):11764–11769, July 2012. 78
- Hirohito Haruki, Junichi Nishikawa, and Ulrich K. Laemmli. The anchor-away technique: Rapid, conditional establishment of yeast mutant phenotypes. *Mol Cell*, 31(6):925–932, 2008. ISSN 1097-2765. 61
- L Hatfield, C A Beelman, A Stevens, and R Parker. Mutations in trans-acting factors affecting mRNA decapping in *Saccharomyces cerevisiae*. *Molecular and Cellular Biology*, 16(10):5830–5838, October 1996. 78
- F He, A Brown, and A Jacobson. Upf1p, Nmd2p, and Upf3p are interacting components of the yeast nonsense-mediated mRNA decay pathway. *Molecular and cellular biology*, 17(3):1580–1594, 1997. ISSN 0270-7306. 9
- Doeke Hekstra, Alexander R. Taussig, Marcelo Magnasco, and Felix Naef. Absolute mRNA concentrations from sequence-specific calibration of oligonucleotide arrays. *Nucleic Acids Res*, 31(7):1962–1968, 2003. 38

REFERENCES

- G. A. Held, G. Grinstein, and Y. Tu. Modeling of DNA microarray data by using physical properties of hybridization. *Proc Natl Acad Sci U S A*, 100(13):7575–7580, 2003. 38
- G. A. Held, G. Grinstein, and Y. Tu. Relationship between gene expression and observed intensities in DNA microarrays: a modeling study. *Nucleic Acids Res*, 34(9):e70, 2006. 38
- Lynna M. Hereford and Michael Rosbash. Regulation of a set of abundant mRNA sequences. *Cell*, 10(3):463–467, 1977. 41
- F Holstege, E Jennings, J Wyrick, T Lee, C Hengartner, M Green, T Golub, E Lander, and R Young. Dissecting the regulatory circuitry of a eukaryotic genome. *Cell*, 95(5):717–728, 1998. 10, 12, 13, 44, 45
- J. Houseley and D. Tollervey. The many pathways of RNA degradation. *Cell*, 136(4):763–776, 2009. 53
- Jonathan Houseley, John LaCava, and David Tollervey. RNA-quality control by the exosome. *Nat Rev Mol Cell Biol*, 7(7):529–539, July 2006. ISSN 1471-0072. 8
- C L Hsu and A Stevens. Yeast cells lacking 5' → 3' exoribonuclease 1 contain mRNA species that are poly(A) deficient and partially lack the 5' cap structure. *Mol Cell Biol*, 13(8):4826–4835, 1993. 7
- Wenqian Hu, Thomas J. Sweet, Sangpen Chamnongpol, Kristian E. Baker, and Jeff Coller. Co-translational mRNA decay in *Saccharomyces cerevisiae*. *Nature*, 461(7261):225–229, September 2009. ISSN 0028-0836. 12, 65, 76
- Toshifumi Inada. Quality control systems for aberrant mRNAs induced by aberrant translation elongation and termination. *Biochimica et Biophysica Acta (BBA) - Gene Regulatory Mechanisms*, (0):–, 2013. ISSN 1874-9399. 3
- Olivier Jaillon, Khaled Bouhouche, Jean-Francois Gout, Jean-Marc Aury, Benjamin Noel, Baptiste Saudemont, Mariusz Nowacki, Vincent Serrano, Betina M. Porcel, Beatrice Segurens, Anne Le Mouel, Gersende Lepere, Vincent Schachter, Mireille Betermier, Jean Cohen, Patrick Wincker, Linda Sperling, Laurent Duret, and Eric Meyer. Translational control of intron splicing in eukaryotes. *Nature*, 451(7176):359–362, January 2008. ISSN 0028-0836. 3

REFERENCES

- Silvia Jimeno-González, Line Lindegaard Haaning, Francisco Malagon, and Torben Heick Jensen. The Yeast 5'-3' Exonuclease Rat1p Functions during Transcription Elongation by RNA Polymerase II, February 2010. ISSN 1097-2765. 42, 49
- A Johnson and R Kolodner. Strand exchange protein 1 from *Saccharomyces cerevisiae*. A novel multifunctional protein that contains DNA strand exchange and exonuclease activities. *The Journal of biological chemistry*, 266(21):14046–14054, 1991. 8
- Paul Jorgensen, Joy L. Nishikawa, Bobby-Joe Breitskreutz, and Mike Tyers. Systematic identification of pathways that couple cell growth and division in yeast. *Science*, 297(5580):395–400, July 2002. 46
- Kim M. Keeling, Joe Salas-Marco, Lev Z. Osherovich, and David M. Bedwell. Tpa1p is part of an mRNP complex that influences translation termination, mRNA deadenylation, and mRNA turnover in *Saccharomyces cerevisiae*. *Molecular and Cellular Biology*, 26(14):5237–5248, 2006. 74
- M. Kenzelmann, S. Maertens, M. Hergenroth, S. Kueffer, A. Hotz-Wagenblatt, L. Li, S. Wang, C. Ittrich, T. Lemberger, R. Arribas, S. Jonnakuty, M. C. Hollstein, W. Schmid, N. Gretz, H. J. Grne, and G. Schtz. Microarray analysis of newly synthesized RNA in cells and animals. *Proceedings of the National Academy of Sciences*, 104(15):6164–6169, April 2007. 11
- Stephanie Kervestin and Allan Jacobson. NMD: a multifaceted response to premature translational termination. *Nat Rev Mol Cell Biol*, 13(11):700–712, November 2012. ISSN 1471-0072. 9
- Jennifer A. Kruk, Arnob Dutta, Jianhua Fu, David S. Gilmour, and Joseph C. Reese. The multifunctional Ccr4-Not complex directly promotes transcription elongation. *Genes & Development*, 25(6):581–593, March 2011. 4, 76
- Meenakshi Kshirsagar and Roy Parker. Identification of Edc3p as an enhancer of mRNA decapping in *Saccharomyces cerevisiae*. *Genetics*, 2004. 6, 13
- Jean-Philippe Lambert, Leslie Mitchell, Adam Rudner, Kristin Baetz, and Daniel Figeys. A novel proteomics approach for the discovery of chromatin-associated protein networks. *Molecular & Cellular Proteomics*, 8(4):870–882, 2009. 61

REFERENCES

- Alice Lebreton, Rafal Tomecki, Andrzej Dziembowski, and Bertrand Seraphin. Endonucleolytic RNA cleavage by a eukaryotic exosome. *Nature*, 456(7224):993–996, 2008. 12
- Kuo-Ming Lee and Woan-Yuh Tarn. Coupling pre-mRNA processing to transcription on the RNA factory assembly line. *RNA*, 10(3):386–396, 2013. 2
- Fabrice Lejeune and Lynne E Maquat. Mechanistic links between nonsense-mediated mRNA decay and pre-mRNA splicing in mammalian cells. *Current Opinion in Cell Biology*, 17(3):309–315, 2005. ISSN 0955-0674. `jc:titlej`Nucleus and gene expression/`ce:titlej`. 9
- Eve Lenssen, Nicole James, Ivo Pedruzzi, Frederique Dubouloz, Elisabetta Cameroni, Ruth Bisig, Laurent Maillet, Michel Werner, Johnny Roosen, Katarina Petrovic, Joris Winderickx, Martine A. Collart, and Claudio De Virgilio. The Ccr4-Not complex independently controls both Msn2-dependent transcriptional activation—via a newly identified Glc7/Bud14 type I protein phosphatase module—and TFIID promoter distribution. *Mol Cell Biol*, 25(1):488–498, January 2005. 4
- Eve Lenssen, Nowel Azzouz, Agnes Michel, Emilie Landrieux, and Martine A. Collart. The Ccr4-Not complex regulates Skn7 through Srb10 kinase. *Eukaryotic Cell*, 6(12):2251–2259, December 2007. 4
- CharlesY. Lin, Jakob Lovén, PeterB. Rahl, RonaldM. Paranal, ChristopherB. Burge, JamesE. Bradner, TongIhn Lee, and RichardA. Young. Transcriptional amplification in tumor cells with elevated c-Myc. *Cell*, 151(1):56–67, September 2012. ISSN 0092-8674. 11, 12, 80
- Hai-Yan Liu, Vasudeo Badarinarayana, Deborah C. Audino, Juri Rappsilber, Matthias Mann, and Clyde L. Denis. The NOT proteins are part of the CCR4 transcriptional complex and affect gene expression both positively and negatively. *EMBO J*, 17(4):1096–1106, February 1998. ISSN 0261-4189. 5, 13, 76
- Hudan Liu and Megerditch Kiledjian. Scavenger decapping activity facilitates 5' to 3' mRNA decay. *Molecular and Cellular Biology*, 25(22):9764–9772, 2005. 72
- Hudan Liu, Nancy D. Rodgers, Xinfu Jiao, and Megerditch Kiledjian. The scavenger mRNA decapping enzyme dcpS is a member of the HIT family of pyrophosphatases. *EMBO J*, 21(17):4699–4708, September 2002. ISSN 0261-4189. 8, 72

REFERENCES

- Quansheng Liu, Jaclyn C. Greimann, and Christopher D. Lima. Reconstitution, activities, and structure of the eukaryotic RNA exosome. *Cell*, 127(6):1223–1237, December 2006. ISSN 0092-8674. 8
- Xin Liu, David A. Bushnell, and Roger D. Kornberg. RNA polymerase II transcription: Structure and mechanism. *Biochimica et Biophysica Acta (BBA) - Gene Regulatory Mechanisms*, 1829(1):2–8, January 2013. ISSN 1874-9399. 1
- P Loflin, C Chen, N Xu, and A Shyu. Transcriptional pulsing approaches for analysis of mRNA turnover in mammalian cells. *Methods (San Diego, Calif.)*, 17(1):11–20, 1999. 10
- Mark S. Longtine, Amos Mckenzie III, Douglas J. Demarini, Nirav G. Shah, Achim Wach, Arndt Brachat, Peter Philippsen, and John R. Pringle. Additional modules for versatile and economical PCR-based gene deletion and modification in *Saccharomyces cerevisiae*. *Yeast*, 14(10):953–961, 1998. 29
- Rona Lotan, Vicky Goler Bar-On, Liat Harel-Sharvit, Lea Duek, Daniel Melamed, and Mordechai Choder. The RNA polymerase II subunit Rpb4p mediates decay of a specific class of mRNAs. *Genes & Development*, 19(24):3004–3016, 2005. 13, 76
- Rona Lotan, Vicky Goler-Baron, Lea Duek, Gal Haimovich, and Mordechai Choder. The Rpb7p subunit of yeast RNA polymerase II plays roles in the two major cytoplasmic mRNA decay mechanisms. *The Journal of Cell Biology*, 178(7):1133–1143, 2007. 13, 76
- Laurent Maillet and Martine A. Collart. Interaction between Not1p, a component of the Ccr4-Not complex, a global regulator of transcription, and Dhh1p, a putative RNA helicase. *J Biol Chem*, 277(4):2835–2842, January 2002. 5
- Debora Makino, Marc Baumgärtner, and Elena Conti. Crystal structure of an RNA-bound 11-subunit eukaryotic exosome complex. *Nature*, 495(7439):70–75, 2013. 8
- Francisco Malagon, Maria L. Kireeva, Brenda K. Shafer, Lucyna Lubkowska, Mikhail Kashlev, and Jeffrey N. Strathern. Mutations in the *Saccharomyces cerevisiae* RPB1 gene conferring hypersensitivity to 6-azauracil. *Genetics*, 172(4):2201–2209, April 2006. 49

REFERENCES

- Naglis Malys and John E. G. McCarthy. Dcs2, a novel stress-induced modulator of m7GpppX pyrophosphatase activity that localizes to P bodies. *Journal of Molecular Biology*, 363(2):370–382, 2006. ISSN 0022-2836. 72
- Tom Maniatis and Robin Reed. An extensive network of coupling among gene expression machines. *Nature*, 416(6880):499–506, 2002. 10.1038/416499a. 76
- Christian Miller, Björn Schwalb, Kerstin Maier, Daniel Schulz, Sebastian Dümcke, Benedikt Zacher, Andreas Mayer, Jasmin Sydow, Lisa Marcinowski, Lars Dolken, Dietmar E Martin, Achim Tresch, and Patrick Cramer. Dynamic transcriptome analysis measures rates of mRNA synthesis and decay in yeast. *Mol Syst Biol*, 7:–, January 2011. 11, 13, 30, 31, 32, 34, 37, 38, 39, 40, 41, 46, 75
- Melanie A. Miller and Wendy M. Olivas. Roles of puf proteins in mRNA degradation and translation. *Wiley Interdisciplinary Reviews: RNA*, 2(4):471–492, 2011. ISSN 1757-7012. 74
- Stefania Millevoi and Stéphan Vagner. Molecular mechanisms of eukaryotic pre-mRNA 3'-end processing regulation. *Nucleic Acids Research*, 38(9):2757–2774, 2010. 2
- John P. Morrissey, Julie A. Deardorff, Clarissa Hebron, and Alan B. Sachs. Decapping of stabilized, polyadenylated mRNA in yeast pab1 mutants. *Yeast*, 15(8):687–702, 1999. ISSN 1097-0061. 7
- D Muhlrاد, C J Decker, and R Parker. Deadenylation of the unstable mRNA encoded by the yeast MFA2 gene leads to decapping followed by 5'→3' digestion of the transcript. *Genes & Development*, 8(7):855–866, 1994. 2, 12
- D Muhlrاد, CJ Decker, and R Parker. Turnover mechanisms of the stable yeast PGK1 mRNA. *Mol Cell Biol*, 15(4):2145–2156, April 1995. 72
- Denise Muhlrاد and Roy Parker. The yeast EDC1 mRNA undergoes deadenylation-independent decapping stimulated by Not2p, Not4p, and Not5p. *The EMBO journal*, 24(5):1033–1045, 2005. 6
- Sarah E. Munchel, Ryan K. Shultzaberger, Naoki Takizawa, and Karsten Weis. Dynamic profiling of mRNA turnover reveals gene-specific and system-wide regulation of mRNA decay. *Mol Biol Cell*, pages mbc.E11–01–0028, 2011. 11, 34, 41, 45, 46

REFERENCES

- G Neely, Keiji Kuba, Anthony Cammarato, Kazuya Isobe, Sabine Amann, Liyong Zhang, Mitsushige Murata, Lisa Elmén, Vaijayanti Gupta, Suchir Arora, Rinku Sarangi, Debasis Dan, Susumu Fujisawa, Takako Usami, Cui ping Xia, Alex Keene, Nakissa Alayari, Hiroyuki Yamakawa, Ulrich Elling, Christian Berger, Maria Novatchkova, Rubina Koglgruber, Keiichi Fukuda, Hiroshi Nishina, Mitsuaki Isobe, J Pospisilik, Yumiko Imai, Arne Pfeufer, Andrew Hicks, Peter Pramstaller, Sai Subramaniam, Akinori Kimura, Karen Ocorr, Rolf Bodmer, and Josef Penninger. A global *in vivo* drosophila RNAi screen identifies NOT3 as a conserved regulator of heart function. *Cell*, 141(1):142–153, 2010. 5
- Frank R. Neumann and Paul Nurse. Nuclear size control in fission yeast. *The Journal of Cell Biology*, 179(4):593–600, 2007. 46
- Tracy Nissan, Purusharth Rajyaguru, Meipei She, Haiwei Song, and Roy Parker. Decapping activators in *Saccharomyces cerevisiae* act by multiple mechanisms. *Mol Cell*, 39(5):773–783, 2010. 78
- M Nonet, C Scafe, J Sexton, and R Young. Eucaryotic RNA polymerase conditional mutant that rapidly ceases mRNA synthesis. *Molecular and Cellular Biology*, 7(5):1602–1611, May 1987. 44
- Takbum Ohn, Yueh-Chin Chiang, Darren J. Lee, Gang Yao, Chongxu Zhang, and Clyde L. Denis. CAF1 plays an important role in mRNA deadenylation separate from its contact to CCR4. *Nucleic Acids Res*, 35(9):3002–3015, May 2007. 5
- Andrew M. Page, Kristina Davis, Catherine Molineux, Richard D. Kolodner, and Arlen W. Johnson. Mutational analysis of exoribonuclease I from *Saccharomyces cerevisiae*. *Nucleic Acids Research*, 26(16):3707–3716, August 1998. 78
- M Page, B Carr, K Anders, A Grimson, and P Anderson. SMG-2 is a phosphorylated protein required for mRNA surveillance in *Caenorhabditis elegans* and related to Upf1p of yeast. *Molecular and cellular biology*, 19(9):5943–5951, 1999. 9
- Salvatore San Paolo, Stepanka Vanacova, Luca Schenk, Tanja Scherrer, Diana Blank, Walter Keller, and André P Gerber. Distinct roles of non-canonical poly(A) polymerases in RNA metabolism. *PLoS Genet*, 5(7):e1000555, 07 2009. 9, 74
- Roy Parker and Ujwal Sheth. P bodies and the control of mRNA translation and degradation. *Mol Cell*, 25(5):635–646, 2007. 1, 6, 8, 12, 78

REFERENCES

- José E. Pérez-Ortín, Lola de Miguel-Jiménez, and Sebastián Chávez. Genome-wide studies of mRNA synthesis and degradation in eukaryotes. *Biochimica et Biophysica Acta (BBA) - Gene Regulatory Mechanisms*, 1819(6):604–615, June 2012. ISSN 1874-9399. 14
- Guy R. Pilkington and Roy Parker. Pat1 contains distinct functional domains that promote P-body assembly and activation of decapping. *Molecular and Cellular Biology*, 28(4):1298–1312, 2008. 13
- Michal Rabani, Joshua Z Levin, Lin Fan, Xian Adiconis, Raktima Raychowdhury, Manuel Garber, Andreas Gnirke, Chad Nusbaum, Nir Hacoheh, Nir Friedman, Ido Amit, and Aviv Regev. Metabolic labeling of RNA uncovers principles of RNA production and degradation dynamics in mammalian cells. *Nat Biotech*, 29(5):436–442, May 2011. ISSN 1087-0156. 31
- Purusharth Rajyaguru, Meipei She, and Roy Parker. Scd6 targets eIF4G to repress translation: RGG motif proteins as a class of eIF4G-binding proteins, January 2012. ISSN 1097-2765. 74
- Carmen Ramirez, Cristina Vilela, Karine Berthelot, and McCarthy, John. Modulation of eukaryotic mRNA stability via the cap-binding translation complex eIF4F. *Journal of molecular biology*, 318(4):951–962, 2002. 7
- Jeffrey A. Ranish, Natalya Yudkovsky, and Steven Hahn. Intermediates in formation and activity of the RNA polymerase II preinitiation complex: holoenzyme recruitment and a postrecruitment role for the TATA box and TFIIB. *Genes & Development*, 13(1):49–63, 1999. 32
- Steven I. Reed. The selection of amber mutations in genes required for completion of start, the controlling event of the cell division cycle of *S. cerevisiae*. *Genetics*, 95(3):579–588, 1980. 4
- Susana Rodríguez-Navarro and Ed Hurt. Linking gene regulation to mRNA production and export. *Current Opinion in Cell Biology*, 23(3):302–309, 2011. ISSN 0955-0674. 2
- Maria J Ruiz-Echevarría and Stuart W Peltz. The RNA Binding Protein Pub1 Modulates the Stability of Transcripts Containing Upstream Open Reading Frames. *Cell*, 101(7):741–751, June 2000. ISSN 0092-8674. 74

REFERENCES

- Alan B. Sachs and Julie A. Deardorff. Translation initiation requires the PAB-dependent poly(A) ribonuclease in yeast. *Cell*, 70(6):961–973, September 1992. ISSN 0092-8674. 4
- Nerea Sanvisens, M. Carmen Bañó, Mingxia Huang, and Sergi Puig. Regulation of ribonucleotide reductase in response to iron deficiency. *Molecular Cell*, 44(5):759–769, December 2011. ISSN 1097-2765. 74
- Mark Schena, Dari Shalon, Ronald W. Davis, and Patrick O. Brown. Quantitative monitoring of gene expression patterns with a complementary DNA microarray. *Science*, 270(5235):467–470, October 1995. 10
- Manfred Schmid and Torben Heick Jensen. Nuclear quality control of RNA polymerase II transcripts. *WIREs RNA*, 1(3):474–485, November 2010. ISSN 1757-7012. 13, 74
- Karyn Schmidt and J. Scott Butler. Nuclear RNA surveillance: role of TRAMP in controlling exosome specificity. *WIREs RNA*, 4(2):217–231, March 2013. ISSN 1757-7012. 3
- Karyn Schmidt, Zhenjiang Xu, David H. Mathews, and J. Scott Butler. Air proteins control differential TRAMP substrate specificity for nuclear RNA surveillance. *RNA*, 2012. 9, 74
- Björn Schwalb, Daniel Schulz, Mai Sun, Benedikt Zacher, Sebastian Dümcke, Dietmar Martin, Patrick Cramer, and Achim Tresch. Measurement of genome-wide RNA synthesis and decay rates with dynamic transcriptome analysis (DTA). *Bioinformatics*, 2012. 31
- D Schwartz, C J Decker, and R. Parker. The enhancer of decapping proteins, Edc1p and Edc2p, bind RNA and stimulate the activity of the decapping enzyme. *RNA*, 9(2):239–251, 2003. 7
- Christine E. Seidman, Kevin Struhl, Jen Sheen, and Timm Jessen. *Introduction of Plasmid DNA into Cells*, chapter 1, page Unit 1.8. John Wiley & Sons, Inc., 2001. ISBN 9780-471-14272-0. 27
- Martin Seizl, Holger Hartmann, Friederike Hoeg, Fabian Kurth, Dietmar E. Martin, Johannes Söding, and Patrick Cramer. A conserved GA element in TATA-less RNA polymerase II promoters. *PLoS ONE*, 6(11):e27595, 11 2011a. 32

REFERENCES

- Martin Seizl, Laurent Larivière, Toni Pfaffeneder, Larissa Wenzek, and Patrick Cramer. Mediator head subcomplex Med11/22 contains a common helix bundle building block with a specific function in transcription initiation complex stabilization. *Nucleic Acids Research*, 39(14):6291–6304, 2011b. 32
- Michael Selitrennik, Lea Duek, Rona Lotan, and Mordechai Choder. Nucleocytoplasmic shuttling of the Rpb4p and Rpb7p subunits of *Saccharomyces cerevisiae* RNA polymerase II by two pathways. *Eukaryotic Cell*, 5(12):2092–2103, 2006. 76
- Ophir Shalem, Orna Dahan, Michal Levo, Maria Rodriguez Martinez, Itay Furman, Eran Segal, and Yitzhak Pilpel. Transient transcriptional responses to stress are generated by opposing effects of mRNA production and degradation. *Mol Syst Biol*, 4:–, October 2008. 10, 44
- D Shalon, S J Smith, and P O Brown. A DNA microarray system for analyzing complex DNA samples using two-color fluorescent probe hybridization. *Genome Research*, 6(7):639–645, July 1996. 10
- A. J. Shatkin. Capping of eucaryotic mRNAs. *Cell*, 9(4, Part 2):645–653, December 1976. ISSN 0092-8674. 2
- Ujwal Sheth and Roy Parker. Decapping and decay of messenger RNA occur in cytoplasmic processing bodies. *Science*, 300(5620):805–808, May 2003. 6
- Christopher J Shoemaker and Rachel Green. Translation drives mRNA quality control. *Nat Struct Mol Biol*, 19(6):594–601, June 2012. ISSN 1545-9993. 13, 74
- Christopher J. Shoemaker, Daniel E. Eyler, and Rachel Green. Dom34:Hbs1 promotes subunit dissociation and peptidyl-tRNA drop-off to initiate No-Go decay. *Science*, 330(6002):369–372, 2010. 9
- Ann-Bin Shyu, Miles F. Wilkinson, and Ambro van Hoof. Messenger RNA regulation: to translate or to degrade. *EMBO J*, 27(3):471–481, 2008. 13
- Michal Skružný, Claudia Schneider, Attila Rácz, Julian Weng, David Tollervey, and Ed Hurt. An endoribonuclease functionally linked to perinuclear mRNP quality control associates with the nuclear pore complexes. *PLoS Biol*, 7(1):e1000008, 01 2009. 70, 74

REFERENCES

- Dmitriy Skvortsov, Diana Abdueva, Christina Curtis, Betty Schaub, and Simon Tavar. Explaining differences in saturation levels for affymetrix genechip arrays. *Nucleic Acids Res*, 35(12):4154–4163, 2007. 38
- Jachen A. Solinger, Donatella Pascolini, and Wolf-Dietrich Heyer. Active-site mutations in the Xrn1p exoribonuclease of *Saccharomyces cerevisiae* reveal a specific role in meiosis. *Mol Cell Biol*, 19(9):5930–5942, 1999. 61
- Audrey Stevens. [20] 5'-exoribonuclease 1: Xrn1. In Allen W. Nicholson, editor, *Ribonucleases - Part B*, volume 342 of *Methods in Enzymology*, pages 251–259. Academic Press, 2001. 8
- Katja Sträßer, Seiji Masuda, Paul Mason, Jens Pfannstiel, Marisa Oppizzi, Susana Rodriguez-Navarro, Ana G. Rondon, Andres Aguilera, Kevin Struhl, Robin Reed, and Ed Hurt. TREX is a conserved complex coupling transcription with messenger RNA export. *Nature*, 417(6886):304–308, May 2002. ISSN 0028-0836. 72, 74
- Mai Sun, Björn Schwalb, Daniel Schulz, Nicole Pirkl, Stefanie Etzold, Laurent Lariivière, Kerstin C. Maier, Martin Seizl, Achim Tresch, and Patrick Cramer. Comparative dynamic transcriptome analysis (cDTA) reveals mutual feedback between mRNA synthesis and degradation. *Genome Research*, 2012. 11, 14, 56, 61
- Silvia A. Synowsky and Albert J. R. Heck. The yeast ski complex is a hetero-tetramer. *Protein Science*, 17(1):119–125, January 2008. ISSN 1469-896X. 70
- Ivan Topisirovic, Yuri V. Svitkin, Nahum Sonenberg, and Aaron J. Shatkin. Cap and cap-binding proteins in the control of gene expression. *WIREs RNA*, 2(2):277–298, 2011. ISSN 1757-7012. 2
- Tatjana Trcek, Daniel Larson, Alberto Moldón, Charles Query, and Robert Singer. Single-molecule mRNA decay measurements reveal promoter-regulated mRNA stability in yeast. *Cell*, 147(7):1484–1497, 2011. 14
- M Tucker and R Parker. Mechanisms and control of mRNA decapping in *saccharomyces cerevisiae*. *Annual review of biochemistry*, 69:571–595, 2000. 7
- Morgan Tucker, Marco A. Valencia-Sanchez, Robin R. Staples, Junji Chen, Clyde L. Denis, and Roy Parker. The transcription factor associated Ccr4 and Caf1 proteins

REFERENCES

- are components of the major cytoplasmic mRNA deadenylase in *Saccharomyces cerevisiae*. *Cell*, 104(3):377–386, 2001. 4, 5, 13
- Morgan Tucker, Robin R Staples, Marco A Valencia-Sanchez, Denise Muhlrads, and Roy Parker. Ccr4p is the catalytic subunit of a Ccr4p/Pop2p/Notp mRNA deadenylase complex in *Saccharomyces cerevisiae*. *EMBO J*, 21(6):1427–1436, March 2002. 53, 76
- Naoyuki Uchida, Shin-Ichi Hoshino, and Toshiaki Katada. Identification of a human cytoplasmic poly(A) nuclease complex stimulated by poly(A)-binding protein. *The Journal of biological chemistry*, 279(2):1383–1391, 2004. 6
- Jeroen van de Peppel, Patrick Kemmeren, Harm van Bakel, Marijana Radonjic, Dik van Leenen, and Frank C P Holstege. Monitoring global messenger RNA changes in externally controlled microarray experiments. *EMBO Rep*, 4(4):387–393, April 2003. 12, 13
- E. L. van Dijk, C. L. Chen, Y. Aubenton Carafa, S. Gourvenec, M. Kwapisz, V. Roche, C. Bertrand, M. Silvain, P. Legoix-Ne, S. Loeillet, A. Nicolas, C. Thermes, and A. Morillon. XUTs are a class of Xrn1-sensitive antisense regulatory non-coding RNA in yeast. *Nature*, advance online publication:–, June 2011. ISSN 1476-4687. 8
- Štěpánka. Vaňáčková, Jeannette Wolf, Georges Martin, Diana Blank, Sabine Dettwiler, Arno Friedlein, Hanno Langen, Gérard Keith, and Walter Keller. A New Yeast Poly(A) Polymerase Complex Involved in RNA Quality Control. *PLoS Biol*, 3(6):e189, 04 2005. 74
- Valmik K. Vyas, Cristin D. Berkey, Takenori Miyao, and Marian Carlson. Repressors Nrg1 and Nrg2 regulate a set of stress-responsive genes in *Saccharomyces cerevisiae*. *Eukaryotic Cell*, 4(11):1882–1891, 2005. 64
- Dong Wang, David A. Bushnell, Xuhui Huang, Kenneth D. Westover, Michael Levitt, and Roger D. Kornberg. Structural basis of transcription: Backtracked RNA polymerase II at 3.4 angstrom resolution. *Science*, 324(5931):1203–1206, 2009. 3
- Lingna Wang, Marc S. Lewis, and Arlen W. Johnson. Domain interactions within the Ski2/3/8 complex and between the Ski complex and Ski7p. *RNA*, 11(8):1291–1302, 2005. 70

REFERENCES

- Yulei Wang, Chih Long Liu, John D. Storey, Robert J. Tibshirani, Daniel Herschlag, and Patrick O. Brown. Precision and functional specificity in mRNA decay. *Proc Natl Acad Sci U S A*, 99(9):5860–5865, 2002. 12, 13, 44
- Zuoren Wang and Megerditch Kiledjian. Functional link between the mammalian exosome and mRNA decapping. *Cell*, 107(6):751–762, December 2001. ISSN 0092-8674. 8
- K. Wiederhold and L. A. Passmore. Cytoplasmic deadenylation: regulation of mRNA fate. *Biochem Soc Trans*, 38(6):1531–6, 2010. Wiederhold, Katrin Passmore, Lori A Medical Research Council/United Kingdom Research Support, Non-U.S. Gov't Review England Biochemical Society transactions *Biochem Soc Trans*. 2010 Dec;38(6):1531-6. 12
- Akio Yamashita, Tsung-Cheng Chang, Yukiko Yamashita, Wenmiao Zhu, Zhenping Zhong, Chyi-Ying A Chen, and Ann-Bin Shyu. Concerted action of poly(A) nucleases and decapping enzyme in mammalian mRNA turnover. *Nat Struct Mol Biol*, 12(12):1054–1063, December 2005. ISSN 1545-9993. 12, 72
- Daniel Zenklusen, Daniel R Larson, and Robert H Singer. Single-RNA counting reveals alternative modes of gene expression in yeast. *Nat Struct Mol Biol*, 15(12):1263–1271, December 2008. ISSN 1545-9993. 41
- Zhenguo Zhang, Dedong Xin, Ping Wang, Li Zhou, Landian Hu, Xiangyin Kong, and Laurence Hurst. Noisy splicing, more than expression regulation, explains why some exons are subject to nonsense-mediated mRNA decay. *BMC Biology*, 7(1):23, 2009. ISSN 1741-7007. 3
- Jacob Zhurinsky, Klaus Leonhard, Stephen Watt, Samuel Marguerat, Jürg Bähler, and Paul Nurse. A coordinated global control over cellular transcription. *Curr Biol*, 20(22):2010–2015, November 2010. ISSN 0960-9822. 76

Abbreviations

Table 5.1: Abbreviations

Abbreviation	
cDTA	comparative dynamic transcriptom analysis
DTA	dynamic transcriptom analysis
NMD	non sense mediated decay
ORF	open reading frame
PCR	polymerase chain reaction
rpm	rotation per minute
UTR	untranslated region
v/v	volume per volume
w/v	weight per volume

Curriculum Vitae

Mai Sun Born on 7th, April, 1983
In Beijing, Peoples Republic of China

Research Experiences

2009 PhD thesis in Prof. Dr. Patrick Cramer lab, Gene Center, Ludwig-Maximilians-Universität München

2008 Research internship in Prof. Dr. Paul Knochel lab, Organic Chemistry, Ludwig-Maximilians-Universität München

2008 Research internship in Prof. DI Dr. Ernst Wagner lab, Pharmaceutical Biotechnology, Center for System-based Drug Research, Ludwig-Maximilians-Universität München

2007 Research internship and master thesis in Prof. Dr. Patrick Cramer lab

2004 Research internship and bachelor thesis in Prof. Wanru Sun lab, state key laboratory of microbial resources, the institute of microbiology, Chinese academy of science

Education

2009 PhD in Biochemistry, Ludwig-Maximilians-Universität München, Germany

2007 MSc in Chemistry and Biochemistry with 1.5 (German system²), Ludwig-Maximilians-Universität München, Germany

2001 BSc in Biotechnology, Beijing Normal University, P. R. China

Awards and scholarship

2009 Römer-Preis of Dr. Klaus Römer-Stiftung for Master thesis

2010 Scholarship of CeNS-IDK (Center of Nano Science-Internationale Doktorandkolleg)

2012 Hertwig award of Helmholtz Gesellschaft

Workshops and Conferences

2010 3rd SFB TR5 (Deutsche Forschungsgemeinschaft (DFG) Sonderforschungsbereich chromatin) Symposium 2010 - CHROMATIN, Munich, Germany

2010 Hands-on training at EBI-EMBO practical course on analysis and informatics of transcriptomics data, European bioinformatics institute, Hinxton, UK

²German grade:1–1.5: Very Good; 1.5–2.5: Good; 2.5–3.5: Satisfactory; 3.5–4: Sufficient; 5: Not sufficient

2010 EMBO Conference Series - From Functional Genomics to Systems Biology, Heidelberg, Germany

2011 The 62. Mosbacher Kolloquium - Mechanisms of RNA-mediated regulation, Mosbach, Germany

2012 CSHL conference: "Systems Biology: Global Regulation of Gene Expression", Cold spring harbor, US

2012 EMBO Conference Series - The complex life of mRNA, Heidelberg, Germany

Publications

2012 **Global analysis of eukaryotic mRNA degradation reveals Xrn1-dependent buffering of transcript levels** Mai Sun¹, Björn Schwalb¹, Nicole Pirkl, Kerstin C. Maier, Arne Schenk, Henrik Failmezger, Achim Tresch, and Patrick Cramer, *Manuscript submitted*

¹ These authors contributed equally

2012 **Comparative dynamic transcriptome analysis (cDTA) reveals mutual feedback between mRNA synthesis and degradation** Mai Sun¹, Björn Schwalb¹, Daniel Schulz¹, Nicole Pirkl, Stefanie Etzold, Laurent Larivière, Kerstin C. Maier, Martin Seizl, Achim Tresch, Patrick Cramer, *Genome Research*, **2012** 22(7):1350-9

¹ These authors contributed equally

2012 **Measurement of genome-wide RNA synthesis and decay rates with Dynamic Transcriptome Analysis (DTA)** Björn Schwalb, Daniel Schulz, Mai Sun, Benedikt Zacher, Sebastian Dömcke, Dietmar Martin, Patrick Cramer, Achim Tresch, *Bioinformatics*, **2012** 28(6):884-5.

-
- 2012 **CTD Tyrosine Phosphorylation Impairs Termination Factor Recruitment to RNA Polymerase II** Andreas Mayer, Martin Heidemann, Michael Lidschreiber, Amelie Schreieck, Mai Sun, Corinna Hintermair, Elisabeth Kremmer, Dirk Eick, Patrick Cramer, *Science*, **2012**. 336:1723-1725.
- 2010 **A Tandem SH2 Domain in Transcription Elongation Factor Spt6 Binds the Phosphorylated RNA Polymerase II C-terminal Repeat Domain (CTD)** Mai Sun, Laurent Larivière, Stefan Dengl, Andreas Mayer, Patrick Cramer, *J Biol Chem*, 2010. 285:41597-41603.
- 2009 **Structure and *in Vivo* Requirement of the Yeast Spt6 SH2 Domain** Stefan Dengl, Andreas Mayer, Mai Sun, Patrick Cramer, *J Mol Biol*, **2009**. 389:211-225.
- 2009 **LiCl-mediated preparation of functionalized benzylic indium(III) halides and highly chemoselective palladium-catalyzed cross-coupling in a protic cosolvent** Yi-Hung Chen, Mai Sun, Paul Knochel, *Angew Chem Int Ed Engl*, **2009**. 48:2236-2239.